Scientific Journal for faculty of Science - Sirte University

ISSN: 2789-858X

Volume1 Issue No.1 October 2021

Bi-annual Peer-review Journal

Legal Deposit Number: 990/2021

sjsfsu@su.edu.ly
journal.su.edu.ly/index.php/JSFSU

DOI: http://www.doi.org.10.37375/issn.2789-858X eISSN: 2789-858X

Scientific Journal for the Faculty of Science-Sirte University (SJFSSU)

Legal Deposit Number: 990/2021

http://journal.su.edu.ly/index.php/JSFSU/index sjsfsu@su.edu.ly

Bi-annual Peer-Reviewed Journal

Volume 1, Issue 1, October 2021

Advisory Scientific Committee of the SJFSSU

No	Name	Specialisation	Organisation	Country
1	**Prof. Dr. Ahmad F. Mahgoub**	Zoology	Science Faculty, **Sirte** University	Libya
2	**Prof. Dr. Salem A. Abuhassia**	Statistics	Science Faculty, **Omar Al-Mukhtar** University	Libya
3	**Prof. Dr. Marei M. El-Ajaily**	Chemistry	Science Faculty, **Benghazi** University	Libya
4	**Prof. Dr.Huda Shaaban Elgubbi**	Botany	Science Faculty, **Misurata** University	Libya
5	**Prof. Dr. Nasser H. Sweilam**	Applied Maths	Science Faculty, **Cairo** University	Egypt
6	**Prof. Dr. Osama Ahmed Hlal**	Geology	Science Faculty, **Tripoli** University	Libya
7	**Prof. Dr. Mohamed A. Elssaidi**	Environment Sciences	Engineering and Technical Sciences Faculty, **Sebha** University	Libya
8	**Prof. Dr. Ebrahim M. Daghman**	Microbiology	Science Faculty, **Misurata** University	Libya
9	**Prof. Dr. Ali Mohamed Awin**	Mathematics	Science Faculty, **Tripoli** University	Libya
10	**Prof. Dr. Ebrahim A. Elmerhaq**	Information Technology	Information Technology Faculty, **Tripoli** University	Libya
11	**Prof. Dr. Rafa A. Azzarroug**	Physics	Science Faculty, **Benghazi** University	Libya
12	**Prof. Dr. Osams M. Shalabiea**	Astronomy	Science Faculty, **Cairo** University	Egypt
13	**Prof. Dr. Abdualhamid S. Alhaddad**	**Environment Sciences & Natural Resources**	Science Faculty, **Misurata** University	Libya

Editor in-Chief's Word

In the name of Allah, the Most Gracious, the Most Merciful.

The praise is to Allah, Lord of the worlds, and prayers and peace is upon the prophet Muhammad, and upon his family and his companions.

At the outset, we are delighted to congratulate all members of the editorial board of the journal and all the teaching fraternity of the faculty of science at Sirte university on the launch of the first scientific journal of our faculty. Moreover, we would like to commend the efforts made by the Dean of the faculty, which bore fruit in establishing this scientific platform. Furthermore, we hope that this journal will be a scientific platform that musters academics from inside and outside the university in the field of basic sciences and their applications to share and exchange their experiences and scientific research. The editorial board of the journal will be keen to adhere to the common quality standards for scientific publications by following certain rules for writing scientific research, investigating honesty and scientific accuracy. We ask Allah to grant us success so that this journal contributes to raising the university's classification and progress at both the local and regional levels.

This journal will provide its services to the teaching community in the vital sectors and will contribute effectively to the process of building the society.

This journal aims to enrich the culture of scientific research and encourages academics to engage in scientific research. We also aspire that this journal puts its unique mark to distinguish among other local and non-local scientific journals. With Allah's help, we will strive to ensure that the journal obtains the recognized quality standards, whether at the local or regional level.

My deep appreciation to the editorial board, reviewers and researchers who make our journal a vehicle for their research works.

Peace, mercy and blessings of Allah are upon you.

Prof. Dr. Abdalla Salem Radwan

Editor in chief

Editorial Director's Word

In the name of Allah, the Most Gracious, the Most Merciful.

The praise is to Allah, Lord of the worlds, and prayers and peace is upon the prophet Muhammad, and upon his family and his companions.

To begin with, it is my great pleasure to congratulate all the members of the editorial board of the Scientific Journal for the Faculty of Science-Sirte University (SJFSSU, henceforth) and all the faculty members and its administrative and technical staff on the release of the first issue of the SJFSSU. The SJFSSU specializes in publishing an original scientific research that fulfils the academic integrity requirements and meets the common scientific requirements. We hope that the SJFSSU will be a valuable scientific platform for academics from inside and outside the university.

Secondly, the SJFSSU aims to consolidate scientific research and encourage everyone in the academic community to engage in the field of scientific research and publish one's work to make valuable contributions to the community. The editorial board of the SJFSSU is keen to abide to the common quality standards by adhering to the ethics of scientific research and the investigation of accuracy and scientific honesty. We pray to Allah to help us in our endeavours so that the SJFSSU projects an honourable impression of the science faculty in particular and of Sirte University in general, and that it contributes to elevating the university's classification and progress at both the local and regional levels.

Thirdly, we also aspire that the SJFSSU will take a prestigious position among other scientific journals. With Allah's help, we will strive to ensure that the SJFSSU obtains the standards of quality that are recognized either at the local or regional levels and continuity of issuing this journal.

In conclusion, it is my great pleasure to thank everyone who involved in the release of this issue, starting with the editorial board, peer reviewers and researchers who chose our journal as a platform to publish their research works. Any feedback or comments are very welcomed.

Peace, mercy and blessings of Allah are upon you.

Assoc.Prof. Haniyah A. Saed Ben Hamdin

Editorial Director

About the Scientific Journal for the Faculty of Science-Sirte University (SJFSSU)

The Scientific Journal for the Faculty of Science-Sirte University (SJFSSU, henceforth) is a bi-annual peer-reviewed and open accessed journal issued electronically by the faculty of science at Sirte University. The SJFSSU aims to encourage research in the scientific community and publish papers reporting original work that are of high standards and contribute to the development of knowledge in all fields of applied and pure (theoretical) science, namely mathematics, statistics, physics, chemistry, zoology, botany, microbiology, astronomy, computer sciences, information technology, geology, environment sciences and oceanography.

The SJFSSU accepts all types of articles such as research articles, review articles, topical review, case study/case reports, monograph, short communication, letters, conference/symposium special issues, editorials research articles and methodology articles.

Any opinions or views expressed in this journal do not reflect the opinions or views of the SJFSSU or its members. Moreover, the designation and the presentation of materials do not reflect any opinion whatsoever of the SJFSSU in terms of legal status of any country, territory…etc.

Policy and Publication Ethics of the Scientific Journal for the Faculty of Science-Sirte University (SJFSSU)

General Rules:

1. Any manuscript submitted to the SJFSSU must contain an original work which has been neither previously published, nor it is under consideration by another journal, conference, workshop or symposium.
2. The submitted manuscript must fulfil the common requirements of the scientific research, including presenting the problem, reviewing the relevant literature, analysing data, discussing results and draw the conclusion and the recommendations.
3. The SJFSSU accepts all types of articles such as research articles, review articles, topical review, case study/case reports, monograph, short communication, letters, conference/symposium special issues, editorials, research articles and methodology articles.
4. An author is required to write his or her manuscript carefully according to the basic and technical rules of the SJFSSU.
5. The SJFSSU only accepts manuscripts written in English language.
6. The subject of the submitted manuscript must be in the specified categories of the SJFSSU.
7. All individuals involved in the publishing process: from authors, editorial board, peer reviewers, must comply with standards of ethical behaviour.
8. All submitted manuscripts are subject to double-blind and peer-review process that is the author will be unaware of the reviewer's identity, and also the reviewer is unaware of the author's identity.

Author/s Rresponsibility:

1. The author is alone responsible for the proofreading and spelling check of his or her submitted manuscript.
2. The SJFSSU editorial committee has the right to make any editorial changes on the manuscript which is accepted for publication.
3. An author is banned from submitting his or her manuscript to the SJFSSU in a period of three years if he or she decides to withdraw his or her manuscript whilst it is undergoing review process, furthermore he or she must pay all the expenses incurred in the review process.
4. An author is kindly requested to disclose any affiliations, including financial, consultant or institutional associations that might lead to bias or a conflict of interest.
5. The author alone is responsible for the views, ideas expressed and the accuracy of the data in his or her manuscript. Thus the published papers do not reflect the opinions or views of the SJFSSU or its members. Furthermore, the designation and the presentation of materials do not reflect any opinion whatsoever of the SJFSSU in terms of legal status of any country, territory…etc.
6. Author is required to understand, complete and sign the 'Authorship, Copyright Transfer, Conflicts of Interest and Acknowledgments statement' which can be downloaded from the link: https://drive.google.com/drive/folders/1DZR62rl4U2XVXN9hlCXshOkDspOdU38z?usp=sharing

The signed form should be scanned and attached electronically along with the submitted manuscript.

16. An author has to submit his or her manuscript electronically as a MS-Word file through the journal website via the link: https://journal.su.edu.ly/index.php/SJFSSU/information/authors
17. Without the need to contact the editorial committee with regard to submitted manuscript, an author can easily track his or her submitted manuscript electronically through the journal website via the link: https://journal.su.edu.ly/index.php/SJFSSU/information/authors

Author's Rights:

1. The Author retains the following rights:
   i. All proprietary rights, such as patent rights.
   ii. Using all or part of the material published in his or her article in further research of his or her own filling, provided that permission is granted from the SJFSSU and an adequate acknowledgment should be appropriately credited and referenced for the SJFSSU.

Plagiarism Policy

2. To fulfil the academic integrity requirements, manuscripts submitted to the SJFSSU must adhere to ethical standards and refrain from plagiarism in any way. Thus manuscripts submitted to the SJFSSU must pass an initial check by plagiarism checker software.

3. If any plagiarism or scientific theft is detected in the submitted manuscript then the SJFSSU will contact the author in regard to this matter. If the editorial board of the SJFSSU is not satisfied with the justifications presented by the author, then strict measures will be taken against the author. Moreover, the editorial board forever will not consider any request for publication submitted by the author in the future.

Editors Responsibilities:

1. The editorial committee must ensure a fair double-blind peer-review of the submitted manuscript.
2. The editorial committee will strive to make sure there are no potential conflicts of interests between the author, the editorial and review personnel.
3. The editorial committee will ensure that all the information related to submitted manuscripts is sustained as confidential.

Reviewers Responsibilities:

1. The reviewers must ensure that all the information related to submitted manuscripts is kept as confidential.

2. Reviewer who is unable to review the submitted manuscript for any reason should notify the editorial director to excuse himself or herself from the review process.
3. Reviewers must review the submitted manuscripts objectively according to the journal's evaluation forms and adhere to the specified evaluation period of three months at max.

Review Process

1. If the submitted manuscript initially meets the specified requirements of the SJFSSU and successfully passes the plagiarism check, then directly it should go through the double blind and peer-review process.
2. The submitted manuscript is subject to double blind review by specialized referees suggested by the editorial committee in an undisclosed manner to evaluate the submitted manuscript.
4. The editorial board of the journal informs the author of the opinions of the referees and forwards its assessment report if the manuscript needs any corrections.
5. Any PhD-degree holder with a degree of (assistant professor or higher) who would like to be a referee in the SJFSSU should register and send his or her CV through the SJFSSU website.
6. An author is required to make any minor or major corrections that are suggested by the referees within a stipulated date.

Publishing Process

1. Once the decision is made of accepting the manuscript for publication at the SJFSSU, the author will be notified and facilitated with an acceptance letter to confirm that his or her manuscript is accepted for publication in the upcoming issue of the SJFSSU.
2. Once the issue of the journal has been realised, a soft-copy of each published paper will be sent to the author via his or her email address.

Author Guidelines for Preparing the Manuscript

All submissions should strictly be prepared according to the following guideline:

1. The submitted manuscript should be approximately up to a maximum of 20 pages and a minimum of 5 pages (including tables, figures, references list, appendixes and supplements).
2. The submitted manuscript of types (review articles, topical review) should be approximately up to a maximum 45 pages (including tables, figures, references list, appendixes and supplements).

Rules for the Paper Structure

3. The first page should contain the full title of the manuscript (the title should be concise and informative), then the name(s) of the author(s).
4. Affiliation with contact information including the (The affiliation(s) of the author(s), i.e. institution, (department), city, (state), country). A clear indication and an active, official university email address of the corresponding author.
5. This is followed by the abstract except for review article types which start with the introduction.
6. The abstract length should be of (250) words at the maximum and (150) words at the minimum.
7. In the abstract of the submitted manuscript, the following main points must be available: -

    i. An introductory sentence related to the research topic to attract readers.
    ii. Presentation of the research main point (purpose).
    iii. Description of the method used in the research.
    iv. Presentation of the achieved results.
    v. A concluding sentence that includes a recommendation.
8. The keywords should be 4 to 6, which can be used for indexing purposes.
9. In the introduction of the submitted manuscript, the following main points must be available: -
    i. Introductory sentences related to the research topic to attract readers.
    ii. An adequate background, then the relevant literature review.
    iii. Clearly state the object of the research.
    iv. The limitation of the research.
    v. The structure of the manuscript.
10. In the Material and methods section of the submitted manuscript, the author should provide sufficient details to allow the work to be reproduced by an independent researcher. Methods that are already published should be summarized and indicated by a reference. If quoting directly from a previously published method, use quotation marks and also cite the source. Any modifications to existing methods should also be described.
11. Results should be clear and concise and presented separately from the discussion.
12. The discussion should explore the significance of the results of the work, not repeat them.
13. The main conclusions of the study may be presented in a short Conclusions section, which may stand alone or form a subsection of the Discussion section.
14. Collate acknowledgements in a separate section at the end of the article before the reference list and do not, therefore, include them on the title page, as a footnote to the title or otherwise. List contributions that need acknowledging (e.g., acknowledgments of technical help;

acknowledgments of financial and material support, writing assistance or proof reading the article, financial arrangement, specifying the nature of the support).

15. Within the acknowledgments section, a conflict of interest statement must be included for all manuscripts even if there are no conflicts of interest.
16. If there is more than one appendix, they should be identified as A, B, etc. Formulae and equations in appendices should be given separate numbering: Eq. (A.1), Eq. (A.2), etc.; in a subsequent appendix, Eq. (B.1) and so on. Similarly for tables and figures: Table A.1; Fig. A.1, etc.
17. The author is asked to switch off the 'Track Changes' option in Microsoft Office files as these will appear in the published version.

Text Formatting Rules:

18. Use a normal, plain font (e.g., 10-point Times New Roman) for text.
19. Use italics for emphasis.
20. Use the equation editor or Math Type for equations.
21. Save your file in docx format (Word 2007 or higher).

Headings: Please use no more than three levels of displayed headings.

22. The manuscript (in two columns) should be single line space and the font type (Times New Roman) and the size should be as specified in this table:

Paper title	**14 Bold**
Authors names	10
Abstract	9
Address	10 Italic
Main headings	12 Bold
subheadings	10 Bold
Text	10
Figure and table captions	9

23. The metric system should be used, and the Arabic numbers should be used for page numbers and throughout the running text.
24. Abbreviations, if used should be defined at their first mention in the text and used consistently thereafter, and the non-standard ones should be avoided.
25. Mathematical equations should appear in a sequential order and should be numbered between the brackets ( ).

Tables

26. All tables are to be numbered using Arabic numerals.
27. Tables should always be cited in text in consecutive numerical order. For each table, please supply a table caption (title) explaining the components of the table and an explanatory legend.
28. Identify any previously published material by giving the original source in the form of a reference at the end of the table caption.

29. Footnotes to tables should be indicated by superscript lower-case letters (or asterisks for significance values and other statistical data) and included beneath the table body.

Figures

30. High resolution is required in preparing the figures in the manuscript, the file formats JPEG, PNG are preferred for the figures, images, etc.
31. If the figure, photo… etc. has been published elsewhere, then the original source must be acknowledged and a written permission from the copyright holder must be obtained and submitted with the manuscript.
32. If photographs of people are used, then the photos must be obscured by clouds or a written permission by the concerned person must be obtained.
33. All figures are to be numbered using Arabic numerals.
34. Figure parts should be denoted by lowercase letters (a, b, c, etc)
35. References to figures and tables should be made in a sequential order as they appear in the running text, and should be numbered between the parentheses ( ), e.g. (Fig. 1) and (Tab. 1).
36. Ensure all figure and table citations in the text match the files provided.
37. When preparing your figures, pay attention to the size figures to fit in the column width.
38. Figures should have a short label.

References Style:

39. Enclose the references list at the end of the manuscript accordingly to the APA (American Psychological Association) style (5^{th} to 7^{th}) edition. A guide containing examples of common citation formats in APA can be found at the below link:
https://guides.libraries.psu.edu/apaquickguide/

40. How to create an APA cited paper in Microsoft Word:
https://support.microsoft.com/en-us/office/apa-mla-chicago-%E2%80%93-automatically-format-bibliographies-405c207c-7070-42fa-91e7-eaf064b14dbb

Page margins: The Page margins should be adjusted as,

Top	Bottom	left	Right
2	2	2.5	2

41. To prepare the manuscript, it is highly recommended to use the ready –template that is prepared by the editorial committee which is available electronically on the journal website at the ink:
https://drive.google.com/drive/folders/1DZR62rl4U2XVXN9hlCXshOkDspOdU38z?usp=sharing

Contents

Contents	page
In Vitro Evaluation Of Bacterial Bioagents And Fungicides Efficiency Against *Rhizoctonia Solani* Isolates the Causal Agent of Black Scurf Disease of Potato *Muna N. Ekri, Alsadek M. Ghazala, Abeer M. Al-geblawi, Mohamed A. Zaied*	**1**
The Role of F-Doping and the Sintering Temperature on the Superconductivity And Lattice Constants in Laofege Compounds *T. M. Fayez, Ibrahim A. Saleh, Mustafah M. Abdullah Ahmad*	**12**
Morphological Study of The Effects of Caffeine Beverages can Cause Birth Defects on Swiss White Mice Embryos *Arwa Adress Alnuimy, Hani Mal Allah Hamodi*	**18**
Microfacies Analysis, Diagenetic Aspects and Depositional Environments of The Oligocene-Miocene Rock Units Exposed at Al Bardia Coastal Area, North East Tobruk City, Libya *Farag Ada, Tarek Anan and Amin Gheith*	**24**
Rate Constants and Rheological Properties of The Ultrasonic Degradation of Carboxymethyl Cellulose *Hitham M. Abuissa, Randa F. Elsupikhe, Tahani S. Alfazani*	**32**
Comparison Between Median Filter and Wiener Filter to Get High Accuracy for Blood Vessel Image Extraction *Akram Gihedan, Salma Albargathe, Mohamed Hasni, Waleed Khalafullah, Tarek Nagem*[5]	**39**
Datura Stramonium* Leaf Extract Toxic Effects on Testis in Swiss Albino Mice *Mus Musculus *Soad Mohammed Alwirfli , Abdalla Mohamed, Ateeqah Ghayth Alzwawy , Raja Abdullah Mohammed*	**47**
Quality Assessment of Underground Water before and after Treatment: A Case Study of Tobruk City, Libya *Mohamed Masoud, Abdullah Abdulla, Anwar Abadelrahim and Tahani Y. M. Aeyad*	**53**

Scientific Journal for the Faculty of Science-Sirte University Vol. 1, No. 1 October (2021) 1-11

Scientific Journal for the Faculty of Science-Sirte University
(SJFSSU)
Journal home page: http://journal.su.edu.ly/index.php/JSFSU/index

In Vitro Evaluation of Bacterial Bioagents and Fungicides Efficiency against *Rhizoctonia solani* Isolates the Causal agent of Black Scurf Disease of Potato

Muna N. Ekrim[1], *Alsadek M. Ghazala**[1], *Abeer M. Al-geblawi*[1], *Mohamed A. Zaied*[1]

[1]*Plant Protection Department, Agriculture Faculty, Tripoli University, Libya.*

ARTICLE INFO

Article history:

Received 24 August 2021

Received in revised form 6 September 2021,

Accepted 12 September 2021

Keywords:

In vitro,

Potato,

Bacterial bioagents.Antagonism,

Rhizoctonia solani,

Fungicides.

ABSTRACT

The efficacy of two isolates of bacterial bioagents and two fungicides via, *Rhizoctonia solani* isolates were evaluated *in vitro*. In the dual culture assays, significance inhibition ratio of *R. solani* hyphal growth was obtained in all treatments of *Pesudomonas fluoresnces* and *Bacillis subtilis* compared to control. Also, *Bacillus subtilis* exhibit the highest significant suppression for the mycelial growth of *R. solani* isolates more than *Pseudemonas fluorescens,* and the ratios of inhibition differed according to the bioagents and *R. solani* isolates similar to those results in antifungal activity technique.

The volatile metabolite studies revealed that in the first period (three days) inhibition percentage significantly differed according to the tested isolates of *R. solani* and the applied bioagents, *B. subtilis* gave the highest inhibition (57.41%) in *R. solani* isolate 3. Similarly in *P. fluoresnces* treatments, the highest inhibition was (57.41%) was detected in isolate 3 of *R. solani* considering that the second tested time period (five day inoculation). *B. subtilis* showed highest inhibition value on isolate 1, on the other hand *P. flouresnce* showed high value of inhibition on isolate 2, whereas the lowest inhibition values were produced on isolate 1.Non volatile activity both bacterial bioagents isolates showed different values of inhibition on *R. solani* isolates. On the other hand, Rezolex was most effective against *R. solani* at two concentrations (0.2 and 0.3), however Topsin-M showed fluctuate inhibition values at two concentration used (0.04% and 0.075%). Further incubation of plates showed suppressed the formation of sclerotia by all the antagonists tested.

The results implied that the extent of inhibition by *B. subtilis* and *P. fluoresnces* rovides the use of excellent potential antagonists capable of controlling the *R. solani in vitro*.

1 Introduction

Rhizoctonia solani, is the most widely recognized species of the genus *Rhizoctonia* which originally first described by Julius Kühn on potato in 1858, which is one of the most prevalent and important soil borne fungal pathogen causing destruction of a wide range of economically important crops such as rice, wheat, tomato, potato etc. (Gull, 2008 and Murphy and Riley, 1962). This fungus does not produce asexual spores, and exists as mycelium and sclerotia or sexual spores called basidiospores (Keijer, 1996). Potato (*Solanum tuberosum* L.) is one of the most important crops worldwide belonging to the family Solanaceae grown in around 150 countries spread through the world in both temperate and tropical regions (Adebola et al., 2020 and Siddique et al., 2020).

Unfortunately, commercial cultivars of potato are susceptible to fungal and bacterial diseases leading to

***Corresponding author:**
E-mail: elsadek1969@yahoo.com
DOI: https://doi.org/10.37375/sjfssu.v1i1.113 **SJFSSU 2021**

big losses in yield and quality of products (Walter et al., 2001and Khan et al., 2008). Among the different fungal diseases of potato crop, black scurf disease of potato caused by, *Rhizoctonia solani*, is the most commonly observed disease with the characteristic of black scurf symptoms on tubers and stem canker are the result of *Rhizoctonia* disease complex in potato. Black scurf disease increases gradually and sclerotia may develop on tuber surface even under low infection, .resultantly the control through fungicidal chemistries is not always useful especially when levels of infection are high (Malik Owais et al., 2014). In addition to that, overuse of chemical pesticides has caused soil pollution and harmful effects on human beings. Accordingly, biological control of soil borne diseases has been attracting attention. Many reports or reviews in this area have already appeared. So far, gram-negative bacteria, especially Pseudomonas strains, have been intensively investigated as biological control agents with regard to the production of antimicrobial metabolites, genetic analysis and regulation of some metabolites, and ecological fitness of soil. The gram-positive bacteria, like *Bacillus* spp., however, have been studied less intensively than the gram-negative bacteria. *Bacillus* subtilis is considered to be a safe biological agent, but evaluation of *Bacillus subtilis* has focused primarily on the degree of disease suppression (Asaka and Shoda, 1996).

Therefore, the objective of the present work was to evaluate the antagonistic effect and to determine the efficacy of volatile and non- volatile activity of bioagents *Bacillus subtilis* and *Pseudomonas fluorescens* on mycelial growth of *R. solani* isolates, and to evaluate the effectiveness of two fungicides viz., Rezolex and Topsin M70 at two different concentrations against five isolates of *R. solani* the causal agent of black scurf of potato under in vitro condition

2 Materials and Methods

The antagonistic bacteria Bacillus subtilis and Pseudomonas fluorescences used in the present study, were identified registered with the aid of members of the Botany Department at Saba Bacha Agriculture Faculty, Alexandria University.

2.1 Source of tested bioagents isolates:

The antagonistic bacteria *B. subtilis* and *P. fluorescens* used in the present study were obtained from the Botany Department at Saba Bacha Agriculture Faculty, Alexandria University.

Sclerotia of *Rhizoctonia solani* were collected from infected potato tubers cv. Spunta, showing typical black scurf symptoms, were first washed free of excess soil in tap water. A portion of each tissue was transferred to 2 min in 2% sodium hypochlorite solution then rinsed twice in sterile water. The treated tissue pieces with sclerotia were blot dried and then transferred to petri plates containing sterilized potato dextrose agar (PDA) medium with five pieces per plate. All plates were incubated at 25°C±2 for 7 days. The pure cultures of different isolates of R. solani were stored on PDA medium at 4°C in the dark for experimentation.

2.2 Isolation and Identification of pathogen:

For the isolation of *R. solani*, sclerotia grown on the skin of infected potato tubers cv. Spunta, showing typical black scurf symptoms were first washed free of excess soil in tap water. A portion of each tissue was transferred to 2 min in 2% sodium hypochlorite solution then rinsed twice in sterile water. The treated tissue pieces with sclerotia were blot dried and then transferred to petri plates containing sterilized potato dextrose agar (PDA) medium with five pieces per plate. All plates were incubated at 25 ± 2°C for 7 days. The pure cultures of different isolates of *R. solani* were stored on PDA medium at 4°C in the dark for experimentation. The fungal isolates were identified observing the morphological and microscopic characteristics described by (Parmeter, 1970; Sneh et al., 1991and Tredway & Burpee, 2001).

2.3 Antagonistic Activity of Bacterial Biocontrol Agents:

Dual culture technique:

Antifungal activity of the bacterial bioagents was tested against *R. solani* isolates using dual culture technique (Rabindran and Vidyasekaran, 1996). In this technique *B. subtilis* and *P.fluorescens* were streaked at one side of Petri dish (1 cm away from the edge) containing PDA medium. A disc (5mm in diameter) from seven days old of *R. solani* isolates were placed on the opposite side of the petri dish perpendicular to the bacterial streak and plates were incubated at room temperature (28℃ ± 2) for 7 days. Plates inoculated with fungus only served as control. Three replicates were maintained for each isolate. The experiment was repeated three times. In in vitro tests, inhibition zone was measured when the mycelium of control was completely filled the Petri dishes. The measurements of inhibition zone were taken from edge side of mycelium of bacteria colony. Percent of inhibition is determined according to Cubukcu (2007).

Percentage Inhibition = C – T/C × 100

Where: C = Colony diameter (cm) of the control T = Colony diameter (cm) of the test plate

Antifungal activity of *B. subtilis* and *P. fluorescens* can be tested by dual culture:

The antifungal activity of *B. subtilis* and *P. fluorescens* can be tested by dual culture technique. PDA disk (5 mm) with active mycelium of the pathogen is placed in the center of a Petri dish with PDA; on the same plate, at a distance of 1.5 cm in the four cardinal points, a loopful of antagonistic bacterial isolates is placed. Plates inoculated with the pathogen culture

serve as controls. In order to quantify the antagonistic potential of bacterial isolate, the size of growth inhibition zones measured after 7 days of incubation at 25°C±2 and the percent of radial growth inhibition was calculated according to Jimenez et al. (2018) .

The radial growth of the pathogen was measured and the percentage of inhibition was calculated by adopting from the following formula.

R= CD –TD/ CD X 100

Where,

R= percentage inhibition of test pathogen

CD = Radial growth of test pathogen in control

TD = Radial growth of test pathogen in treatment

Volatile activities:

Petri plates containing 20 ml of PDA were inoculated separately with 5 mm disc of antagonists and incubated at 28°C ±2 for 24 hours. After this lid of each plate was replaced by a bottom containing PDA previously inoculated with the disc of the pathogen and sealed together with paraffin film. The cultures were incubated at 25 °C ± 2, three replicates were used in this experiment. Radial growth was measured at 3and 5 days intervals and inhibition percent was determined using the following formula: Percent of inhibition = C2 − C1/C2 × 100.

Where, C2 means growth of *R. solani* in control and C1 means growth of *R. solani* according to Dennis and Webster (1971).

Non-volatile activities:

The method of Jariwala et al. (1991) with small modifications was used to evaluate the non-volatile activities of bacterial bio-agents. In this method, loop full of bacterial biocontrol agents were inoculated in nutrient broth and incubated for 48 hours at room temperature (25° C ± 2). After the incubation, cultures were centrifuged at 3000 rpm for15min. and the supernatant was used for antibiotic activity. Culture filtrates were added to PD Agar medium at 25%, 50%, 75% and 100% concentration, the pH was adjusted to 6.8 ± 0.2. Then the medium was sterilized and poured in sterile petri plates.7day old actively growing *R. solani* cultures were removed from the edge of the colony using 5mm diameter cork borer and placed at the center of these culture medium and the plates were incubated at room temperature. Three replicates were maintained for each concentration. Plates containing PDA medium with pathogens alone served as control. Radial growth of the fungal colony was measured on 5 day after incubation. Percent of inhibition was determined using the following equation:

Percent of inhibition = C2 − C1/C2 × 100

Where, C2 means growth of *R. solani* in control and C1 means growth of R. *solani* in treatment.

Evaluation of the effectiveness of two fungicides against *Rhizoctonia solani*

This experiment was conducted in vitro in plant pathology lab, dep of plant protection, Faculty of Agriculture, University of Tripoli to evaluate the efficacy of two fungicides belonging to various of chemical groups; namely Rizolex and Topsin-M (Table,1) aginst *R. solani* isolates,by using poisoned food technique (Hawamdeh & Ahmad 2001), in this technique, different fungicide concentrations were prepared in flasks by dissolving requisite quantities of each fungicide in warm media (50ºC). The fungicides were added after the media had been autoclaved. Twenty ml of amended medium was poured in 90 mm sterilized petri dishes and allowed to solidify. Mycelial discs of 5 mm diameter from 7day old culture was inoculated at the center of the petri plate and then incubated at 25°C ± 2 for 7days.Control was maintained without fungicide. Three replicated plates were used for each concentration of every fungicide with completely randomized design (CRD).The inhibition percentage of growth was calculated by using the formula I = (C-T/C) x 100

Where, I = Per cent inhibition of mycelial growth

C = Colony diameter in control (cm)

T = Colony diameter in treatment (cm) that given by Vincent (1927)

Table 1. Fungicides used for in vitro evaluation:

Common name	Trade name	Formulation	IUPAC name	concentrations
Tolclofos-methyl	Rizolex	50%WP	(2,6-dichloro-4-methylphenoxy)-dimethoxy-sulfanylidene-λ^5-phosphane	0.2, 0.3%
Thiophanate-methyl	Topsin-M	70%WP	methyl *N*-[[2-(methoxycarbonylcarbamothioylamino)phenyl]carbamothioyl]carbamate	0.04 , 0.075%

Statistical Analysis:

All experiments were set up in a complete randomized design. One-way ANOVA was used to analyses the differences between antagonistic inhibitor effect and linear growth of pathogenic fungi in vitro. A general linear model option of the analysis system SAS was used to perform the ANOVA (SAS, 1996).

3 Results

3.1 Antagonistic Activity of Bacterial Biocontrol Agents

Dual culture method

The bacterial antagonists *P. fluorescens*, *B. subtilis* showed inhibition in the mycelial growth ratios compared to control, though, inhibition ratios differed according to the bacterial isolates the *R. solani* tested isolates.

The highest inhibition ratio was obtained by B. subtilis (74.10%) on isolate No.3 of *R. solani*, while, the lowest inhibition ratio was obtained on isolate No.5 of *R. solani*. Otherwise the highest inhibition ratio (68.13%) was obtained by *P. fluoresces* on isolate No.3 of *R. solani*, although the least inhibition ratio (13.8%) was obtained in *R. solani* No.1. The formation of sclerotia has been suppressed by all the antagonists used (Table 2 and Fig 1).

Table 2. Effect of *Bacillus subtilis* and *Pseudomonas fluorescens* on mycelial growth inhibition of *Rhizoctonia solani* isolate

Bioagent (B)	Growth inhibition % Isolates of *Rhizoctonia solani* (I)					Mean
	1	2	3	4	5	
B. subtilis	45.00	50.00	74.10	60.56	38.33	53.60
P. fluorescens	13.89	50.56	68.13	58.06	41.67	46.46
Control	0.00	0.00	0.00	0.00	0.00	0.00
Mean	19.63	33.52	47.41	39.54	26.67	33.35
LSD0.05 (B) = 1.054	**LSD0.05 (I) = 1.36**		**LSD0.05 (B x I) =2.355**			

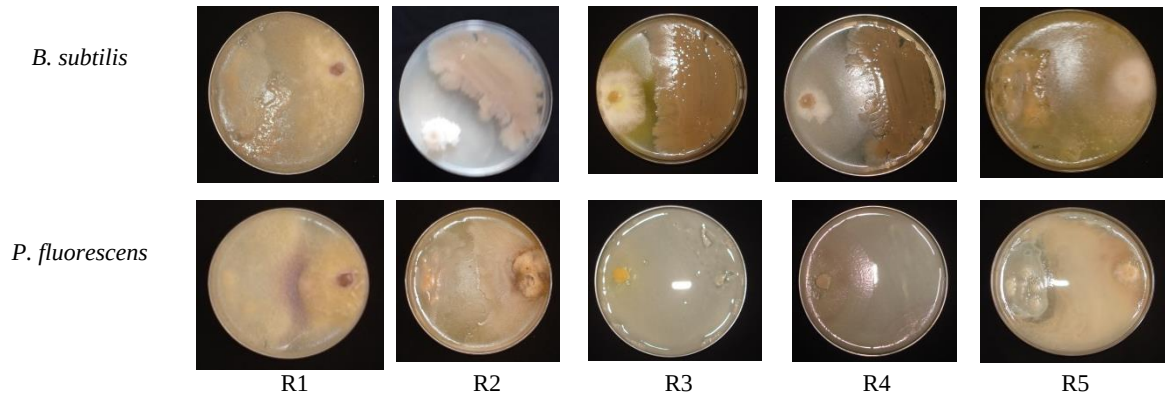

Fig. 1. The antagonistic effect of the tested bacteria (BACs) against *R. solani* isolates 1,2,3,4,5

Antifungal activity of *B. subtilis* and P. fluorescens canbe tested by dual culture:

Significant effect on all *R. solani* isolated used in this experiment was obtained by the two bacterial agents. *B. subtilis* gave highest inhibition value (66.44%) on isolate No.5 of *R. solani*, moreover, the lowest value was detected in isolate No.1 of *R. solani*. Finally, *P. fluoresscens* treatment showed high inhibition level on isolate No.4 of *R. solani* although, the lowest inhibition level was (6.11%) on isolate No.5 of *R. solani* compared to control (Table 3 and Fig. 2)

Table 3. Effect of *Bacillus subtilis* and *Pseudomonas fluorescens* on mycelial growth inhibition of *Rhizoctonia solani* isolates

Bioagents (B)	Growth inhibition % Isolates of *Rhizoctonia solani* (I)					Mean
	1	2	3	4	5	
B. subtilis	31.39	38.33	57.47	34.67	69.44	46.26
P. fluorescens	22.22	52.78	33.89	77.22	6.11	38.44
Control	0.00	0.00	0.00	0.00	0.00	0.00
Mean	17.87	30.37	30.45	37.30	25.19	28.23
LSD0.05 (B) =1.05	**LSD0.05 (I) =1.36**		**LSD0.05 (B x I) =2.36**			

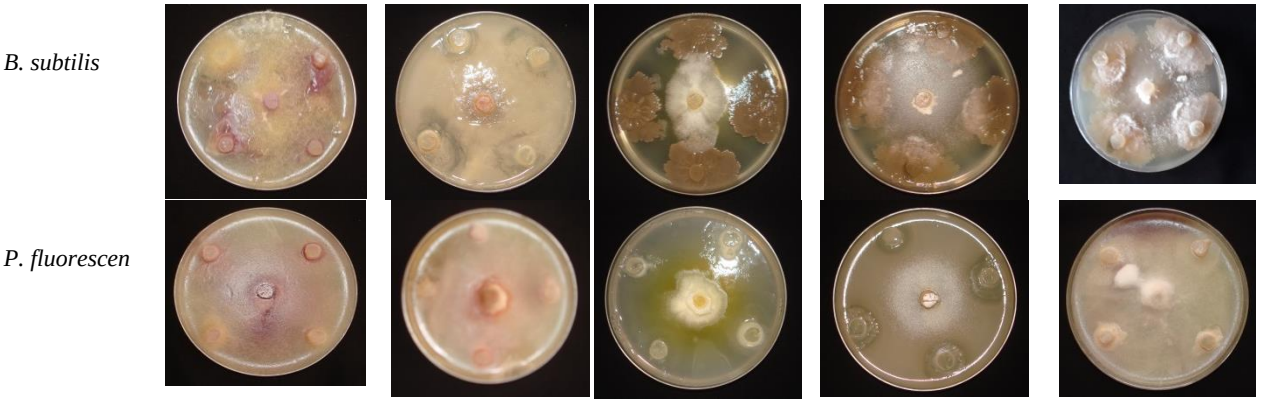

Fig. 2. The antagonistic effect of the tested bacteria (BACs) against *R. solani* isolates by dual culture technique .

Effect of volatile substance produced by *P. fluorescens* and *B. subtilis* on growth of the pathogen.

Two time-periods i.e. three days and five days after inoculation were carried out to determine the percent of inhibition. Inhibition percentages significantly differed according to the tested R. solani isolates and the applied bioagents in the first period. In B. subtilis treatment, the highest inhibition (57.41 %) was recorded in R. solani isolate 3, since, the least inhibition (30.30%) was detected in isolate 5. Similar to those in P. fluorsences treatment, the highest inhibition (57.41%) was detected in isolate 3 of R. solani, and the least percent was obtained on isolate 1 (33.3%). In the second tested time period (five days of inoculation), the highest inhibition value was showed by B. subtilis on isolate 1 (37.08%), meanwhile the least inhibition value was (15.54) on isolate no 5 of R. solani. Moreover, P. flouresences showed high value of inhibition on isolate 2 (39.33), though, the lowest inhibition values were detected on isolate 1 (13.89%) (Table 4)

Tale 4 .Volatile activity of *B. subtilis* and *P. fluorescens* against *R. solani* isolates in two-time period:

Bioagent (B)	Growth inhibition (%) 3 days after inoculation (T) Isolates of *Rhizoctonia solani* (I)					Mean	Growth inhibition (%) in the 5 days after inoculation(T) Isolates of *Rhizoctonia solani* (I)					Mean
	1	2	3	4	5		1	2	3	4	5	
B. subtilis	42.04	25.68	57.41	32.20	30.30	37.53	37.08	17.59	35.56	23.44	15.54	25.84
P. fluorescens	33.3	55.37	57.41	43.33	46.44	47.18	13.89	39.33	24.69	22.20	19.74	23.97
Control	0.00	0.00	0.00	0.00	0.00	0.00	0.00	0.00	0.00	0.00	0.00	0.00
Mean	25.12	27.02	38.27	25.18	25.58	28.23	16.99	18.97	20.08	15.21	11.76	16.6
LSD0.05 B=0.16	**LSD0.05 I= 0.24**		**LSD0.05 T=0.10**									
LSD0.05 IxB=0.37	**LSD0.05 IxT=0.30**		**LSD0.05 BxT = 0.23**		**LSD0.05 IxBxT =0.52**							

Non-Volatile activity

Different concentrations of *bacterial bioagents* (25%, 50%, 75% and 100%) were tested on mycelial growth of *R. solani* isolates (Table 5).

Results obtained by this technique showed that: *B. subtilis* gave different inhibitions values between all tested isolates. The concentrations 75 and 100% gave the highest inhibition values in isolate 2 (64.63 and 70.42% respectively) followed by 60.74% in isolate 4 at concentration 100% considering that the least inhibition value were detected at concentration 25% in isolate 2 (4.17%). Results similar to those obtained by *P. fluorsences*, which showed different inhibition values on *Rhizoctonia* isolates tested. The highest values of inhibition were obtained by concentrations (75, 100%) in isolate (2) 66.22 and 69.37% respectively, followed by 60.37% in isolate 4 at concentration 100%, while the least inhibition value were detected at concentration 25% in isolate (1) 3.3

Table 5. Effect of different concentrations of *Bacillus subtilis* and *Pseudomonas fluorescens* on mycelial growth of *R. solani* isolates.

	Bioagent (B)	Concentration % (C)	Isolates of *Rhizoctonia solani* (I)					
			1	2	3	4	5	
	B. subtilis	**25**	**5.833**	**4.17**	**35.56**	**39.27**	**9.34**	**18.734**
		50	**7.500**	**56.71**	**42.22**	**54.07**	**14.07**	**34.491**
		75	**19.028**	**64.63**	**47.00**	**55.18**	**18.15**	**37.167**
		100	**29.167**	**70.42**	**49.33**	**60.74**	**19.63**	**45.899**
	Control	**-**	**0.000**	**0.000**	**0.000**	**0.000**	**0.000**	**0.000**
	Mean		**12.305**	**39.18**	**34.82**	**41.85**	**12.24**	**27.258**
	P.fluorescens	**25**	**3.355**	**10.74**	**5.17**	**3.70**	**6.22**	**5.837**
		50	**4.889**	**55.00**	**5.43**	**49.26**	**12.70**	**25.455**
		75	**15.926**	**66.22**	**5.76**	**52.22**	**17.44**	**31.513**
		100	**24.889**	**69.37**	**7.23**	**60.37**	**19.63**	**36.297**
	Control	**-**	**0.000**	**0.000**	**0.000**	**0.000**	**0.000**	**0.000**
	Mean		**9.812**	**40.27**	**4.72**	**33.11**	**11.20**	**19.820**
	$LSD_{0.05}$ C= 1.427		**$LSD_{0.05}$ I =1.009**			**$LSD_{0.05}$ CXI= 2.257**		
		$LSD_{0.05}$ B= 0.638		**$LSD_{0.05}$ BXCXI = 3.192**				

Evaluation of the effectiveness of two Fungicides on *R. solani* isolates

Two fungicides were used at two concentrations in vitro to control *R. solani*.

Results showed that Rezolex was the most effective at concentrations (0.2 and 0.3%) on all *R. solani* isolates tested with inhibition values (82.41%) in isolate 1 at concentration 0.2% followed by 79.81% in isolate 1 at concentration 0.3%, where as the least inhibition value was (63.33%) at concentration 0.3% in isolate 4. While Topsin M-70 showed fluctuated inhibition values at two concentrations tested (0.04-0.075%) which was (83.11%) at concentration 00.075% in isolate 3 mean while 2.20 % inhibition value was detected at concentration 0.04% in isolate (1) Table 6. (Fig4&5).

Table 6. Effect of two concentrations of the tested Fungicides on mycelial growth of *R. solani* isolates.

Fungicides	Tretements (T) Concentration %(C)	Growth inhibition (%) 7 days after inoculation Isolates of *Rhizoctonia solani* (I)					Mean
		1	2	3	4	5	
Rezolex	0.2	82.41	69.07	78.15	65.37	75.74	74.148
	0.3	79.81	65.37	63.59	63.33	72.96	69.012
Control	-	0.00	0.00	0.00	0.00	0.00	0.00
Mean		54.07	44.81	47.25	42.90	49.57	47.719
		1	2	3	4	5	
Topsin – M70%	0.04	2.20	47.61	52.78	31.37	29.07	32.606
	0.075	2.75	52.41	83.11	53.70	41.48	46.674
Control	-	0.00	0.00	0.00	0.00	0.00	0.00
Mean		1.65	33.34	45.30	28.36	23.52	26.426
		$LSD_{0.05}$ C= 0.894		$LSD_{0.05}$ I = 1.145		$LSD_{0.05}$ CXI= 1.632	

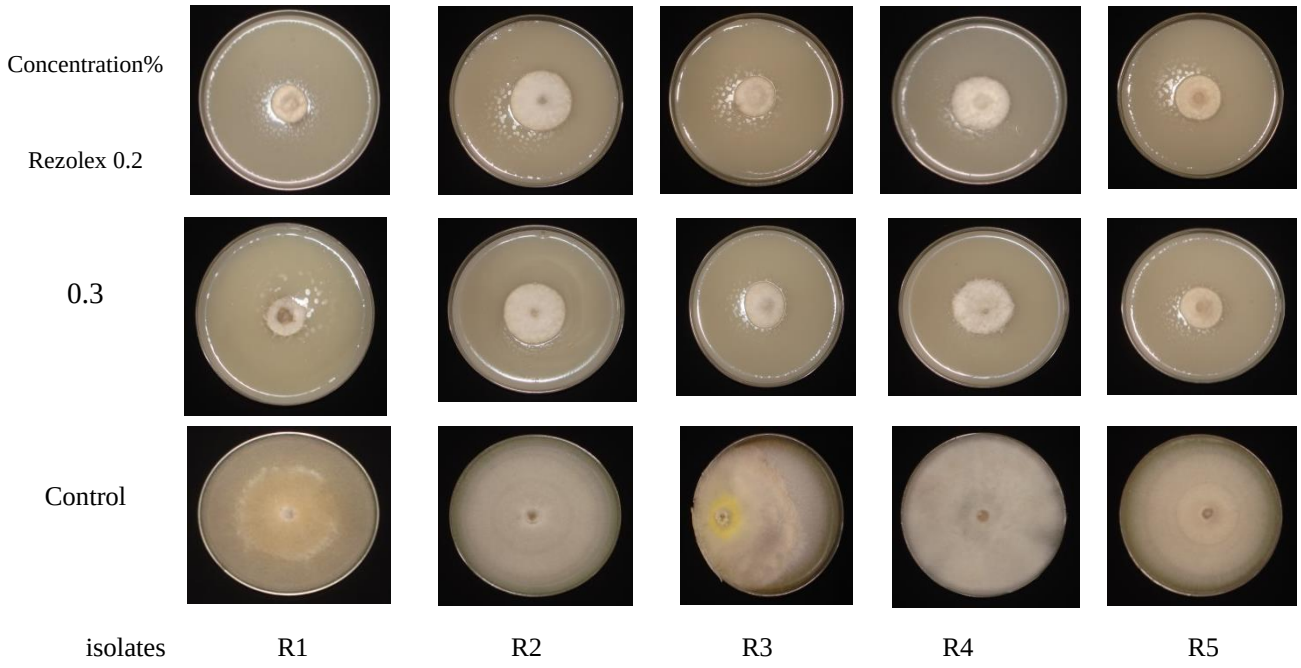

Fig. 4. Effect of two concentrations of the Rezolex on linear growth of *R. solani* isolates

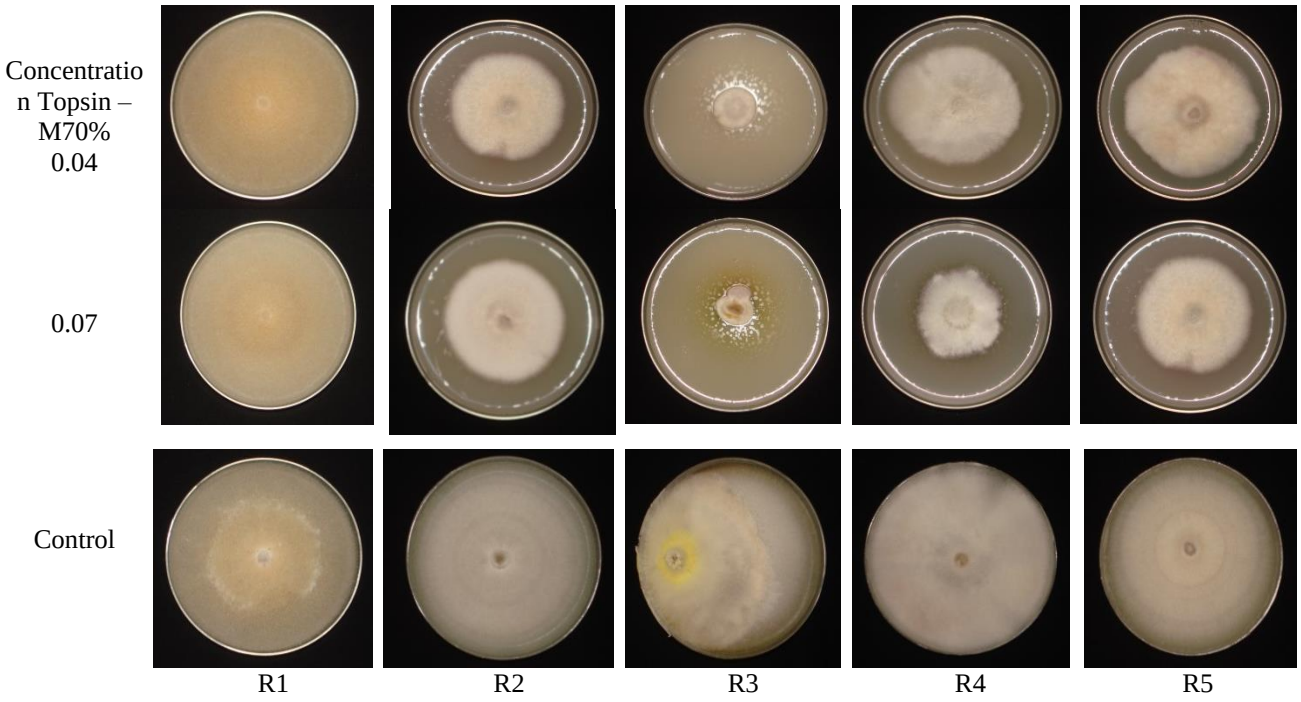

Fig. 5. Effect of two concentrations of the Topsin - M Fungicide on linear growth of *R. solani.*

4 Discussion

Results of the antagonism tests showed that *B. subtillis* was able to inhibited the the mycelium of *R. solani* isolates , this antagonistic action of *Bacillus subtilis* might be due to the antibiotic secretion (Siahmoshteh et al., 2019) enzymes and metabolites which reflect permeability changes in the protoplasmic membrane; competition for nutrients and bulb formation and lysis of the fungal hyphae. Several research workers have been reported that *B. subtilis* produces antibiotics which include iturin A and surfactin and Bacillopeptins and Bacillomycin (Cavaglieri et al., 2005 and Cheng et al., 2019) and this could have contributed to the biological control activity observed in the present study. The antibiotics produced in vitro were generally assumed to be the compounds responsible for biocontrol in vivo. *Bacillus* spp., however, produce a range of other metabolites including biosurfactants (Edwards and Seddon 1992), chitinase and other fungal cell wall-degrading enzymes (Pelletier and Sygusch 1990; Frandberg and Schnurer 1994), volatiles (Fiddaman and Rossall 1993) and compounds which elicit plant resistance mechanisms (Kehlenbeck et al. 1994)

Some isolates of bacteria change the media colour especially near the inhibition zone resulting in mycelial growth retardation *B. subtilis* showed the inhibition and the color of the media turned brown at the antagonized portion on the 7 day after . This may be due to the presence of the antibiotic like Inturin A and Surfactin produced by *B. subtilis*. Akihiro et al. (1993) has reported that *B. subtilis* produced antifungal peptide antibiotic Inturin A and Surfactin. Inturin A has a strong antifungal activity when compared to Surfactin. A purple pigment consistently produced in culture by strain Pseudomonas cepacia, strain 5.5B was isolated and identified as 4,9-dihydroxyphenazine-1,6-dicarboxylic acid dimethyl ester, a phenazine (Kelly Cartwright et al.,1995). On the other hand, Pal et al.(2000) reported that Pseudomonas fluorescens isolate EM85,produced the fluorescent pigment in PDA and antifungal antibiotics.

Moreover, Production of heat labile antifungal substances by *Bacillus* to control different fungal pathogens was reported by several workers (Podile et al., 1987 and Dileepkumar et al., 1988). Cyanides were also considered as volatile metabolites produced by bacterial biocontrol agents (Laha et al., 1996). During antibiosis, both volatile and nonvolatile secondary metabolities have been implicated in restricting the vegetative growth of pathogenic fungi.

In addition to that several studies described that the use of *P. fluorescenes* as a biocontrol agent against plant diseases. The activity of antifungal or antibacterial pseudomonads is traced back to the production of phenazines, 2-4-diacetyl phloroglucinol, pyrrolnitrin, pyoluteorin, cyclic lipopeptides (Liu et al., 2007), and rhizoxin (Loper et al., 2008). In addition to that they play a role in ecological fitness (Chin-A-Woeng et al., 2003).

Moreover, the suppression of *Rhizoctonia* diseases by bacterial bioagents usually attributed to the production of secondary metabolites which are toxic to the pathogen (Whipps, 2001). The results of dual culture studies showed that *P. fluorescenes* inhibited the growth of *R. solani* isolates.Member of the genus pseudomonas spp. Are well known antagonistic fungi (Kriet Low., 1949) .They are known to produce volatile compounds such as hydrogen cyanide (Castric et al.,1983). In vitro inhibition of *R. solani* occurred with the phenazine. Ester Dimethyl Pseudomonas Secondary Metabolite Liquid Culture (Kelly Cartwright et al.,1995).on the otger hand, compounds implicated in biocontrol of *R. solani* are usually antibiotics or fungal cell-wall degrading enzymes. It has been demonstrated that the ability of many strains of rhizobacteria to suppress plant pathogens is dependent on their capacity to produce secondary metabolites which directly inhibit the pathogens, and these include antibiotics, siderophores, bacteriocins, volatile compounds cyanide,enzymes and phytohormons (Homma, 1996).

On the other hand, all chemical fungicides used in this experiment prevent mycelial growth in vitro, but the inhibition rate was different between selected fungicides. In this study, tolclofos-methyl (TME) was the most effective of *R. solani* isolates, and suppressed of sclerotial production. However, Csinos (1985) found that 0.1 ug of TME/ml PDA suppressed sclerotia formation by 40% or more. (Ammar, 2003 and Korra, 2005) reported the inhibitory effect of Topsin M70 against many plant soil-borne pathogenic fungi. In other studies by Srinivas et al, 2014 and Rajput et al, 2014 reported the effectiveness of the active ingredient. Thiophanate methyl in the control of *R. solani* The different levels of reductions of radial growth by the fungicides was more likely due to varying extent of interference of these chemicals with the metabolism of the pathogen involved. In addition to genetic requirement, Deacon (1980) reported that the metabolism of pathogen depends, among other factors, on the substrate composition which could have been the active principles in the fungicides that affect the qualitative state of the fungus. The fungus genetics can affect its sensitivity toward the fungicides as a sensitive or insensitive to a chemical molecule (McGrat, 2009 and Reis et al., 2010), also the difference in the chemical group and the active ingredient of the used fungicides are much supported for the potential variation .The obtained results agreed with Rajput et al., 2016. Considering several systemic as well as non-systemic fungicides have been used which possess good control against *R. solani* (Madhavi et al., 2018).

The difference between both fungicides under study could be attributed to one or more factors, as mode of action of the fungal cell (Watkins et al., 1977), degree

of permeability of cell wall and/or plasma-lemma of fungi for uptake and passage of the fungicide into the fungal cell (Giffin, 1981). The similarity was obvious in terms of response of several isolates to the fungicides and those first reported by Dimond et al. (1941) for thiram. This response may be due to alterations in cell membrane permeability, storage of non dissociated fungicide or detoxification by the fungus (Horsfall, 1956).

5 Conclusion

We conclude that the success of *B. subtilis* and *P. flouresnces* as a potential biocontrol agents encouraged research into new microbial agents as alternatives to chemical control compounds. Whereas application of fungicides is the most convenient and predominant way for disease control. Their use has made it feasible to enhanc

e crop yields and food production. The efficacy of fungicides is influenced by many biological and environmental factors that directly influence the metabolic activities of fungal cells. Sometimes critical concentrations are not effective long-term, as the fungus can become resistant to the fungicide. In the present study, two fungicides showed as effective control agents against *R. solani*, though their efficacy varied among fungicides. These findings need further verification by application of these treatments in infected host plants and to find out the degree of control over the pathogen in vivo conditions.

Conflict of interest: The authors declare that there are no conflicts of interest.

References

Adebola, O. Matthew; Bello, S. Tunde; Seriki, A. Esther and Aremu, B. Mariam. (2020). Evaluation of three plant species to control black scurf disease of Irish potato (*Solanum tuberosum* Linn.). Notulae Scientia Biologicae 12(1):90-99. https://doi.org/10.15835/nsb12110643

Akihiro, O. Takashi A and Makoto, K. (1993). Production of antifungal peptide antibiotic – inturin by *Bacillus subtilis* NB. 22 in solid state fermentation. Journal Fermentation Bioengineering, 75: 23–27.

Ammar, M. I. (2003). Studies on heart rot disease of date palm in Egypt. Ph. D. Thesis, Fac. Agric., Cairo Univ., 121pp.

Asaka, O. and Shoda, M. (1996). Biocontrol of *Rhizoctonia solani* Damping-Off of Tomato with *Bacillus subtilis* RB14. Applied and Environmental Microbiology, Nov., Vol. 62(11): 4081–4085.

Ayed, H.B; Hmidet, N.; Béchet, M.; Chollet, M.; Chataigné, G.; Leclère, V.; Jacques, P. and Nasri, M. (2014). Identification and biochemical characteristics of lipopeptides from *Bacillus mojavensis* A21. Process Biochem. 49: 1699–1707.

Bhuiyan, M. K. A. (1994). Pathological and physiological study of *Rhizoctonia oryzae* causing rice bordered sheath spot disease (p. 39). A Ph.D. thesis submitted to the Department of Plant Pathology, Kynshu University, Fukuoka, Japan.

Cavaglieri, L.; J.R. Orlando, M. I. Rodriguez, S. Chulze and M. Etcheverry (2005). Biocontrol of *Bacillus subtilis* against *Fusarium verticillioides in vitro* and at the maize root level. Research in Microbiology, 156(5-6):748-754.

Cheng, X., X. Ji, Y. Ge, J. Li, W. Qi and K. Qiao (2019). Characterization of Antagonistic *Bacillus*
methylotrophicus isolated from rhizosphere and its biocontrol effects on maize stalk rot. Phytopathology, 109 (4): 571-581.

Chin-A-Woeng T.F.C., Bloemberg, G.V. and Lugtenberg, B.J.J. (2003). Phenazines and their role in biocontrol by *Pseudomonas* bacteria. New Phytol., 157: 503-523.

Compant, S.; Du-Y. B; Nowak, J.; Clement, C.; Barka, E.A. (2005). Use of plant growth promoting bacteria for biocontrol of plant diseases: Principles, mechanisms of action, and future prospects. Appl. Environ Microbiol. 71: 4951–4959.

Csinos, A. S. (1985). Activity of tolclofos-methyl (Rizolex) on *Sclerotium rolsii* and *Rhizoctonia solani* in peanut. Peanut Science 12:32-35.

Cubukcu, N. (2007). Pamuklarda *Verticillium solgunluğu* (*Verticillium dahlia* Kleb.)'na karşı endofitik bakterilerle biyolojik mücadele olanakları. Adnan Menderes Üniversitesi, Fen Bilim-leri Enstitüsü Yüksek Lisans Tezi, 73 (in Turkish).

Deacon, J.W. (1980). Introduction to modern mycology. *Oxford Blackwell Publication.* pp. 48-77.

Dennis, C. and Webster, J. (1971). Antagonist properties of species group of *Trichoderma* II. production of volatile antibiotics. Transactions of British Mycological Society 57: 41 -48.

Dileepkumar, B. S; Podile, A. R and Dube, H. C. (1988). Antagonistic activity of *Bacillus subtilis*
towards *Rhizopus nigricans.* J Biol Control., 2(1): 42-45.

Dimond, A. E; Davis, D; Herberger, J. W] and Stoddard, E. M. (1941). Role of the dosage response curve in the evaluation of fungicides. Conn. Agr. Exp. Sta. Bull., 451:635-667.

Dunlap, C.A.; Schisler, D.A.; Price, N.P.; Vaughn, S.F.(2011). Cyclic lipopeptide profile of three *Bacillus subtilis* strains; antagonists of Fusarium head blight. J. Microbiol. 49, 603–609.

Edwards, S.G. and Seddon, B. (1992). *Bacillus brevis* as a biocontrol agent against *Botrytis cinerea* on protected Chinese cabbage. In *Recent Advances in Botrytis Research* ed. Verhoeff, K., Malathrakis,

N.E. and Williamson, B. pp. 267-271. Wageningen: Pudoc Scientific Publishers.

Fiddaman, P. J and Rossall, S. (1993). The production of antifungal volatiles by *Bacillus subtilis.* Journal of Applied Bacterio1ogy7 (4):119-126.

Frandberg, E and Schniirer, J. (1994). Evaluation of a chromogenic chitooligosaccharide p-nitrophenyl N,W-diacetyl chitobiose, for the measurement of chitinolytic activity of bacteria. *Journal o*f Applied Bacteriology 76, 259-263

Giffin, D. H. (1981). Fungal physiology. John Wiley Sons, New York Chichester Brinsbane, Toronto and Singapore, 383pp.

Gong, A. D ; Li, H. P; Yuan, Q. S; Song, X. S; Yao, W ; He, W.J; Zhang, J. B; Liao, Y.C.(2015). Antagonistic mechanism of iturin A and plipastatin A from *Bacillus amyloliquefaciens* S76-3 from wheat spikes against *Fusarium graminearum*. PLoS ONE 10, e0116871.

Gull, M. (2008). Biological control of pathogenic infection through plant growth promoting Rhizobacteria. Ph. D. dissertation, Quaid-i-Azam University, School of Biotechnology, NIBGE Campus, Pakistan.

Hawamdeh, A. S and Ahmad, S. (2001). In vitro control of *Alternaria solani*, the cause of early blight of Tomato. Online Journal of Biological Sciences 1: 949–950

Horsfall, J. G. (1956). Principles of fungicidal action. Chronica Botanica Co., Waltham Mass., 279pp.

Jariwala, S. V and Bharat, R. (1991). Antagonistic activity of some fungi against

Alternaria solani and *Drechlera oryzae*. *Acta Botanica Indica*, 19(2): 217 - 223.

Jimenez, M. D. C. M; Hernandez, F. D; Alcala, E. I. L; Morales, G. G; Valdes, R.A and Reyes, F. C. (2018). Biological effectiveness of *Bacillus* spp. spp. and *Trichoderma* spp. spp. on apple scab (*Venturia inaequalis*) in vitro and under field conditions. European Journal of Physical and Agricultural Sciences. 6(2):7-17.

Kehlenbeck, H; Krone, C; Oerke, E. C and Schonbeck, F. (1994). The effectiveness of induced resistance on yield of mildewed barley. Journal of Plant Diseases and Protection 101, 11-21.

Keijer, J. (1996). The initial steps of the infection process in *Rhizoctonia solani*. In B. Sneh, S. Jabaji-Hare, S. Neate & G. Dijst (Eds.), *Rhizoctonia* species: Taxonomy, Molecular Biology, Ecology, Pathology and Disease Control (pp. 149-162). Dordrecht: Kulwer Academic Publishers.

Kelly, C. D; Chilton, W. S and Benson, D. M. (1995).Pyrrolnitrin and phenazine production by *Pseudomonas cepacia*, strain 5.5B, a biocontrol agent of *Rhizoctonia solani*. Applied Microbiology and Biotechnology, 43(2):211–216

Khan, R.S; Sjahril, R; Nakamura, I. and Mii, M. (2008). Production of transgenic potato exhibiting enhanced resistance to fungal infections and herbicide applications. *Plant Biotechnol. Rep*., 2, 13-20.

Korra, A. M. E. (2005). Pathological studies on root and corm rot of Banana. Ph. D. Thesis, Fac. Agric., Cairo Univ. 133 pp.

Kreit, L. K. W. (1949).Agriculture Experiment scicontribution.Ntm-101K.

Laha, G. S; Verma, J. P and Singh, R. P. (1996). Effectiveness of Fluorescent *Pseudomonads* in the

management of sclerotial wilt of cotton. *Indian Phytopath.*, 49(1):3-8.

Liu, H; He, Y; Jiang, H; Peng, H; Huang, X; Zhang, X; Thomashow, L. S. and Xu, Y. (2007). Characterization of a phenazine producing strain Pseudomonas chlororaphis GP72 with broad spectrum antifungal activity from green pepper rhizosphere. Curr. Microbiol., 54: 302-306.

Loper, J.E; Henkels, M.D; Shaffer, B.T; Valeriote, F.A. and Gross, H. (2008). Isolation and identification of rhizoxin analogs from *Pseudomonas fluorescens* Pf-5 by using a genomic mining strategy. Appl. Environ. Microbiol., 74: 3085-3093.

Madhavi1, M ; Narayan, R. P; Manohar, K and Aruna, K. C. (2018). Effect of Fungicides and Herbicides against *Rhizoctonia solani* f. sp. *sasakii* Exner Causing Banded Leaf and Sheath Blight in maize (*Zea mays* L.) International Journal of Bio-resource and Stress Management 9(1):142-153.

Murphy, J.; Riley, J.P. (1962). Modified solution method for determination of phosphate in natural water. *Anal. Chem. Acta.* 27, 31-36.

McGrath, M. T. (2009). Fungicides and other chemical approaches for use in plant disease control. Encyclopedia of Microbiology (Third Edition). Pp412-421.

Malik, O; Chohan, S; Naqvi, S and Atif, H. (2014). Occurrence of Black Scurf Disease of Potato in Multan (Punjab) Alongwith Its *in vitro* Chemical and Biotic Elicitor Mediate Management. Journal of Agricultural Science; Vol. 6, No. 9; ISSN 1916-9752 E-ISSN 1916-9760.

Pal, K. K; Tilak, K. V. B. R; Saxena, A. K; Dey, R and Singh, C. S. (2000). Antifungal characteristics of a fluorescent *Pseudomonas* strain involved in the biological control of *Rhizoctonia solani*, Microbiol. Res. 155:233-242.

Pelletier, A and Sygusch, J. (1990). Purification and characterization of three chitosanase activities from *Bacillus megaterium* P1. Applied and Environmental Microbiology 56: 844-848.

Perez, L.M.; Besoain, X.; Reyes, M.; Pardo, G and Montealegre, J. (2002). The expression of extracellular fungal cell wall hydrolytic enzymes in

different *Trichoderma harzianum* isolates correlate with their ability to control *Pyrenochaeta lycopersici*. *Biol. Res.* 35 (3-4): 401-410

Podile, A. R; Prasad, G. S and Dube, H. C. (1987). Partial characterization of antagonistic principle of *Bacillus subtilis* AF-1. J Biol Control., 1(1): 60-65.

Rabindran, R and Vidhyasekaran, P. (1996). Development of a formulation of *Pseudomonas fluorescens* PfALR2 for management of rice sheath blight. Crop protect, 15:715-721

Rajput, L.S; Harlapur, S.I; Venkatesh, I; Aggarwal, S.K. and Choudhary, M. (2016). *In -vitro* study of fungicides and an antibiotic against R*hizoctonia solani,* f.sp. *Sasakii* causing banded leaf and sheath blight of maize. International *Journal of Agriculture Sciences*, Volume 8, Issue 1, pp.-121-134.

Reis, E; Reis, A. and Carmona, M. (2010). Manual de fungicidas; guiapara controlequimico de doencas de plantas. Passo Fundo; UPF. English abstract.

SAS Institute Inc (1996). SAS/STAT user's guide. Version 6. Vol. 2.' 12th edn. (SAS Institute Inc.: Cary, NC), 846 pp

Castric, K. F and Castric, P. (1983). Method for rapid detection of cyanogenic bacteria, Appl, Environ. Microbiol. 45:701-702.

Shafi, J; Tian, H. and Ji, M.(2017). *Bacillus* species as versatile weapons for plant pathogens: A review. Biotechnol. Biotech. Equip. 31, 446–459.

Siahmoshteh, F; Z. Hamidi-Esfahani, D. Spadaro, M. S-G and Razzaghi-Abyaneh, M. (2019). Unraveling the mechanism of antifungal action of *Bacillus subtilis* and *Bacillus amyloliquefaciens* against aflatoxigenic *Aspergillus parasiticus*. 89: 300-307.

Siddique, M. A; Fateh, F. S; Rehman1, Z-U and Saleem, 1. H. (2020) .Black Scurf of Potato Disease Prevalence in the Markets of Federal Capital Territory, Pakistan. 33 (3): 440-444.

Sneh, B; Burpee, L and Ogoshi, A. (1991). Identification of *Rhizoctonia* species. The American phytopathological society APS Press. St. Paul, Minnesota, USA.

Srinivas, P; Ratan, V; Reddy, P. N and Gopireddy, B. M. (2014). In-vitro evaluation of fungicides, biocontrol agents and plant extracts against rice sheath blight pathogen *Rhizoctonia solani*. International Journal of Applied &Pharmaceutical Biotechnology, Vol. 58 (36), pp. 3284-3294.

Tredway, L. P and Burpee, L. L. (2001). *Rhizoctonia* diseases of turfgrass. The plant Health Instructor.

Walter, R.S; Rosemary, L; Gary, F.D. and Weingartner, D.P. (2001). *Compendium of potato diseases.* St Paul, MN, USA: American Phytopathological Society.

Watkins, J. E; Littefield, L. J and Statler, G. D. (1977). Effect of systemic fungicide 4-n-butyl-1,2,4- triazole on the development of *Puccinia recondite* f.sp. *tritici* in wheat. Phytopathology, 67: 985.

Whipps, J.M. (2001). Microbial interactions and biocontrol in the rhizosphere. J. Exp. Bot. 511, 487–511.

Zalila-Kolsi, I.; Mahmoud, A.B.; Ali, H.; Sellami, S.; Nasfi, Z.; Tounsi, S. and Jamoussi, K.(2016). Antagonist e_ects of *Bacillus* spp. strains against *Fusarium graminearum* for protection of durum wheat (*Triticum turgidum* L. subsp. *durum*). Microbiol. Res. 192, 148–158.

Zhao, Y.; Selvaraj, J.N.; Xing, F.; Zhou, L.; Wang, Y.; Song, H.; Tan, X.; Sun, L.; Sangare, L.; Folly, Y.M.E.; *et al*.(2014). Antagonistic action of *Bacillus subtilis* strain SG6 on *Fusarium graminearum*. PLoS ONE 9, e92486.

Scientific Journal for the Faculty of Science-Sirte University
(SJFSSU)
Journal home page: http://journal.su.edu.ly/index.php/JSFSU/index

The role of F-doping and the Sintering Temperature on the Superconductivity and Lattice Constants in LaOFeGe Compounds

T. M. Fayez[1], Ibrahim A. Saleh[2], Mustafah M. Abdullah Ahmad[1]*

[1] *Physics Department, Science Faculty, Sebha University, Libya*

[2] *Physics Department, Science Faculty, Benghazi University, Libya*

ARTICLE INFO

Article history:

Received 03 September 2021

Received in revised form 21 September 2021

Accepted 21 September 2021

Keywords:

Superconductivity,

Quaternary oxypnictides,

Electrical resistivity,

Fourpoint probe,

Solid state reaction method.

ABSTRACT

The most prominent indicator of superconductivity is the superconducting transition temperature (T_c) that refers to three points. The onset transition temperature (T_{onset}) is defined as the deviation point away from the *ρ(T)* straight line (onset of the drop in resistivity). The midpoint transition temperature ($T_{midpoint}$) is defined as the temperature, where resistivity becomes 50% of its value at T_{onset}. The zero-resistance transition temperature ($T_{\rho\approx0}$) is defined as the temperature, in which the resistance is identically zero or only immeasurably small. These indicators of temperatures associated with some factors. In this article, the X-ray diffraction and electrical resistivity measurements of $LaO_{1-x}F_xFeGe$ samples are reported. This compound was successfully synthesized via a solid state reaction method with the presence of germanium Ge in the conduction layer. Furthermore, some factors affecting the superconducting transition temperature were studied, which are the F-doping dependence of T_{onset}, $T_{midpoint}$, and lattice parameters, and sintering temperature dependence of T_{onset}.

1 Introduction

Iron-based LnOFeAs phase is not a superconductor and displayed an anomalous change in the slope of ρ(T) resistivity measurement curve. The anomaly transition point related to the spin-density wave fluctuations and structural phase transition was at 150 (Kamihara et al., 2008), 145 (Chen et al., 2008), 155 (Prakash et al., 2010), 140 (Martinelli et al., 2008), 135 (Wang et al., 2008), and 124 K (Jun Li et al., 2008) for compounds LaOFeAs, CeOFeAs, PrOFeAs, SmOFeAs, GdOFeAs, and TbOFeAs, respectively. Conversely, nickel-based quaternary oxypnictides LaONiP and LaONiAs exhibited superconducting transition in resistivity measurements with critical transition temperature T_{onset}=4 K ($T_{\rho\approx0}$=2 K) (Watanabe et al. 2007, Tegel et al., 2008) and T_{onset}=2.4 K (Tρ≈0=2 K) (Watanabe et al., 2008), respectively.

Moreover, in iron-based 1111-phase, only the LaOFeP compound (Liang et al., 2007, Hamlin et al., 2008) was a superconductor at T_{onset}=5 K ($T_{\rho\approx0}$=3.2 K) (Kamihara et al., 2006).

Superconductivity could be obtained from LnOFeAs phase through replacement of O^{2-} with F^- (i.e., F-doping), with the resulting phase being the $LnO_{1-x}F_xFeAs$ compound. Superconducting transition temperature T_{onset} of $LaO_{1-x}F_xFeAs$ was at 17 (Dong et al., 2008), 28 (Dong et al., 2008), 24.6 (Gao et al., 2008), and 30 K (Kamihara et al., 2008) for x=0.03, 0.06, 0.10, and 0.11, respectively. The F-doping dependence of T_c and T_{onset} on $LaO_{1-x}F_xFeAs$ (Kamihara et al., 2008), after superconductivity appears, T_c is nearly unchanged up to x=0.14, and the highest T_c=26 K (T_{onset}= 30 K) is attained at the F-content x=0.11.

*Corresponding author:
E-mail: tar.ahmad@sebhau.edu.ly
DOI: https://doi.org/10.37375/sjfssu.v1i1.139

Replacement La in $LaO_{1-x}F_xFeAs$ compound with other rare earth elements (Ce, Pr, Nd, Sm, Eu, Gd, Tb, Dy, and Tm) led to superconductors with T_{onset} > 28 K. T_{onset}=42.5 (Prakash et al., 2009), 52 (Ren et al., 2008), 52 (Jia et al., 2008), 56.1 (Wang et al., 2010, Iida et al., 2013), 36.6 (Peng et al., 2008), 45.9 (Bos et al., 2008, Kuzmicheva et al., 2018), and 45.4 K (Bos et al., 2008) for compounds $CeO_{0.8}F_{0.2}FeAs$, $PrO_{0.89}F_{0.11}FeAs$, $NdO_{0.82}F_{0.18}FeAs$, $SmO_{0.8}F_{0.2}FeAs$, $GdO_{0.83}F_{0.17}FeAs$, $TbO_{0.8}F_{0.2}FeAs$, and $DyO_{0.9}F_{0.1}FeAs$, respectively. Two rare earth elements, Eu and Tm, did not display superconducting transition in resistivity measurements of $LnO_{0.84}F_{0.16}FeAs$ phase; instead, resistivity ρ(T) displayed metallic behavior (Gen-Fu et al., 2008).

Superconductivity in LnOFeAs phase can also be obtained by partially replacing the trivalent ion Ln^{3+} with a bivalent dopant, such as Sr^{2+}, Pb^{2+}, or a tetravalent dopant, such as Th^{4+} in the LnO layer. As a result, superconducting transition T_{onset} of superconductors Sr-doped $La_{0.87}Sr_{0.13}OFeAs$ (Wen et al., 2008) and Pb-doped $La_{8.0}Pb_{0.2}OFeAs$ (Che et al., 2008) was at 25.6 ($T_{\rho\approx0}$=15 K) and 11.6 K ($T_{\rho\approx0}$=9.7 K), respectively. In Th-doping, which provides the insulating layer with an extra positive charge, superconductors $Nd_{0.8}Th_{0.2}OFeAs$ (Xu et al., 2008), $Gd_{0.8}Th_{0.2}OFeAs$ (Wang et al., 2008), $Tb_{0.9}Th_{0.1}OFeAs$ (Jun Li et al., 2008), and $Tb_{0.8}Th_{0.2}OFeAs$ (Jun Li et al., 2008) were successfully synthesized, exhibiting transition temperature T_{onset} in resistivity measurements at 47, 56, 45, and 52 K, respectively, all higher than the recorded values for Sr- and Pb-doped compounds.

The third method of doping in the LnO layer consists of replacing the trivalent ion Ln^{3+} and monovalent ion F^- with two dopants, and is referred to as double doping. For K doping in $LaO_{1-x}F_xFeAs$ compound, the onset of superconducting transition was practically unaffected by the addition of K, with onset T_{onset} occurring at 26.20 and 26.45 K for $(La_{0.85}K_{0.15})(O_{0.85}F_{0.15})FeAs$ and $(La_{0.8}K_{0.2})(O_{0.8}F_{0.2})FeAs$, respectively (Prakash et al., 2008). Replacing potassium (K^{1+}) with Ce or Yb increased transition temperature T_{onset} to 29 K for $La_{0.2}Ce_{0.8}O_{0.9}F_{0.1}FeAs$ (Gen-Fu et al., 2008) and 31.3 K for $La_{0.9}Yb_{0.1}O_{0\cdot8}F_{0\cdot2}FeAs$ (Prakash et al., 2010).

Superconductivity can be also achieved by doping in the conduction layer MPn (M=transition metals, and Pn=pnictogen). For Co-doped $LaOFe_{1-x}Co_xAs$ samples, the T_{onset} was at 11.2, 14.3, and 6 K for x=0.05, 0.11, and 0.15, respectively (Sefat et al., 2008). Co-doping for $PrOFe_{1-x}Co_xAs$ samples showed T_{onset} at 4.7, 14.2, and 5.9 K for x=0.05, 0.1, and 0.15, respectively (Prakash et al., 2010). For $SmOFe_{1-x}Co_xAs$ samples, T_{onset} (=15.2 K) was unchanged at two levels of doping x=0.10 and 0.15 (Qi et al., 2008), whereas T_{onset} was affected by the change in doping from x=0.10 to x=0.15 for Co-doping in La-oxypnictide and Pr-oxypnictide samples. Ir-doped $SmOFe_{0.85}Ir_{0.15}As$ compounds provided the critical transition temperature T_{onset} close to 17.3 K (Chen et al., 2009), which is greater than that for Co-doping. In (Singh et al., 2009), researcher reported one case of increased transition temperature T_{onset} with doping in the conducting layer when $LaO_{0.8}F_{0.2}FeAs$ was synthesized with Sb-doping. The doping in this case was in both layers and led to the enhancement of transition temperature to 30.1 K for compound $LaO_{0.8}F_{0.2}FeAs_{0.95}Sb_{0.05}$. Singh et al. (Singh et al., 2014) prepared the $SmO_{0.88}F_{0.12}FeAs_{1-x}P_x$ compound with double-doping in both layers, and they observed a suppression in the superconducting transition temperature.

The critical superconducting transition temperature for 1111-oxyarsenide compounds is affected by a number of factors, mainly the density of conduction carriers in the insulating and conduction layers, which is altered with doping. Although hole or electron-doping suppressed the anomalous behavior to induce superconductivity, some phases did not show superconductivity: $La_{0.80}Sr_{0.20}OFeAs$ (T_{onset}=25.6 K for x=0.13) (Wen et al., 2008), $LaOFe_{0.80}Co_{0.20}As$ (T_{onset}=14.3 K for x=0.11) (Sefat et al., 2008), $PrOFe_{0.70}Co_{0.30}As$ (T_{onset}=14.2 K for x=0.10) (Prakash et al., 2010), $EuO_{0.84}F_{0.16}FeAs$, and $TmO_{0.84}F_{0.16}FeAs$ (Gen-Fu et al., 2008). For nonsuperconducting $La_{0.80}Ce_{0.20}OFeAs$ compound (Che et al., 2008), the doping was at the same oxidation state (La^{3+} was replaced with Ce^{3+}), and as a result, anomaly point T_{anom} still existed and appeared at 155 K.

Concentration and lattice parameters are also factors that affect superconducting transition temperature. Doping dependence of T_c, a, and c for hole-doped $La_{1-x}Sr_xOFeAs$ sample showed that a and c increased monotonously with Sr-doping concentration and a consequent increase in T_c. This expansion in lattice constants is because the radius of Sr^{2+} is larger than that of La^{3+} (Mu et al., 2008). In contrast with electron doping, T_c increased with the shrinkage of lattice parameters, whereby the electron-doped $SmO_{1-x}F_xFeAs$ sample showed that a and c decreased monotonously with the increase in F-doping concentration x in the range of $0 \leq x \leq 0.20$, and T_c increased with the increase in concentration x in the same range (Yang et al., 2009).

When hole doping was applied in the FeAs layer for $PrOFe_{1-x}Co_xAs$ sample, the lattice parameters decreased with the increase in Co concentration x ($0 < x < 0.3$), but T_c increased from 4.7 K for x=0.05 to 14.2 K for x=0.1. However, transition temperature T_c decreased with higher Co-doping concentration $x > 0.1$ (T_c=5.9 K for x=0.15, T_c=4 K for x=0.20 and 0.30) (Prakash et al., 2010). A similar behavior of doping dependence of T_c, a, and c in double-doped compound $La_{1-x}Ce_xO_{0.9}F_{0.1}FeAs$ (x=0, 0.2, 0.4, 0.6, and 0.8) was observed. Lattice parameters a and c slightly decreased with the change in Ce concentration (a=4.029˚A and c= 8.726˚A at x=0, and a=3.994˚A, c=8.598˚A at x=0.8) whereas T_c increased from 24.99 K at x=0 to 29 K at

x=0.8 with the presence of an abnormal point in the phase diagram $T_c(x)$ at x=0.60 (T_c= 28.01 K) (Che et al., 2008). In contrast to the case of $La_{1-x}Ce_xO_{0.9}F_{0.1}FeAs$, the transition temperature for $LaO_{0.8}F_{0.2}FeAs_{1-x}Sb_x$ compound (double-doping in both layers) decreased from 30.1 K at Sb concentration x=0.05 to 28.6 K at Sb concentration x=0.10. However, by increasing the doping level from x=0.05 to x=0.10, lattice parameters *a* and *b* increased because of the larger size of the Sb ion compared with the As ion (Singh et al., 2009).

The effect of sintering temperature on the superconducting properties of $SmO_{0.8}F_{0.2}FeAs$ was reported by Wang et al. (Wang et al., 2010). Onset transition temperature of the samples sintered at 850 ºC was 53.5 K. Samples sintered at 1000 ºC displayed a transition temperature of 56.1 K whereas those sintered at 1200 ºC displayed a transition temperature of 50.8 K. Samples sintered at 1000 ºC had the highest transition temperature, the lowest *ρ(T)*, and the highest residual resistivity ratio *ρ*(300 K)/*ρ*(57 K), indicating low impurity scattering and enhanced carrier density (Wang et al., 2010). However, the highest onset transition temperature was related to specific sintering temperature, where T_{onset} was 41 K for $SmO_{0.7}F_{0.3}FeAs$ sample sintered by a two-step approach at 500 ºC for 15 h and then at 900 ºC for 40 h (Wang et al., 2010), and it was 54.6 K for sintering at 1160 ºC for 40 h (Ma et al., 2008).

2 Materials and Methods

A polycrystalline sample of $LaO_{1-x}F_xFeGe$ (x=0, 0.11, 0.13) was synthesized by heating a mixture of high-purity starting materials (i.e., dehydrated La_2O_3, Fe, LaF_3 powders, Ge grains, and La pieces), which were weighed with stoichiometric amounts of molar mass according to nominal compositions in the following formula for undoped compound LaOFeGe:

$$La+3Fe+3Ge+La_2O_3 \rightarrow 3LaOFeGe \quad (1)$$

For F-doped compound, the stoichiometric formula is:

$$(1+x)\ La + 3Fe + 3Ge + (1-x)\ La_2O_3 + x\ LaF_3 \rightarrow 3LaO_{1-x}F_xFeGe \quad (2)$$

The present method involves two steps. First, 2 g of the starting materials (Table 1) were mixed thoroughly, pressed into a pellet 13 mm in diameter through a manual hydraulic press under a load of 12 metric tons, and then placed between two boats of Tungsten inside a chamber evacuated at 10^{-5} Torr. The pellet was heated at high current by electrical poles at both ends of the boats. Current was applied in the following order: 120 A for 2 h, 160 A for 3 h, and 100 A for 2 h. The product was smashed and grinded at each electric current set-up to make it more homogeneous and was then pressed into a pellet. Second, the final pellet was sealed in an evacuated silica tube at 10^{-3} Torr and then annealed in a furnace under the following conditions: 500 °C for 12 h, 600 °C for 24 h, and 800 °C for 12 h. Then, the pellet was cooled to room temperature gradually. In heat treatments, an electric current of 160 A through the boats (heating source) causes a temperature of around 1000 ºC, which is appropriate for solid-state reaction with consideration for the comparison of melting-point temperatures of the starting materials. Heat treatment for a long time was conducted in the furnace, where the samples were first heated at 500 ºC and then sintered at a temperature range of 600 ºC (i.e., 2/3 of the melting point of La and Ge) to 800 ºC (i.e., 6/7 of the melting point of La and Ge), which is the most suitable temperature range to obtain an adequately annealed sample. Sample preparation, except for the annealing, was conducted in a glove box under high-purity Nitrogen. The samples were cut and polished into a thin bar shape 6 mm long, 1 mm wide, and 1 mm thick for use in measuring DC resistivity.

Table 1. Stoichiometric amounts for starting materials of nominal compositions $LaO_{1-x}F_xFeGe$ according to formulas 1 and 2.

	Starting materials (gm)				
Content X	La Purity: 99.9%	Fe 99.9%	Ge 99.999%	La_2O_3 99.5%	LaF_3 99%
0	0.3268	0.3941	0.5127	0.7664	0
0.11	0.3623	0.3937	0.5121	0.6813	0.0506
0.13	0.3688	0.3936	0.5119	0.6659	0.0598

3 Results

Figure 1 shows the X-ray diffraction patterns of $LaO_{1-x}F_xFeGe$ (x=0, 0.11, 0.13). All main peaks of the samples can be well determined based on the tetragonal oxypnictide structure LnOMPn, which is indexed to the tetragonal ZrCuSiAs-type structure reported previously (Kamihara et al., 2008, Liang et al., 2007, Hamlin et al., 2008, Kamihara et al., 2006, Che et al., 2008, Chen et al., 2008, Gao et al., 2008). A small amount of the impurity phases LaOF and Fe_2Ge were detected. Secondary phases were observed in most LnOMPn oxypnictide phases (Kamihara et al., 2008, Gao et al., 2008).

The lattice parameters *a* and *c* (table 2) were calculated by the least-squares method of the measured peak positions using equation:

$$\sin^2(\theta_{hkl}) = \frac{\lambda^2}{4}\left(\frac{h^2+k^2}{a^2} + \frac{l^2}{c^2}\right) \quad (3)$$

For electrical resistivity measurements *ρ(T)*, table 2 shows the F-doping dependence of T_{onset} ,

$T_{midpoint}$ and lattice parameters for $LaO_{1-x}F_xFeGe$ samples. The effect of sintering temperature on the transition temperature of F-content samples as shown in table 3.

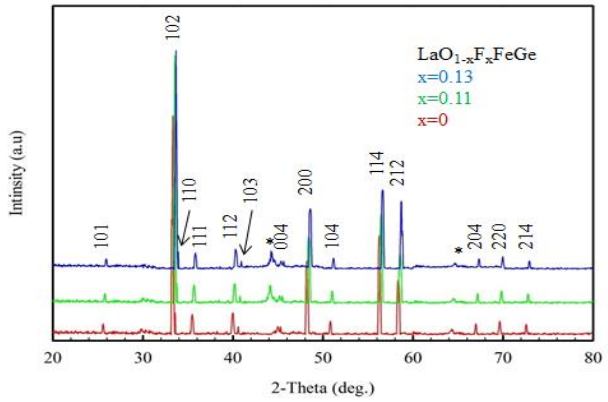

Figure 1. X-ray diffraction pattern of the nominal $LaO_{1-x}F_xFeGe$ samples. The impurity phases LaOF and Fe_2Ge are marked by an asterisk.

Table 2. F-doping dependence of T_{onset} , $T_{midpoint}$, and lattice parameters for $LaO_{1-x}F_xFeGe$ compound.

F content	T_{onset}	$T_{midpoint}$	a [nm]	c [nm]
0	-	-	0.380686	0.815796
0.11	19.7	18.8	0.38178	0.81367
0.13	21.3	20.6	0.379226	0.808415

Table 3. Sintering temperature dependence of transition temperature for $LaO_{1-x}F_xFeGe$ compound.

Sintering temperature [K]	800	850	900
F content		T_{onset} [K]	
x=0.11	19.7	21.2	20.3
x= 0.13	21.3	22.1	22.3

4 Discussion

The lattice parameters of LaOFeGe, a=0.380686 nm and c=0.815796 nm, were found to be smaller than those of the LnOFeAs family reported previously (Kamihara et al., 2008, Chen et al., 2008, Wang et al., 2008, Bos et al., 2008, Chen et al., 2009). Considering that F- has a smaller ionic size than O2-, the peaks shifted to the right-hand side for the F-doped samples. In comparison with the undoped sample, the lattice parameters of F-doped samples decrease with greater F-doping concentration. This result indicates the successful substitution of O by F. For x=0.11, a=0.381786 nm, and c=0.813679 nm and for x=0.13, a=0.379226 nm, and c=0.808415 nm, the c-lattice parameter decreased with the increase in x content (x=0, 0.11, 0.13). By comparing the *a*-lattice parameter with the increase in x content for all samples with each other, the *a* (x=0.13) < *a* (x=0) and *a* (x=0.13) < *a* (x=0.11). However, an expansion in the *a*-lattice parameter was observed, *a* (x=0.11) > *a* (x=0), which is attributed to the impurity phase stacking along the *a*-axis of the x=0.11 phase.

As shown in table 2, T_{onset} and $T_{midpoint}$ increase slightly with increasing F-doping content. For table 3, onset transition temperature of the sample x=0.11 sintered at 800ºC was 19.7 K. Sample sintered at 850ºC displayed a transition temperature of 21.2 K whereas those sintered at 900ºC displayed a transition temperature of 20.3 K. Samples (x=0.11 and 0.13) sintered at 850 ºC had the highest transition temperature.

5 Conclusion

The quaternary compound $LaO_{1-x}F_xFeGe$ were prepared using a two-step solid-state reaction method because the method gives a more homogeneous sintering of the compound in two separate steps of heat treatment. Moreover, this method enables the formation of the initial binary phases when most of the raw materials are direct chemical elements with one or two compounds. The crystal structure of tetragonal LnOMPn oxypnictide (Ln=rare-earth, M=transition metals, and Pn=pnictogen) is characterized by the lattice parameters *a* and *c*. The content x, ionic size of the dopant, and sintering temperature, all affect lattice parameters.

The majority of undoped tetragonal LnOMPn oxypnictides are not superconductors, and only some phases, such as LaOFeP and LaONiP, exhibit a transition to the superconducting state. According to the available data, superconductivity occurs exclusively in oxyarsenide phases under the required condition of electron or hole doping. The previous experimental material suggests that a number of factors affect the critical transition temperature for superconducting 1111 oxypnictides. Doping levels, as well as external factors such as sintering temperature all affect superconductivity. In general, no direct evidence or rule has been discussed to predict the transition behavior in resistivity after doping. However, certain factors cause changes in the interactions among electrons (i.e., electron scattering and electron-phonon scattering).

Conflict of interest: The authors declare that there are no conflicts of interest.

References

Y. Kamihara, T. Watanabe, M. Hirano and H. Hosono. (2008) Iron-based layered superconductor La[$O_{1-x}F_x$]FeAs

(x=0.05-0.12) with T_c=26 K, Journal of the American Chemical Society. 130(11), pp.3296-3297.

G. F. Chen, Z. Li, D. Wu, G. Li, W. Z. Hu, J. Dong, P. Zheng, J. L. Luo and N. L. Wang. (2008) Superconductivity at 41 K and its competition with spin-density-wave instability in layered $CeO_{1-x}F_xFeAs$. Physical Review Letters. 100(24), pp.247002.

J. Prakash, S. J. Singh, D. Das, S. Patnaik and A. K. Ganguli. (2010) New oxypnictide superconductors: $PrOFe_{1-x}Co_xAs$. Journal of Solid State Chemistry. 183(2), pp.338-343.

A. Martinelli, M. Ferretti, P. Manfrinetti, A. Palenzona, M. Tropeano, M. R. Cimberle, C. Ferdeghini, R. Valle, C. Bernini, M. Putti and A. S. Siri. (2008) Synthesis, crystal structure, microstructure, transport and magnetic properties of SmFeAsO and $SmFeAs(O_{0.93}F_{0.07})$. Superconductor Science and Technology. 21(9), pp.095017.

C. Wang, L. Li, S. Chi, Z. Zhu, Z. Ren, Y. Li, Y. Wang, X. Lin, Y. Luo, S. Jiang, X. Xu, G. Cao and Z. Xu. (2008) Thorium-doping-induced superconductivity up to 56 K in $Gd_{1-x}Th_xFeAsO$. Europhysics Letters. 83(6), pp.67006.

L. -Jun Li, Y. -Ke Li, Z. Ren, Y. -Kang Luo, X. Lin, M. He, Q. Tao, Z. -Wei Zhu, G. -Han Cao and Z. -An Xu. (2008) Superconductivity above 50 K in $Tb_{1-x}Th_xFeAsO$. Physical Review B. 78(13), pp.132506.

T. Watanabe, H. Yanagi, T. Kamiya, Y. Kamihara, H. Hiramatsu, M. Hirano and H. Hosono. (2007) Nickel-based oxyphosphide superconductor with a layered crystal structure LaNiOP. Inorganic Chemistry. 46(19), pp.7719-7721.

M. Tegel, D. Bichler and D. Johrendt. (2008) Synthesis, crystal structure and superconductivity of LaNiPO. Solid State Sciences. 10(2), pp.193-197.

T. Watanabe, H. Yanagi, Y. Kamihara, T. Kamiya, M. Hirano and H. Hosono. (2008) Nickel-based layered superconductor LaNiOAs. Journal of Solid State Chemistry. 181(8), pp.2117-2120.

C. Y. Liang, R. C. Che, H. X. Yang, H. F. Tian, R. J. Xiao, J. B. Lu, R. Li and J. Q. Li. (2007) Synthesis and structural characterization of LaOFeP superconductors. Superconductor Science and Technology. 20(7), pp.687-690.

J. J. Hamlin, R. E. Baumbach, D. A. Zocco, T. A. Sayles and M. B. Maple. (2008) Superconductivity in single crystals of LaFePO. Journal of Physics: Condensed Matter. 20(36), pp.365220.

Y. Kamihara, H. Hiramatsu, M. Hirano, R. Kawamura, H. Yanagi, T. Kamiya and H. Hosono. (2006) Iron-based layered superconductor: LaOFeP. Journal of the American Chemical Society.128(31), pp.10012-10013.

J. Dong, H. J. Zhang, G. Xu, Z. Li, G. Li, W. Z. Hu, D. Wu, G. F. Chen, X. Dai, J. L. Luo, Z. Fang and N. L. Wang. (2008) Competing orders and spin-density-wave instability in $La(O_{1-x}F_x)FeAs$. Europhysics Letters. 83(2), pp.27006.

Z. Gao, L. Wang, Y. Qi, D. Wang, X. Zhang and Y. Ma. (2008) Preparation of $LaFeAsO_{0.9}F_{0.1}$ wires by the powder-in-tube method. Superconductor Science and Technology. 21(10), pp.105024.

J. Prakash, S. J. Singh, S. Patnaik and A. K. Ganguli. (2009) Superconductivity in $CeO_{1-x}F_xFeAs$ with upper critical field of 94 T. Physica C. 469(2-3), pp.82-85.

Z. A. Ren, J. Yang, W. Lu, W. Yi, G. C. Che, X. L. Dong, L. L. Sun and Z. X. Zhao. (2008) Superconductivity at 52 K in iron based F doped layered quaternary compound $Pr[O_{1-x}F_x]FeAs$. Materials Research Innovations. 12(3), pp.105-106.

Y. Jia, P. Cheng, L. Fang, H. Luo, H. Yang, C. Ren, L. Shan, C. Gu, and Hai-Hu Wen. (2008) Critical fields and anisotropy of $NdFeAsO_{0.82}F_{0.18}$ single crystals. Applied Physics Letters. 93(3), pp.032503.

C. Wang, Z. Gao, L. Wang, Y. Qi, D. Wang, C. Yao, Z. Zhang and Y. Ma. (2010) Low-temperature synthesis of $SmO_{0.8}F_{0.2}FeAs$ superconductor with T_c=56.1 K. Superconductor Science and Technology. 23(5), pp.055002.

K. Iida, J. Hanisch, C. Tarantini, F. Kurth, J. Jaroszynski, S. Ueda, M. Naito, A. Ichinose, I. Tsukada, E. Reich, V. Grinenko, L. Schultz, B. Holzapfel. (2013) Oxypnictide SmFeAs(O,F) superconductor: a candidate for high-field magnet applications, Scientific Reports. 3:2139, pp.1-5.

C. Peng, F. Lei, Y. Huan, Z. XiYu, M. Gang, L. HuiQian, W. ZhaoSheng and W. HaiHu. (2008) Superconductivity at 36 K in gadolinium-arsenide oxides $GdO_{1-x}F_xFeAs$. Science China Physics, Mechanics and Astronomy. 51(6), pp.719-722.

J.-W. G. Bos, G. B. S. Penny, J. A. Rodgers, D. A. Sokolov, A. D. Huxley and J. P. Attfield. (2008) High pressure synthesis of late rare earth RFeAs(O,F) superconductors; R=Tb and Dy. Chemical Communications. 31, pp.3634-3635.

T. Kuzmicheva, A. Sadakov, A. Muratov, S. Kuzmichev, Y. Khlybov, L. Kulikova, Y. Eltsev. (2018) Magnetic, superconducting and electron-boson properties of GdO(F)FeAs oxypnictides, Physica B: Condensed Matter. 536, pp.793-797.

C. Gen-Fu, L. Zheng, W. Dan, D. Jing, L. Gang, H. Wan-Zheng, Z. Ping, L. Jian-Lin and W. Nan-Lin. (2008) Element substitution effect in transition metal oxypnictide $Re(O_{1-x}F_x)TAs$ (Re=rare earth, T=transition metal). Chinese Physics Letters. 25(6), pp.2235-2238.

Hai-Hu Wen, G. Mu, L. Fang, H. Yang and X. Zhu. (2008) Superconductivity at 25 K in hole doped ($La_{1-x}Sr_x$)OFeAs. Europhysics Letters. 82(1), pp.170

. C. Che, L. Wang, Z. Chen, C. Ma, C. Y. Liang, J. B. Lu, H. L. Shi, H. X. Yang and J. Q. Li. (2008) Superconductivity in ($La_{1-x}Ce_x$)($O_{0.9}F_{0.1}$)FeAs and ($La_{1-x}Pb_x$)OFeAs. Europhysics Letters. 83(6), pp.66005.

M. Xu, F. Chen, C. He, H-W. Ou, J-F. Zhao and D-L. Feng. (2008) Synthesis of a new member in iron-based layered superconductor: $Nd_{0.8}Th_{0.2}$OFeAs with T_c=38K. Chemistry of Materials. 20(23), pp.7201-7203.

J. Prakash, S. J. Singh, S. L. Samal, S. Patnaik and A. K. Ganguli. (2008) Potassium fluoride doped LaOFeAs multi-band superconductor: Evidence of extremely high upper critical field. Europhysics Letters. 84(5), pp.57003.

J. Prakash, S. J. Singh, S. Patnaik and A. K. Ganguli. (2010) Superconductivity at 31.3 K in Yb-doped La(O/F)FeAs Superconductors. Journal of Chemical Sciences. 122(1), pp.43-46.

A. S. Sefat, A. Huq, M. A. McGuire, R. Jin, B. C. Sales, D. Mandrus, L. M. D. Cranswick, P. W. Stephens and K. H. Stone. (2008) Superconductivity in $LaFe_{1-x}Co_xAsO$. Physical Review B. 78(10), pp.104505.

Y. Qi, Z. Gao, L. Wang, D. Wang, X. Zhang and Y. Ma. (2008) Superconductivity in Co-doped SmFeAsO, Superconductor Science and Technology. 21(11), pp.115016.

Y. L. Chen, C. H. Cheng, Y. J. Cui, H. Zhang, Y. Zhang, Y. Yang and Y. Zhao. (2009) Ir doping-induced superconductivity in the SmFeAsO system. Journal of the American Chemical Society. 131(30), pp.10338-10339.

S. J. Singh, J. Prakash, S. Patnaik and A. K. Ganguli. (2009) Enhancement of the superconducting transition temperature and upper critical field of $LaO_{0.8}F_{0.2}$FeAs with antimony doping. Superconductor Science and Technology. 22(4), pp.045017.

S. J. Singh, Jun-ichi Shimoyama, A. Yamamoto, H. Ogino and K. Kishio. (2014) Effects of phosphorous doping on the superconducting properties of SmFeAs(O,F), Physica C: Superconductivity and its Applications. 504, pp.19-23.

G. Mu, L. Fang, H. Yang, X. Zhu, P. Cheng and Hai-Hu Wen. (2008) Doping dependence of superconductivity and lattice constants in hole doped $La_{1-x}Sr_x$FeAsO. Journal of the Physical Society of Japan. 77, pp.15-18.

J. Yang, Z.-An Ren, G.-Can Che, W. Lu, X.-Li Shen, Z.-Cai Li, W. Yi, X.-Li Dong, Li-Ling Sun, F. Zhou and Z.-Xian Zhao. (2009) The role of F-doping and oxygen vacancies on the superconductivity in SmFeAsO compounds. Superconductor Science and Technology. 22(2), pp.025004.

L. Wang, Y. Qi, D. Wang, Z. Gao, X. Zhang, Z. Zhang, C. Wang and Y. Ma. (2010) Low-temperature synthesis of $SmFeAsO_{0.7}F_{0.3-\delta}$ wires with a high transport critical current density. Superconductor Science and Technology. 23(7), pp.075005.

Y. Ma, Z. Gao, L. Wang, Y. Qi, D. Wang and X. Zhang. (2008) One step synthesis of $SmO_{1-x}F_x$FeAs bulks with T_c=54.6 K: High upper critical field and critical current density. arXiv:0806.2839.

G. F. Chen, Z. Li, G. Li, J. Zhou, D. Wu, J. Dong, W. Z. Hu, P. Zheng, Z. J. Chen, H. Q. Yuan, J. Singleton, J. L. Luo and N. L. Wang. (2008) Superconducting properties of the Fe-based layered superconductor $LaFeAsO_{0.9}F_{0.1-\delta}$. Physical Review Letters. 101(5), pp.057007.

Z. Gao, L. Wang, Y. Qi, D. Wang, X. Zhang and Y. Ma. (2008) Preparation of LaFeAsO0.9F0.1 wires by the powder-in-tube method. Superconductor Science and Technology. 21(10), pp.105024.

Scientific Journal for the Faculty of Science-Sirte University
(SJFSSU)
Journal home page: http://journal.su.edu.ly/index.php/JSFSU/index

Morphological study of the Effects of Caffeine Beverages Can Cause Birth Defects on Swiss White Mice Embryos

Arwa Adress Alnuimy[1], Hani Mal Allah Hamodi* [2]

[1]*Biology Department, College of Education for Pure Sciences, Mosul University, Mosul, Iraq*

[2]*Biology Department, College of Education for Pure Sciences, Mosul University, Mosul, Iraq*

ARTICLE INFO

Article history:

Received 5 August 2021

Received in revised form 8 September 2021

Accepted 30 September 2021

Keywords:

Embryos,

Malformations,

Caffeine beverages,

Mice embryos.

ABSTRACT

The current study was conducted to identify the effects of different doses of Arabic coffee, black tea and Coca-Cola syrup on the possibility of birth defects in Swiss white mice embryos. (25) pregnant female mice were used in the study, divided into five experimental groups, including the control group dosed with distilled water, and four experimental groups were dosed with concentrations (4000-2500-2000-1000) mg/kg body weight for Arabic coffee and black tea and (2,3,4,6 ml/kg) for Coca-Cola syrup; once a day, from the seventh day until the eighteenth day of pregnancy.

The results of the current study showed cases of abortion and fetal death at varying degrees and many abnormalities in white mouse embryos due to the different concentrations of the beverages used were characterized by the appearance of elongated and enlarged embryos. The elongation and deformation of the fetus, And the embryos mutated. Small embryos folded like a ball and curved in the shape of letter C, and the severity of the deformities increased by the appearance of mutated embryos resembling the body of a fish and deformed embryos similar to a water mermaid and not fully developed and the appearance of the head in the shape of a blurred triangle, as well as forward with a pointed end resembling a bird's beak, and brain deformation through depression in the posterior cranial region of the skull, and for the first time a new deformation is a cerebral Meningomyelocele in the form of a cystic tumor in the posterior brain region.

1 Introduction

In most countries around the world, social beverages are now one of the most popular drinks, but how does it look when consumed in large amounts during pregnancy, causing miscarriages, damages, deformities, and birth defects (AL-Rasheedi,2009). Currently, commercial advertisements in various media outlets are widely observed by companies and factories that produce such drinks strikingly in order to highlight their nutritional importance, which has caused a large number of people to over-consume them without any reference to the negative effects of unusually using them. Caffeine increases the amount of energy in the body and stimulates the muscles to oxidize fat and protein (Yen *et al*.,2005). Caffeine crosses the placental wall to the fetus and increases the likelihood of spontaneous abortion, as well as a lack of fetal growth and congenital malformations within the womb, which sometimes leads to fetal loss and death (Weng and Odouli,2008). There are very few studies on the effect of caffeine beverages on fetus levels and fetal development, especially during pregnancy (Bech *et al*.,2005). Three types of coffee beverages, Arabic coffee, black tea and Coca-Cola syrup, have been selected in the current study. Many studies have focused on the benefits and importance of these drinks in the first place (Greenberg *et al*.,2006). Very small studies (Bech *et al*.,2007).

Corresponding author:
E-mail: arwabio2020@uomosul.edu.iq
DOI: https://doi.org/10.37375/sjfssu.v1i1.65 **SJFSSU 2021**

This matter has stopped embryologists from paying attention to studying the various deformities that occur during the embryonic development process, their types, causes and mechanisms of formation under the name of Congenital malformations. Teratology (Ashmead,2003), that many pregnant women frequently drink coffee and tea and over-drink various soft drinks without concern. The health damage caused by these high doses of used drinks. The fact that women who drank four or more cups of coffee increased the function of the placenta and thus the death of the fetus (CARE,2008) (Bierrnacki *et al*.,2000). Given the lack of studies to clarify the effects of caffeine beverages on birth defects, this study was conducted. Therefore, the aim of study to identify the teratogenic effects of caffeinated beverages on the fetuses of pregnant albino mice

2. Materials and Methods

Mice were selected at (9-12) weeks of age for both sexes, their average weight was (2 ± 23) g, and the mice were healthy and healthy. The mice were placed under standard laboratory conditions throughout the study period. Females ready for fertilization have been placed with males at the rate of one male with three females in each cage. And the fertilization was confirmed by the observation of the vaginal plug in the morning of the following day. The date of mating is day zero of pregnancy, and the next day is the first day of mating (10).

2.1 Drinks Used

I used Arabic coffee that was bought from the local market. The aqueous solution was prepared for coffee by dissolving (1-4) grams of coffee in (50) ml of distilled water, boiling the solution for two minutes and

stirring continuously to simulate what is being prepared and used by humans, use caffeine black tea purchased from the local market and prepare the aqueous solution of black tea by boiling (1-4) grams of black tea in (50) ml of distilled water And boiling the solution for three minutes, as a simulation of what is prepared and used by humans, as for the Coca-Cola drink, is to use a ready-made drink packed in 330 ml metal cans.

2.3 Concentrations used

(25) pregnant female mice, which were divided into five groups and included in the control group and were dosed with distilled water, and four experimental groups were dosed with an aqueous solution of Arabica coffee at an increase in body weight (4000,2500,2000,1000) mg/kg In comparison to the study's median lethal dose (LD50) of (5 g / kg body weight) orally (43.5 mg caffeine / kg) which was reached through this study, Black tea with progressive concentrations (4000,2500,2000,1000) mg/kg body weight in comparison to (LD50) and its amount (6 g/kg body weight) orally (39 mg caffeine / kg), which was achieved in this study and Coca-Cola syrup, the concentrations used are (2 ml, 3 ml, 4 ml, 6 ml) In comparison to the median lethal dose (LD50) of (200 ml/kg body weight) orally (0.86 mg caffeine/kg) obtained in this research, daily and once orally with a gavage absorbent needle starting on the seventh day of pregnancy (Organogenesis stage) until the 18th day of pregnancy (The day of the autopsy).

2.2 Experimental Design

Table 1 Shows the experimental design

Dosing period	Groups	Arabic coffee concentrate: mg / kg	Black tea concentrate: mg / kg	Coca-Cola syrup concentrate ml / kg	The number of potions available	The number of mice
An oral dose of The seventh day to the eighteenth day of pregnancy	**The control**	**Distilled water**	**Distilled water**	**Distilled water**	**11**	**5**
	Experimental (1)	1000	1000	2	11	5
	Experimental (2)	2000	2000	3	11	5
	Experimental (3)	2500	2500	4	11	5
	Experimental (4)	4000	4000	6	11	5

3. Results

The results of the study showed the incidence of partial and total abortion to varying degrees. The results of the current study showed miscarriage and fetal death at varying degrees in experimental groups dosed with the drinks used, as observed when aqueous solution of

Arabic coffee was administered at a concentration of 4000 mg/kg body weight; the rate of abortion was 33 per cent and the death of some pregnant mice on the 15th day of pregnancy. The experimental group fed an aqueous solution of black tea at a concentration of 4000 mg/kg of body weight had a 29 percent miscarriage rate. On the 14th day of pregnancy, several pregnant mice had partial miscarriages and died.used, the current study found several abnormalities in white mouse embryos due to the various concentrations of the drinks use.

Figure a: embryo for control group

Figure b: The embryo of a deformed mouse is undefined. Dosed with an aqueous solution of Arabic coffee containing 4000 mg/kg body weight.

In terms of the findings of the study of abnormalities in embryos at various doses of the drinks used, the current study found several abnormalities in white mouse embryos due to the various concentrations of the drinks used. The embryos were elongated and enlarged, the fetus was elongated and deformed, and the embryos were mutated (Figures b, c).

Figure c: Completely mutated mouse embryo. Dosed with aqueous solution of Arabic coffee at a concentration of 4000 mg/kg of body weight.

Indicating that regular dosing of the aqueous solution of black tea caused deformities in pregnant mouse embryos and it curved in the shape of the letter C, and the emergence of mutated embryos that resemble the body of a fish (Figure d).

Figure d: A completely mutant mouse embryo with a fish-like body is shown from the front. Dosed with a 4000 mg/kg body weight concentration of black tea aqueous solution

Whereas the results showed that when dosed with Coca-Cola syrup, the percentage of mutilated embryos was different from what it is in coffee and tea, achieving (37-90 %) at concentrations of 3,4,6 ml/kg of body weight, and it was represented by the appearance of deformed embryos that looked like a water mermaid (Figure e) and distorted metamorphosed embryos (Figure f).

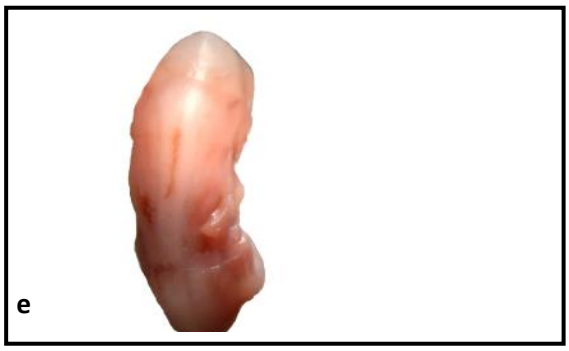

Figure e: A malformed water nymph-like mouse fetus missing front and hind limbs is seen from the back. Coca-Cola was given at a concentration of 4 mL per kilogram of body weight.

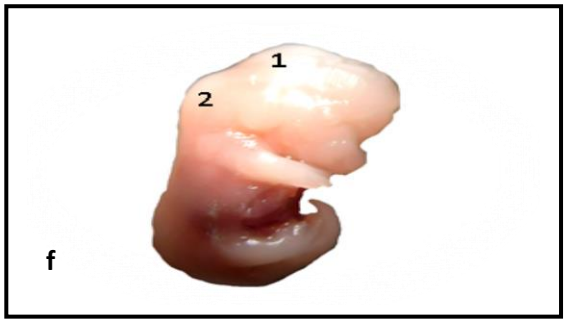

Figure f: A mutant mouse fetus with ischemic meningocele (1) and myelomeningocele in the dorsal anterior region is shown in a lateral view (2). Coca-Cola syrup was used as a dosing agent. 6ml per kilogram of body weight.

Results also showed small, deformed, mutated and incomplete embryos when dosed at a concentration of 6 ml/kg of body weight of Coca-Cola syrup ,Results also showed that the head was deformed by 75 %-85.5 % when dosed with an aqueous solution of Arabic coffee, and that the appearance of a cleft lip (Figure g) The appearance of the head in the form of a blurred triangle (Figure h)

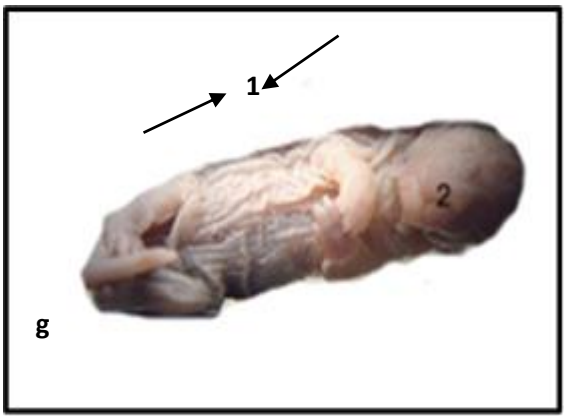

Figure g: Anterior view of a white mouse fetus reveals that the fetus appears elongated and enlarged (1), cleft lip (CL) (2). Dosed with an aqueous solution of Arabic coffee containing 2000 mg / kg body weight

Figure h: The head of a malformed mouse embryo stopped developing and took on an unclear triangular appearance. Dosed with 4000 mg of Arabic coffee per kg of body weight in an aqueous solution.

It reflects congestion and enlargement of the head in comparison to the rest of the body, distortion of the facial features of the nose, bulging eyes, and hemorrhage in the brain region when dosing with an aqueous solution of black tea and deformation of the head by (70%) (Figure i).

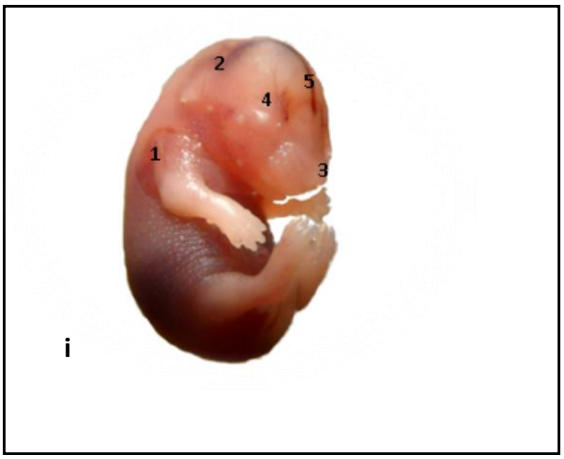

Figure i: Fetal curvature (1), congestion (CON) and enlargement of the head (2), deformation of nasal facial features (3), exophthalmos (4), and bleeding (BL) in the brain area (5) are all seen in this lateral view of a tiny white mouse fetus. Aqueous black tea solution at a concentration of 1000 mg / kg of body weight was given.

In addition to the formation of a head with a pointed end that resembles the beak of a bird, the brain is deformed by depression in the posterior cranial region of the skull (Figure k). Whereas, the severity of phenotypic head anomalies, when taken with Coca-Cola syrup, increased to a higher rate of 88% and was represented for the first time by the development of a new malformation, which is a cerebral meningocele in the form of a cystic tumor in the posterior brain region (Figure m), Compared to the control group (Figure a).

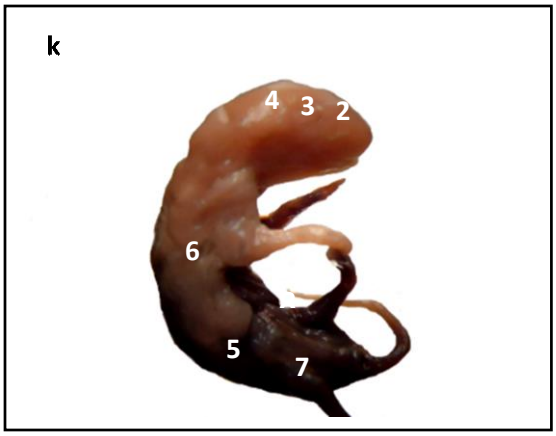

Figure k: Lateral figure of a white mouse embryo displaying round head with pointed end (1), occlusion of the eyes (2), loss of the auricle (3), posterior cranial depression (4), skin deformity and laxity (5), skeletal malformation, haemorrhage (7), abdominal atrophy and dissolution (8). At a concentration of 4000 mg / kg of body weight in an aqueous solution of blackte

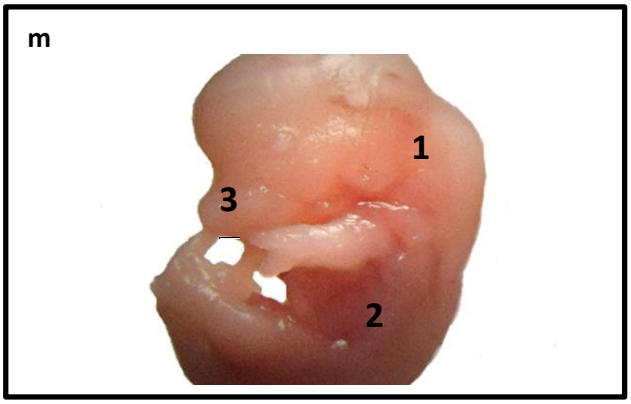

Figure m: Deformation and convexity of the trunk, differentiation of a congested cystic tumor (1), hyperemia of the dorsal area (2), and deformation and enlargement of the nasal characteristics are all visible in this lateral figure of a malformed mouse fetus (3). Coca-Cola was given at a concentration of 4 mL per kilogram of body weight.

4. Discussion

The study's findings revealed varied degrees of partial and entire abortion. The present study's findings revealed varying degrees of miscarriage and fetal mortality in experimental groups given the drinks. Excessive coffee intake and its caffeine content, which occurred at higher rates than other beverages, resulted in a doubling of the risk to the fetus within the uterus and a rise in the incidence of spontaneous and complete abortion during pregnancy (Hey ,2007), which could be due to the increase in contractions induced by stimuli containing caffeine. (Ullman *et al*., 1992).

The current study discovered several abnormalities in white mouse embryos due to various concentrations of the drinks used. The embryos were elongated and enlarged, the fetus was elongated and deformed, and the embryos were mutated, according to the findings of the study of abnormalities in embryos at various doses of the drinks used these findings backed up what was previously stated (Ormerod ,2001). Regular dosing of an aqueous solution of black tea produced abnormalities in pregnant mouse embryos, according to the findings. It curled in the shape of the letter C, as well. And the appearance of mutant embryos that resemble a fish's body and the reason may be attributed to the amount of caffeine in excessive doses of black tea, as indicated by the emergence of mutated embryos that resemble the body of (Grosso and Bracken,2005). When dosed with Coca-Cola syrup, the consequence was the emergence of malformed embryos that resembled a water mermaid, and distorted metamorphosed embryos. This may be due to the effect of Coca-Cola syrup, which contains caffeine in inhibiting growth during the stage of organogenesis, causing a lack of growth (Jana *et al.*,1994), or perhaps explaining the reason for increased fetal resorption and stunted growth of the fetus during the period of organogenesis on the sixth day of pregnancy (Al-Mamouri,2001), When Coca-Cola syrup was dosed at a concentration of 6 ml/kg of body weight, the results revealed tiny, malformed, mutated, and incomplete embryos and the cause may be attributed to damage to developing placenta that begins to function on the ninth day of pregnancy. Decreases in the exchange of nutrients between the fetus and the mother and reduces the process of protein building in the embryos, leading to delayed growth, low weights and the appearance of small embryos (Padmanabhan *et al*.,1981).

When given an aqueous solution of Arabic coffee, the head was deformed by 75 percent to 85.5 percent, and the appearance of a cleft lip was also seen this was similar to that indicated by (Matijasevich *et al*.,2005). The head appears to be in the shape of a blurring triangle and this combined with what the researcher pointed out (Hammoudi, 2005). When given an aqueous solution of black tea, it causes congestion and growth of the head in relation to the rest of the body, distortion of the facial characteristics of the nose, bulging eyes, and hemorrhage in the brain region, as well as deformation of the skull (70 %). The brain is deformed by depression in the posterior cranial region of the skull, in addition to the creation of a head with a pointed end that resembles a bird's beak, and that's in line with what reported in Fazal and Jalali, 2002.

When combined with Coca-Cola syrup, the severity of phenotypic head malformations grew to an 88 percent rate, which was represented for the first time by the development of a novel malformation, a cerebral meningocele in the shape of a cystic tumor in the posterior brain region this perhaps the explanation is due to the combination of maternal consumption of Caffeine-containing stimuli and the risk of developing brain myeloma (Rogwei *et al*., 2011).

5. Conclusion

The study showed that caffeinated drinks have congenital anomalies on the fetus and the pregnant mother should be careful when consuming.

Acknowledgements

This work was supported by the department of biology, college of education for pure sciences, Mosul university.

Conflict of interest: The authors declare that there are no conflicts of interest.

References

Al-Mamouri, Rafah, Hani Abdel-Latif. (2001). The effect of alcohol on implantation of embryos and fertility in the mouse. *Master Thesis*, College of Medicine, Tikrit University, Iraq.

AL-Rasheedi, A.A.(2009).study of effect of energy drinks on Biochemical and histological marks in Rats. Arab. J. Chem. 2 (1):113-126.

Ashmead ,T. M.(2003).Smoking and pregnancy .J. mater. Fet. and Neon. Medic.;14:297-304.

Bech, B. H., Nohr, E. A., Vaeth, M., Henriksen, T. B., & Olsen, J. (2005). Coffee and fetal death: a cohort study with prospective data. American journal of epidemiology, 162(10), 983–990. https://doi.org/10.1093/aje/kwi317.

Bech, B. H., Obel, C., Henriksen, T. B., & Olsen, J. (2007). Effect of reducing caffeine intake on birth weight and length of gestation: randomised controlled trial. BMJ (Clinical research ed.), 334(7590), 409. https://doi.org/10.1136/bmj.39062.520648.BE.

Bierrnacki,B.; Wofodarezyk.; B. and Minta,M.(2000).Effect of sodium valporate on rat embryo development invitro. Bull .Vet. Inst. Pulawy .,44:201-205.

CARE Study Group (2008). Maternal caffeine intake during pregnancy and risk of fetal growth restriction: a large prospective observational study. BMJ (Clinical research ed.), 337, a2332. https://doi.org/10.1136/bmj.a23329.

Higdon, J.V.; and Frei, B.(2006) Coffee and health:A review of recent human research. Crit Rev Food Sci Nutr.;46(2):101-123.

Fazal ,A.; and Jalali ,M. (2002). Experimentally – induced exencephaly and spina bifida in mice. Archives of Iranian-medicine,5(3),179-183. https://www.sid.ir/en/journal/ViewPaper.aspx?id=13074.

Greenberg, J. A., Boozer, C. N., & Geliebter, A. (2006). Coffee, diabetes, and weight control. The American journal of clinical nutrition, 84(4), 682–693. https://doi.org/10.1093/ajcn/84.4.682.

Grosso, L. M., & Bracken, M. B. (2005). Caffeine metabolism, genetics, and perinatal outcomes: a review of exposure assessment considerations during pregnancy. Annals of epidemiology, 15(6), 460–466. https://doi.org/10.1016/j.annepidem.2004.12.011.

Hammoudi, Hani Malallah. (2005). Study of the effect of paracetamol (acetaminophen) on the embryonic development of the Swiss white rat Mus musculus. Journal of Education and Science, Volume (7), Issue 1: 165-149.

Hey E. (2007). Coffee and pregnancy. BMJ (Clinical research ed.), 334(7590), 377. https://doi.org/10.1136/bmj.39122.395058.80.

Jana, N., Vasishta, K., Jindal, S. K., Khunnu, B., & Ghosh, K. (1994). Perinatal outcome in pregnancies complicated by pulmonary tuberculosis. Int J Gynaecol Obstet, 44(2), 119–124. https://doi.org/10.1016/0020-7292(94)90064-7

Matijasevich, A., Santos, I. S., & Barros, F. C. (2005). Does caffeine consumption during pregnancy increase the risk of fetal mortality? A literature review. Cadernos de saude publica, 21(6), 1676–1684. https://doi.org/10.1590/s0102-311x2005000600014

Ormerod P. (2001). Tuberculosis in pregnancy and the puerperium. Thorax, 56(6), 494–499. https://doi.org/10.1136/thorax.56.6.494

Padmanabhan, R., Singh, G., & Singh, S. (1981). Malformations of the eye resulting from maternal hypervitaminosis A during gestation in the rat. Acta anatomica, 110(4), 291–298. https://doi.org/10.1159/000145439

Rogwei, Y.E.; Aiguo, R.; Zhang, Le.; Zhiwen, Li.; Jianmeng, Liu.; Lijun Pei.; and Xiaoying ,Z.(2011).Tea Drinking as a Risk Factor for Neuraltube Defects in Northern China. Epidemiology. 22. (4);22:491-496.

Ullman, A., Beutsch, J. Wilber T.D. (1992). The role of drug R4486 in early miscarriage. Journal of Science, 8(7): 19-12.

Weng X, Odouli R, Li DK. (2008).Maternal caffeine consumption during pregnancy and the risk of miscarriage: a prospective cohort study. Am J Obstet Gynecol. 198(3):279.e1-8. doi: 10.1016/j.ajog.2007.10.803. Epub 25. PMID: 18221932.

Yen WJ, Wang BS, Chang LW, Duh PD. (2005).Antioxidant properties of roasted coffee residues. J Agric Food Chem. 6;53(7):2658-63. doi: 10.1021/jf0402429.

Scientific Journal for the Faculty of Science-Sirte University Vol. 1, No. 1 October (2021) 24-31

Scientific Journal for the Faculty of Science-Sirte University
(SJFSSU)
Journal home page: http://journal.su.edu.ly/index.php/JSFSU/index

Microfacies Analysis, Diagenetic Aspects and Depositional Environments of the Oligocene-Miocene Rock Units Exposed at Al Bardia Coastal Area, North East Tobruk City, Libya

Farag Adam[1], *Tarek Anan*[2] *and Amin Gheith*[2]

[1] *Geology Department, Science Faculty, Tobruk University, Tobruk, Lybia*

[2] *Geology Department, Science Faculty, Mansoura University, Mansoura, Egypt*

ARTICLE INFO

Article history:

Received 16 August 2021

Received in revised form 30 September 2021

Accepted 6 October 2021

Keywords:

Microfacies,

Wadi Shamas,

Wadi Rizk,

Al Khowaymat Formation ,

Al Faidiyah Formation,

Al Jaghbub Formation.

ABSTRACT

The Oligocene-Miocene carbonate succession exposed at Wadi Shamas and Wadi Rizk in the coastal area of Al Bardia was investigated to determine their depositional environments. This succession includes from base to top; Al Khowaymat, Al Faidiyah and Al Jaghbub Formation s. It was found that Al Khowaymat Formation is characterized by three microfacies associations (foraminiferal bioclastic(packstone, Wackestone and floatstone) rich with foraminifera and bivalves pointing to deposition within intertidal to lagoonal conditions related to regressed sea level with relatively high agitation due to the presence of bivalves and shell banks. Al Faidiyah Formation has three microfacies associations (packstone, floatstone and grainstone) rich in algae, bivalves, bryozoans and foraminifera indicating deposition in prograding advanced sea with deeper sub-environments from shallow energetic. Al Jaghbub Formation have four microfacies associations (packstone, floatstone, dolomitic wackestone and rudstone) rich with bryozoa, algae, bivalves and foraminifera, indicating deposition in tidal flats to mid ramp conditions. Micritization, dissolution and replacement are the main diagenetic processes affected the studied carbonate rocks.

1 Introduction

The study area lies within Al Bardia area, northeast Libya. It is the first sheet from east Libya contiguous to the Libyan Egyptian border (Fig, 1), lying between longitudes 24˚ 00′ and the Egyptian border nearly at 25˚ 00′ E and between latitudes 31˚ 00′ and the Mediterranean Sea nearly at 32˚ 00′ N. The area covers approximately 10,450 km2 (El-Deftar and Issawi, 1977).

As the authors aware, few authors study Oligocene-Miocene carbonate rocks at Al Bardia area (Annoscia 1968, Bellini 1969, Pietersz 1968, Imam 1999, El Safory and Muftah 2007, and Muftah et al., 2017).

This work aims to determine facies development, besides diagenetic and depositional environments of Al Khowaymat, Al Faidiyah, and Al Jaghbub formations. The study area located at the eastern border of the Al Bardia area encompassing two Wadis; Rizk and Shamas (Fig,2). The area was affected by post Miocene faulting. The two Wadis are located about 150 km from Tobruk city. The two Wadis are 3 Km apart. Based upon the detailed field study and facies characteristics, the different successions exposed are stratigraphically consisting from the base to top of the Al Khowaymat Formation, Al Faidiyah Formation and Al Jaghbub Formation ranging in age from Early Oligocene to Middle Miocene.

2 Materials and Methods

During field trips to the study area, two sections (Wadi Rizk and Wadi Shamas) were sampled and described bed by bed for each lithological changes and sedimentary structures. Thirty-five rock samples were collected according to their variations in color, texture, lithology, sedimentary structures and faunal content.

Corresponding author:
E-mail: faraj.admi@tu.edu.ly
DOI: https://doi.org/10.37375/sjfssu.v1i1.78

In addition, some macrofossils (bivalves, echinoderms) were collected. Twenty thin sections have been prepared and examined using the polarizing microscope to knom their texture, mineralogical components and faunal content. The depositional environments and subsequent diagenetic changes have been determined. Microfacies of limestone were named following the classification of Dunham (1962) with the modifications of Embry and Klovan (1971).

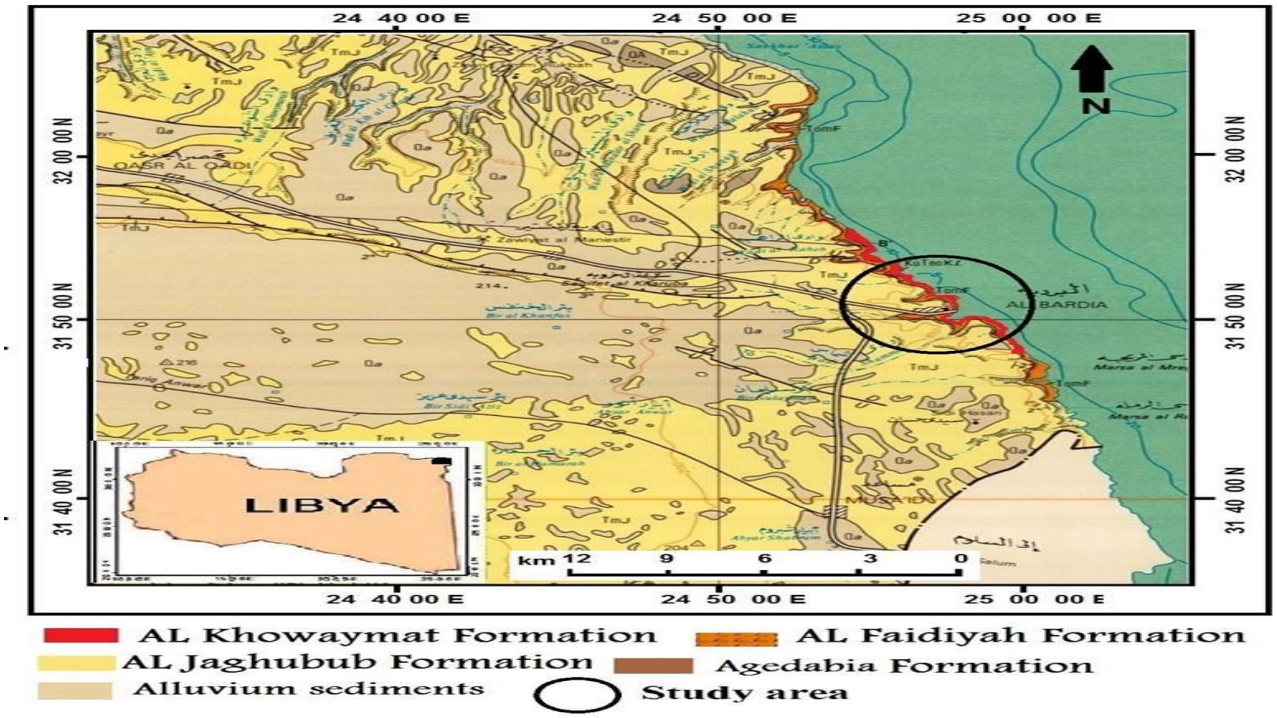

Fig. 1: Geological map of the Al Bardia area

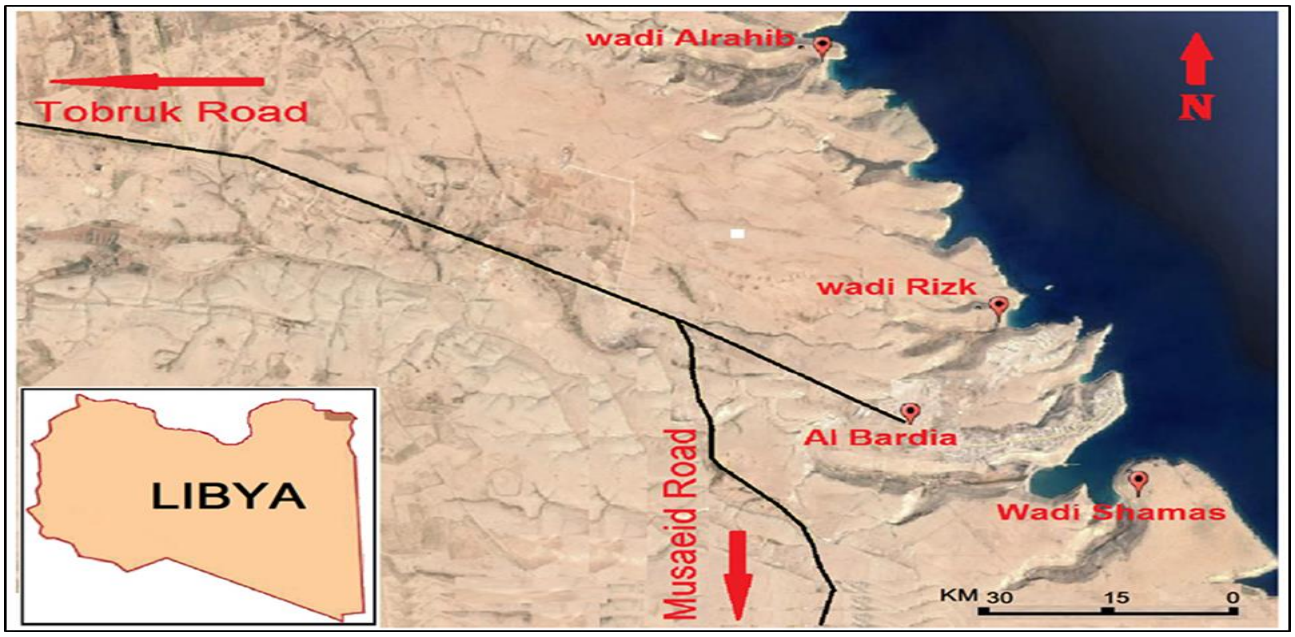

Fig.2. Landsat image showing the location of the studied Wadis Rizk and Shamas at the Al Bardia Area, northeast Libya.

2.1 Lithostratigraphy of the study area

The Al Khowymat Formation (Late Eocene-Early Oligocene) is the oldest rock unit in the study area and covers the northern part of it. It extended parallel to the Mediterranean Sea as a small strip west of the Al Bardia area (El Deftar and Issawi, 1977). This rock unit was originally described by Mazhar and lssawi (1977) in its type locality, Al Khowaymat village, a few kilometres southeast of Bir Habas. Its age was determined as Upper Eocene to Lower Oligocene with a thickness of 25 m.

The second Formation Al Faidiyah (Late Oligocene-Early Miocene) represents the oldest Miocene rock unit exposed in the study area. Pietersz (1968) is the first one who introduced the term Al Faidiyah Formation to describe calcareous rocks and shale that overlie the Shahat Formation in Al Jabal Al Akhdar area in its type section (Qaryat Al Faidiyah). Pietersz (1968) assigned this rock unit a Late Oligocene-Early Miocene age. The third Al Jaghbub Formation (Early-Middle Miocene) is represented by fossiliferous sandy to argillaceous limestone with subordinate calcareous shale. In the studied area, the Al Jaghbub Formation conformably overlies the Al Faidiyah Formation (Plate 1). The contact between the two formations occurs at the first appearance of carbonate or marl beds over the clay beds of the Al Faidiyah Formation (Fig.3,4)

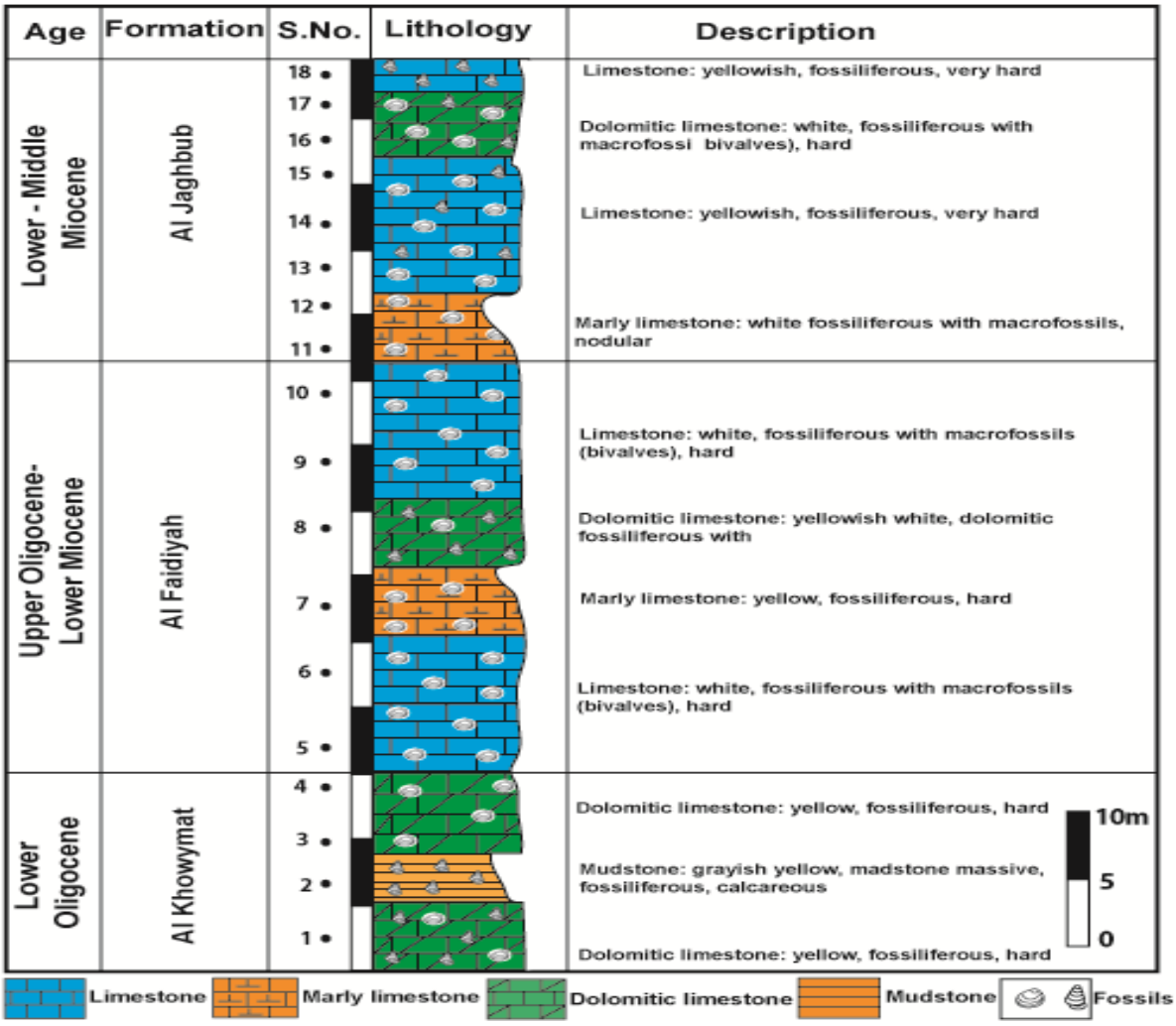

Fig.3: Lithostratighraphic column of the studied rock units at Wadi Rizk.

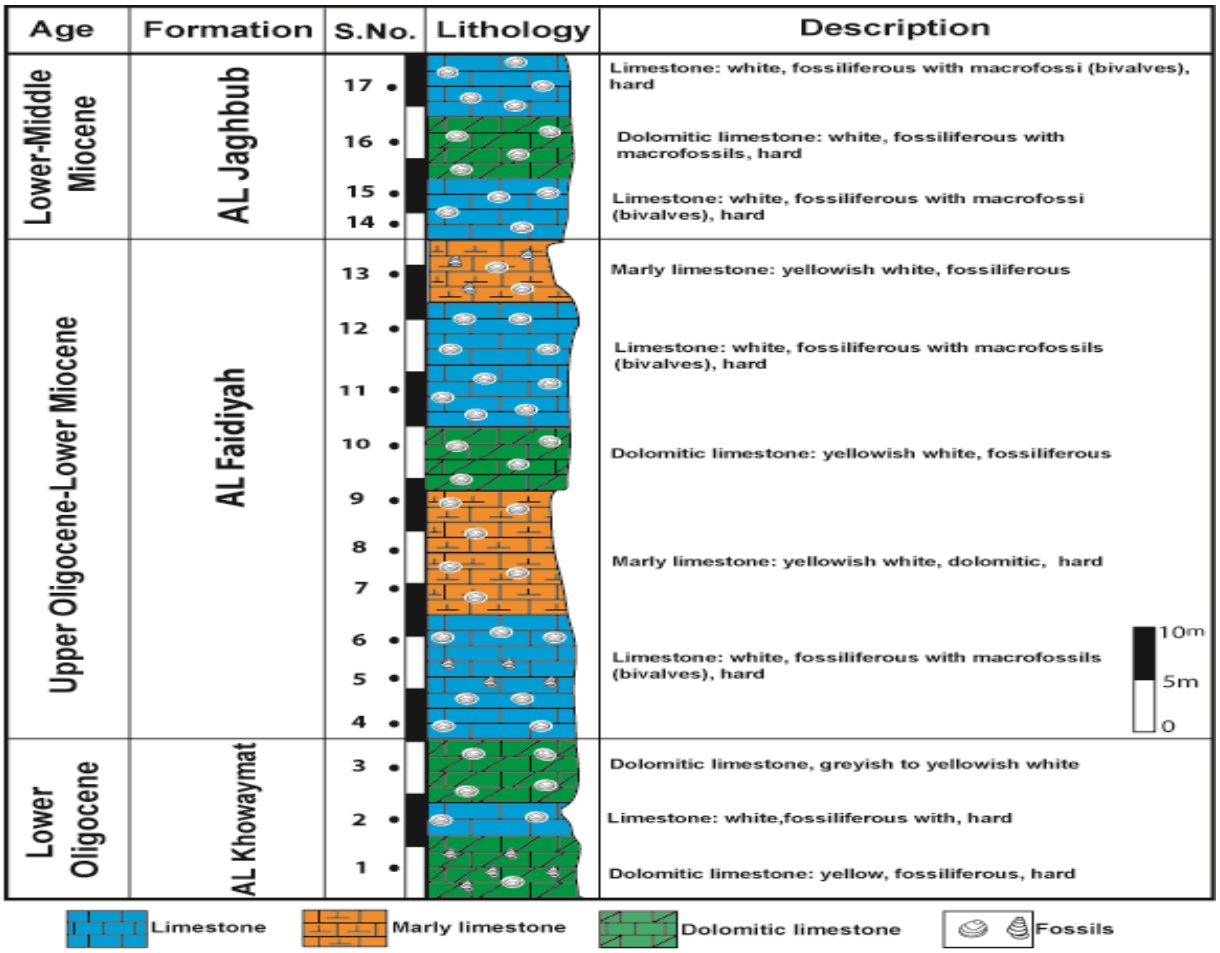

Fig.4: Lithostratighraphic column of the studied rock units at Wadi Shamas

3. Results

The common microfacies associations and their depositional environments prevailed during deposition of the Lower Oligocene and Lower-Middle Miocene rock units, exposed at Wadi Rizk and Wadi Shamas are determined. The analysis is complemented by comparison with both recent and ancient analogous carbonate systems. Diagenetic process was taken special attention utilizing comprehensive petrographic study.

1. Al Khowaymat Formation (Late Eocene-Early Oligocene.)

Five samples have been thin sectioned (three samples from Wadi Shams and two samples from Wadi Rizk) and studied under the polarizing microscope. The following microfacies types are recorded:

1.1 Foraminiferal bioclastic packstone (Wadi Shamas, Sample. No.1).

1.2 Bivalve bioclastic floatstone (Wadi Shamas, Sample. No3).

1.3 Pelagic foraminiferal wackstone (Wadi Rizk, Sample. No.2).

2. Al Faidiyah Formation (Late Oligocene-Early Miocene.

Eleven thin sections are examined in Al Faidiyah Formation (seven samples from Wadi Shmas and four samples from Wadi Rizk). The microfacies associations recognized are given below from bottom to top.

2.1 Bryozoa bioclastic packstone (Wadi Shamas, Sample. No.6).

2.2 Foraminiferal bioclastic floatstone (Wadi Shamas, Sample. No.9).

2.3 Algal foraminiferal bioclastic grainstone (Wadi Shamas, Sample. No.12).

2.4 Bivalve algal bioclastic grainstone (Wadi Rizk, 5).

***3. Al Jaghbub Formation (Early-Middle Miocene*).**

Twelve thin sections have been investigated from Wadi Shamas and Wadi Rizk to represent Al Jaghbub Formation.

The most common microfacies associations detected are summarized below, from bottom to top.

3.1Bryozoa algal rudstone (Wadi Shamas, Sample. No.14).

3.2 Dolomitized wackestone (Wadi Shamas, Sample. No.16).

3.3 Foraminifera bryozoa grainstone (Wadi Rizk, Sample. No.14).

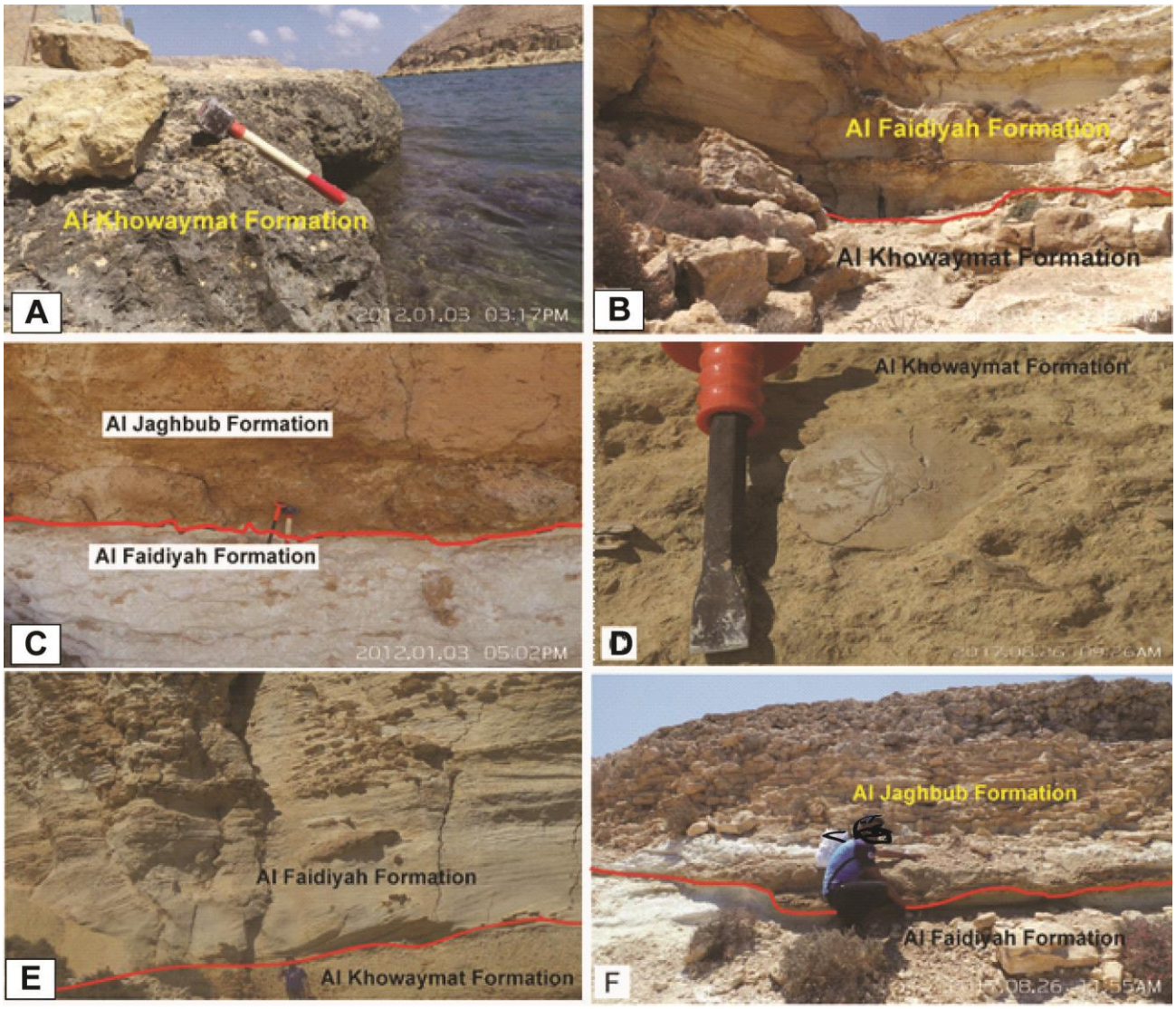

Plate 1: Field photographs showing: A) The upper part of the Al Khowaymat Formation at Wadi Shamas. composed mainly of dolomitic limestone. (Notice the color change of the lower part due to the action of seawater). B) The contact between the Al Khowaymat Formation and the Al Faidiyah Formation at Wadi Shamas. C) The contact between the Al Faidiyah Formation and the Al Jaghbub Formation at Wadi Shamas. D) Echinoderms in the Al Khowaymat Formation at Wadi Rizk. E) The contact between the Al Khowaymat Formation and the Al Faidiyah Formation at Wadi Rizk. F) The contact between the Al Faidiyah Formation and the Al Jaghbub Formation at Wadi Rizk.

4. Discussion

Microfacies associations recorded in Al Khowaymat Formation are discussed and their components are described and interpreted in the following:

Foraminiferal bioclastic packstone (Wadi Shamas, Sample. No.1) is composed of a framework micritized matrix. Allochems are tightly packed, grain supported sand to gravel-sized. They are represented by echinod spines, bryozoa, ostracods, foraminifera, bivalve fragments that cemented by mosaic sparry calcite. Echinod spines are circular or elliptical in cross-section with smaller broken fragments (Plate,2A). These recorded allochems are cemented by coarse grained, well crystallized dolomite mixed with mosaic calcite cement. Diagenesis is represented by dissolution of micritic matrix and large carbonate fragments that replaced by coarse grained sparry calcite. Due to the presences of ostracods, bryozoa, foraminifera, and bivalves, an intertidal foreshore to lagoonal setting is suggested for this microfacies. This association matches with SMF 12 and FZ 6 of Wilson (1975) and Flügel (2004).

Bivalve bioclastic floatstone (Wadi Shamas, Sample.No3) is represented by fossil debris of gravel-sized includes; ostracods, gastropods, bivalve fragments, echinoderms, bryozoa and algae floating in the micritic matrix. Sometimes allochems are cemented with drusy mosaic equant calcite crystals. Most of the internal cavities of the shells are entirely recrystallized into Sperry calcite with micritic envelope.
Diagenesis can be observed from dissolution of the carbonate mud matrix and recrystallization of medium to coarse sparry calcite surrounding the allochems. Most voids and fossil chambers show recrystallization of coarse spars. Most allochems suffered dissolution and recrystallization of spars with mosaic structure (Plate, 2B). Micritization process accompanied burial is noticed from assimilated most of the allochems boundaries which admixed into the matrix. The most common diagenetic feature is the, development of coarse-grained sparry mosaic calcite in some patches in the expense of micritic matrix. This association indicates deposition in relatively shallow marine energetic conditions with relatively high agitation (inner shelf bays). This microfacies is matching well with SMF8 and FZ7 of Wilson (1975) and Flügel (2004).

Pelagic foraminiferal wackstone (Wadi Rizk, Sample. No.2) is composed mainly of cryptocrystalline carbonate (micrite) matrix enriched with allochems. Allochems are represented by well-defined scattered pelagic foraminiferal, curved bivalves and echinoderms, ostracods, algae, and bryozoa floating within the matrix (Plate, 2C) Diagenesis process accompanied burial has noticed from sparitization of most foraminiferal chambers. Deposition of this microfacies was prevailed within relatively quiet less energetic marine conditions; mid to outer shelf setting is suggested. This association is concordant with SMF9 and FZ7 of Wilson (1975) and Flügel (2004). While the microfacies detected in Al Faidiyah Formation include the following associations; Bryozoa bioclastic packstone(Wadi Shamas, Sample. No.6) where allochems are represented mostly by numerous altered bryozoa, echinoderms, bivalves and foraminifera that embedded in a cryptocrystalline carbonate matrix. Some fossils stained with iron (Plate,2D). Diagenetic alterations in this microfacies are represented by dissolution and replacement with sparry calcite crystals that filled most foraminiferal chambers. This facies was deposited in quiet less energetic marine conditions. Mid to outer shelf marine setting is suggested for this microfacies. This association matches with (SMF3) and (FZ1) of Wilson (1975) and Flügel (2004).
Foraminiferal bioclastic floatstone **(Wadi Shamas, Sample. No.9),** this microfacies is made up of echinoderms, nummulites, gastropods, bivalve fragments, bryozoa and algae. The internal cavities of the shells are entirely recrystallized into coarse crystalline sparry calcite (Plate 2E). Diagenesis in this microfacies are represented by dissolution, recrystallization and dolomitization. This microfacies indicates deposition in relatively energetic shallow marine conditions (inner shelf bays. This microfacies is matching with SMF8 and FZ7 of Wilson (1975) and Flügel (2004).

Algal foraminiferal bioclastic grainstone **(Wadi Shamas, Sample. No.12),** consists of numerous allochems and coarse sparry calcite. The allochems are generally represented by bryozoa, bivalves (oyster), gastropods, coralline red algae, echinoderms and foraminifera (Plate, 2F). The internal cavity of the shells is entirely recrystallized into, mosaic coarse crystalline calcite. The cement is coarse to medium sparite filled pore spaces and partly filled shell cavities.

Bivalve algal bioclastic grainstone **(Wadi Rizk, Sample No.5)** consists of numerous allochems and coarse interlocking mosaic of sparry calcite. The allochems are represented by bivalve fragments, coralline red algae, bryozoa, ostracods that cemented with sparry calcite (Plate, 3A). The internal cavity of the shells is entirely filled with coarse crystalline calcite mosaic, indicating active recrystallization process during burial process. The cement is coarse to medium sparite filled pore spaces and partly filled cavities of most shells. Diagenesis is evident from recrystallization features seen in the sparite cement and partially to complete replacement of the allochems.
Microfacies associations recorded in Al Jaghbub Formation (Early-Middle Miocene) Formation are discussed and their components are described and interpreted in the fol

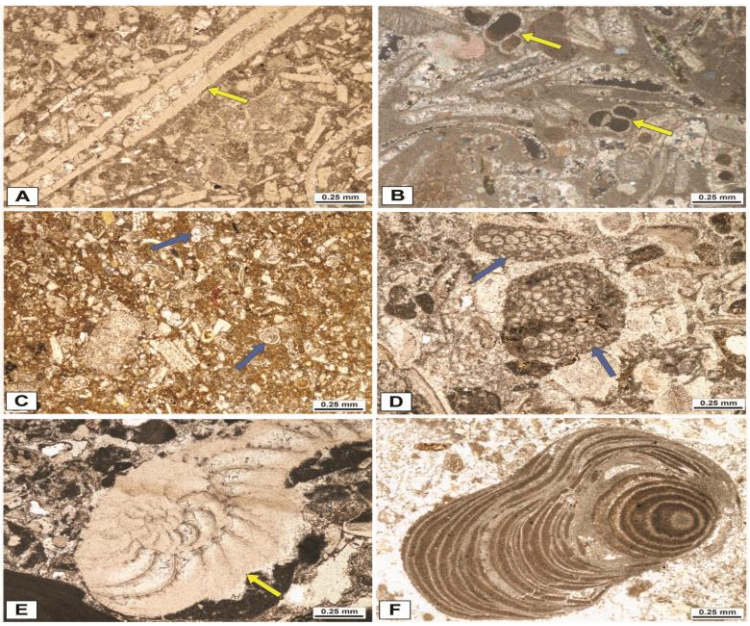

Plate 2: Photomicrographs showing: A) Foraminiferal bioclastic packstone microfacies. Al Khowaymat Formation, S. No. 1,Wadi Shamas PPL. B) Bivalve bioclastic floatstone microfacies. Bivalve fragments and gastropods (arrows) are scattered in a micritc matrix, Al Khowaymat Formation, S. No. 3, Wadi Shamas XPL, C) Pelagic foraminiferal wackestone microfacies. Planktonic foraminifera are abundant, Al Khowaymat Formation, S. No. 3,Wadi Rizk PPL. D) Bryozoa bioclastic packstone microfacies, Al Faidiyah Formation, S. No. 5, Wadi Shamas PPL. E) Algal foraminiferal packstone/floatstone microfacies. The bivalve fragments are recorded with its large size, Al Faidiyah Formation, S. No. 9, Wadi Shamas PPL. F) Algal foraminiferal bioclastic grainstone microfacies, Al Faidiyah Formation, S. No. 10, Wadi Shamas PPL

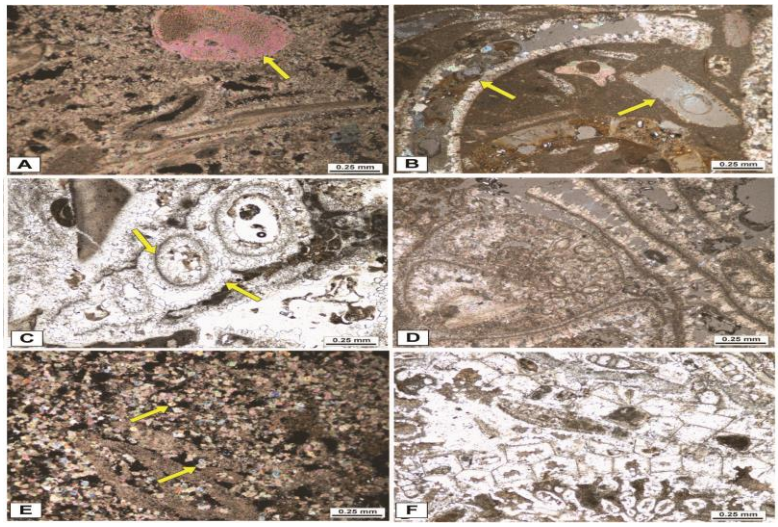

Plate 3: Photomicrographs showing: A) bivalve algal bioclastic grainstone microfaces. Echinoderm plates are recorded (arrow), Al Faidiyah Formation, S. No. 5 new, Wadi Rizk XPL. B) Bivalve bryozoan floatstone microfacies. Bivalve fragments are encountered and filled with drusy calcite (arrows), Al Faidiyah Formation, XPL, S. No. 9, Wadi Rizk. C) Bivalve grainstone microfacies. Gastropods are abundant (arrows), Al Faidiyah Formation PPL, S. No. 10, Wadi Rizk. D) bryozoa algal rudstone microfacies, Al Jaghbub Formation, S.No. 15,Wadi Shamas (XPL). E) dolomitized wackestone microfacies. Dolomite rhombs (arrows) are observed in the groundmass, Al Jaghbub Formation, S.No. 15,Wadi Shamas XPL. F) Foraminifera bryozoa grainstone microfacies, Al Jaghbub Formation, S. No. 11, Wadi Rizk PPL.

5. Conclusion

The paleoenvironmental conditions deduced from the microfacies associations identified in the Early Oligocene - Middle Miocene sedimentary rock units allow for recognizing different depositional environments. Three microfacies associations are exhibited by Al Khowaymat Formation; these are foraminiferal bioclastic packstone, foraminiferal bioclastic wackestone and bivalve bioclastic floatstone indicating deposition within intertidal to shelf lagoon conditions related to regressed sea level to shallow energetic marine conditions with relatively high agitation due to the presence of bivalves and shell banks.

The Al Faidiyah Formation reveals three microfacies associations varied between packstone, floatstone and grainstone rich with algae, bivalves, bryozoans and foraminifera indicating deposition in continuous sea level rise from shallow energetic marine conditions to mid - outer shelf marine settings. The Al Jaghbub Formation offered four

microfacies associations includes, packstone, floatstone, dolomitic wackstone and rudstone enriched with bryozoa, algae, bivalves and foraminifera indicating deposition started during a stable phase of maximum sea level rise during inner shelf marine setting with minor shallow marine fluctuations where a marked sea level drop and shallow intertidal and supratidal warm coastal sedimentation occurred.

Conflict of interest: The authors declare that there are no conflicts of interest.

References

Annoscia, E., 1968. The bryofauna of Mesomiocenic Al Jaghbub Formation in the eastern Cyrenaica, Libya. In: Said, R., Al Ansary, S., Beckmann, J.P., Viotti, C., Ghorab, M.A., Kerdany, M.T. (Eds.), Proceedings of the 3rd African Micropaleontology Colloquium, Cairo, pp. 37-94.

Bellini E (1969) Geological map of Libya, Sheet NI35-17, scale 1:250 000, Al Baida, Explanatory Booklet. Industrial Research Centre, SPLAJ, Tripoli, 68p.

Dunham RJ (1962) Classification of carbonate rocks according to depositional texture. In: Ham, W.E. (Ed.), Classification of Carbonate Rocks. American Association of Petroleum Geologists, Memoir, 1, pp. 108-121.

El Deftar T, Issawi B (1977) Geological Map of Libya, sheet NH. 35-1 scale 1: 250 000, Al Bardia, Explanatory Booklet, Industrial Research Center, SPLAJ, Tripoli, 93p.

El Safory Y, Muftah A (2007) Oligocene bryozoans from Al Jabal Al Akhdar, Libya. Egyptian Journal of Paleontology, 7: 315-334.

Embry AF, Klovan JE (1971) Absolute water depths limits of Late Devonian paleoecological zones. Geologische Rundschau, 61:672-686.

Flügel E (2004) Microfacies of carbonate rocks. Springer, Berlin, 976 p.

Imam M (1999) Lithostratigraphy and planktonic foraminiferal biostratigraphy of the Late Eocene-Middle Miocene sequence in the area between Wadi Al Zeitun and Wadi Al Rahib, Al Bardia area, northeast Libya. Journal of African Earth Sciences, 28:619-639.

Mazhar A, Issawi B (1977) Geological Map of Libya, sheet NH 34-3 scale 1: 250 000. Zut Musus Explanatory Booklet, Industrial Research Center, SPLAJ, Tripoli, 80 p.

Muftah AM, El Ebaidi SK Al Mahmoudi A, Faraj FH, Khameiss B (2017) New insights on the stratigraphy of Tobruk - Burdi, area Marmarica, NE Libya. Libyan Journal of Science & Technology, 6(1): 30-38.

Pietersz CR (1968) Proposed nomenclature for rock units in Northern Cyrenaica. In: Barr F.T. (Ed.), Geologyand Archaeology of Northern Cyrenaica, Libya, Tripoli, pp. 125-130.

Reading, HG (1996) "Sedimentary Environments and Facies, 3rd Edition, Blackwell Scientific, Oxford, 688p.

Selley RC (1996) "Ancient Sedimentary Environments, 4th Edition, Chapman & Hall, London, 300p.

Wilson JL (1975) Carbonate facies in geologic history. Springer-Verlag, Berlin, Heidelberg, 471 p

Scientific Journal for the Faculty of Science-Sirte University Vol. 1, No. 1 October (2021) 32-38

Scientific Journal for the Faculty of Science-Sirte University
(SJFSSU)
Journal home page: http://journal.su.edu.ly/index.php/JSFSU/index

Rate constants and Rheological Properties of the Ultrasonic Degradation of Carboxymethyl Cellulose

Hitham M. Abuissa[1], Randa F. Elsupikhe[2], Tahani S. Alfazani[2]*

[1]*Chemistry Department, Science Faculty, Ajdabiya University, Ajdabya, Libya*

[2] *Chemistry Department, Science Faculty, Benghazi University, Benghazi, Libya*

ARTICLE INFO

Article history:

Received 24 August 2021

Received in revised form 25 September 2021

Accepted 25 September 2021

Keywords::

Carboxymehtyl cellulose,

Ultrasonic degradation,

Viscosity,

Rate constant.

ABSTRACT

To degrade the polysaccharide with high molecular weight the effectiveness of ultrasound for carboxymethyl cellulose (CMC) in aqueous solution has been studied at a time of 60 min and temperature of 25 ℃ and for polymer solution with concentration up 0.1 g/L. The Huggins equation was appropriate to apply to the intrinsic viscosity of CMC before sonication to understand the influence of salt on degradation, CMC solution was premixed with 0.1 M NaCl, before ultrasonication. Developed a kinetic model, successfully implement to predict and quantify rates of degradation and efficiency. The values of reaction rate constants and reaction orders were found related to the salt and the concentration used, suggesting that, the presence and absence of salts could increase or decrease the degradation by ultrasonic radiation through adjusting the molecular conformation of CMC

1 Introduction

The natural polymers (polysaccharides and proteins), and their degradation methods are of great interest to researchers. The degradation of polysaccharides give oligosaccharides, which are used for many industries and are considred of great importance in the food industry. Cellulose is a polysaccharide with a diverse range of applications that are built up as a linear homopolymer from 1,4-β-glycosidically linked glucose. Figure 1 shows the structural formula of native cellulose (Clasen and Kulick 2001). Carboxymethyl cellulose(CMC) is a cellulose derivative with carboxymethyl groups bound to the hydroxyl groups of the glucose unit (Guo et al 1998; Pourjavadi et al. 2006; Lakshmi et al. 2017).Chemical modified CMC withimproved properties is gaining increasing in many fields, not only because it is low in cost, but also mainly the polysaccharide portions of the products are biocompatible and biodegradable(Sakairi et al. 1998). CMC is an industrially relevant cellulose derivative, which has multiple uses for pharmicutical, food, and cosmetic industries as a thickener and binder (Kokol 2002; Lund et al. 1990; Capitani 2000). In recent years, CMC evoked considerable interest as a Texturing additive for foodstuffs (Samant et al.1993; Ganz 1974) and preparation of hydrogels from graft copolymerization of the hydrophilic monomers onto CMC (Bajpai and Giri 2003; Zaleska et al. 2001; Zaleska et al. 2001). Also, CMC was used in the oil industry as lubricant for drilling, and in the cosmetic industry as a stabilizer and a binder

***Corresponding author*:**
E-mail: hithamaboeisa@yahoo.com
DOI: https://doi.org/10.37375/sjfssu.v1i1.114 **SJFSSU 2021**

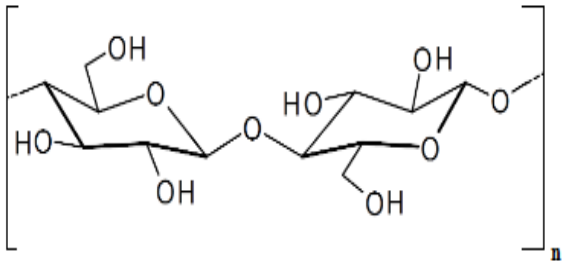

Fig. 1 Structure of water-soluble cellulose derivatives (carboxymethyl cellulose; R^1= CH_2 COONa).

Because of its no toxicity, biodegradability, and biocompatibility, CMC solution has also been widely used as a carrier for a bone graft (Santa-Comba et al. 2001). It is reported that CMC can improve the clinical Properties of calcium sulfate when used as a binder for particulate bone grafts (Reynolds et al. 2007).

In recent decades, many technique for degradation have been applied to polysaccharides, especially CMC, including biodegradation (Ahlgren 1993; Muchova et al 2009), thermal degradation (Soares et al 2005; Srivastava, et al. 2012), chemical degradation (Christensen et al 1993), and ultrasonic degradation (Milas et al. 1986). The advantage of degradation by ultrasonic technique compared to other types of degradation techniques, is one of the best ways to control the molecular weight of degradation products. Furthermore, the degradation polymers by ultrasonic technique don't change their basic chemical structure, as their parent molucule, and this feature cannot be obtained when using other (Basedow and Ebert 1977). Various physicochemical effects, such as radiation pressure, streaming, cavitations, and interface instabilities, that result from high-intensity ultrasound radiations (Mulet et al. 2002).

Cavitations are broadly accepted as the mechanism of ultrasonic degradation of polymers (Basedow and Ebert 1977). Recently, Gogate (Mohod and Gogate 2011) was investigated on some conditions and parameters, in the presence of additives, which affected the ultrasonic degradation of CMC and poly (vinyl alcohol)(PVA). Also, Anti teal (Antti and pntti 2008). Previously worked on ultrasonic degradation of CMC and studied the effect of different molecular mass and concentrations dynamic viscosity measurements. Because the enviromental conditions have a significant effect on the degradation efficiency within the solution, they have been studied to reduce it. In this research paper, we study the effect of salt on the degradation of CMC by ultrasonic radiation in aqueous solution. specifically study the influence of salt on the ultrasonic degradation of CMC in aqueous solution, which provides a possible way to a chive degradation beyond the limits seen in other degradation studied and with a faster degradation rate.

NaCl salt was used over a range of concentration, through the changes in the intrinsic viscosity of the solutions were used to follow the effectiveness of ultrasonic degradation . Also, the degradation kinetics model has been developed and used to quantify and compare degradation rates and rate constants at different environmental conditions.

1.1 Intrinsic viscosity Determination

The objective of rheological measurements of the solutions is to determine the intrinsic viscosity [η] as a function of ultrasonication for quantify the degradation process. The intrinsic viscosity is a measure of individual polymer molecule contribution to the viscosity of the solution. As shown in Eqs (1-3), to obtain the intrinsic viscosity value, solution –viscosity measurements are extrapolated to zero shear – rate (q→0) and infinite dilution (C→0) in order to eliminate the interaction effects between the polymer molecules. Where, η_{sp} is the specific viscosity, η_{rel} is the relative viscosity, η_s is the viscosity of the solvent, and η is the viscosity of the solution. The intrinsic viscosity is determined by measuring the specific viscosities of a solution at its initial polymer concentration, then diluting it several times by the solvent and measuring and calculating the specific viscosity of the polymer.

$$[\eta] = \lim_{\substack{q\to 0 \\ C\to 0}} \frac{\eta_{sp}}{C} \quad (1)$$

$$[\eta] = \eta_{rel} - 1 = \frac{\eta - \eta_s}{\eta_s} \quad (2)$$

$$\eta_{rel} = \frac{\eta}{\eta_s} \quad (3)$$

The relationship between concentration and viscosity of dilute polymer solution can be described by many empirical forms, the most common of which is the Huggins equation (Mohod and Gogate 2011), as shown in Eq.(4), where k is Huggins constant.

$$\frac{\eta_{sp}}{C} = [\eta] + k[\eta]^2 C \quad (4)$$

The Huggen equation can be simplified For applied to very dilute solutions, by removing the second-order term, and, thus, the intrinsic viscosity can be determined from the slope of a plot polymer concentration an against relative viscosity (Antti and pntti 2008).

$$\eta_{rel} = 1 + [\eta]C \quad (5)$$

1.2. Ultrasonic Degradation Kinetics

Generally, the degradation rate can be considered as an order reaction based on the total molar concentration of the polymer, as is shown in Eq.(6).

$$\frac{d[M]_t}{dt} = k[M]_t^n \quad (6)$$

Where [M] is the total concentration of polymer molecules (and fragments) at time t, k is the degradation rate constant, and n is the order of reaction (Taghizadeh, and Mehrdad 2003).

Note that, the value of n is expected to be negative, because the ultrasonic degradation is a mechanical process. By integrating and applying the initial condition at Eq. (6) that, at t=0, $[M]_t = [M]_0$, where $[M]_0$ is the initial total molar concentration of polymer and t is Sonication time, Eq. (7) is obtained:

$$[M]_t^{1-n} - [M]_0^{1-n} = (1-n)kt \quad (7)$$

The total molar concentration of polymer, which increases as degradation occurs, is related to the number-average molecular weight and polymer concentration in solution, as shown in Eq. (8). The viscosity average molecular weight, M_v is related to intrinsic viscosity through Mark–Houwink equation (White and Kim 2008), Eq. (9), and the number average molecular weight through Eq. (10).

$$[M] = \frac{C}{M_n} \quad (8)$$

$$[\eta] = KM_v^{\alpha} \quad (9)$$

$$M_n = [(1+\alpha)\Gamma[(1+\alpha)]^{\frac{1}{\alpha}} M_v \quad (10)$$

Where α and K are the Mark-Houwink constant, and Γ is the standard gamma function. Furthermore, the values of $\Delta\eta$ determined from Eq.(12) (Taghizadeh, and Abdullahi 2011).

$$M = \left(\frac{KC^{\alpha+1}}{\sqrt{2}(1+\alpha)\Gamma(1+\alpha)}\right)^{\frac{1}{\alpha}} \Delta\eta \quad (11)$$

Where, $\Gamma(1+\alpha) = \int_0^{\infty} e^{-t}t^{\alpha}$, and

$$\Delta\eta = \left(\frac{1}{\eta_{sp} - ln\eta_{rel}}\right)^{1/(2\alpha)}$$

By substituting Eq. (11) in (7) yields Eq (12)

$$\Delta\eta^{1-n} - \Delta\eta_0^{1-n} = (1-n) \times \left(\frac{\sqrt{2}(1+\alpha)\Gamma(1+\alpha)}{KC^{\alpha+1}}\right)^{\frac{(1-n)}{\alpha}} kt \quad (12)$$

or

$$\Delta\eta^{1-n} - \Delta\eta_0^{1-n} = kt \quad (13)$$

2. Materials and Methods

2.1 Material and Solution Preparation

The Powder material Supplied by local Libyan Company (Jowfe) and used without Further Purification. Sodium chloride (NaCl) was purchased from Fluke (Sigma-Aldrich, Germany). Mother Solution of 1g/L concentration was prepared by adding a known weight of the Polymer to a fixed volume of double distilled water and dissolving with magnetic stirring, giving a clear solution. Some extra double distilled water was then added up to the required volume. A centrifuge was used at 2200rpm for 20 min to remove air bubbles from the solutions. After centrifuging, the solutions were ready for ultrasonic processing.

2.2 Density Measurement

By filtering Small samples of the centrifuged carboxymethyl cellulose solutions, the dissolved amount of CMC was measured. The evaporate solvent and dissolved material were determined gravimetrically, by adding aliquots to small flasks and heated overnight at 80°C. All the measurements were performed in triplicate.

2.3 Sonication Treatment and Viscosity Measurement

The carboxymethyl cellulose solutions (25ml, 0.1g/L) were transferred into a cooling cell, and Sonicated by using a BANDELIN electronic, Heinrichstrabe 3-4 D-12207 Berline, Ger ate- type UW 2200, Pro-Nr. GB599.00003718.001. The amplifier frequency was fixed at 20 KHz, and the amplitude was fixed at 40%, which corresponds to approximately 95W of power. The temperature of the solutions in the cell was controlled by replacing the water in the water ice Path. After Sonication process, all solution were prepared at concentration of 0.1M of salt by adding necessary amount of salt, in order to make sure that all viscosity measurements were taken at the same ionic strength. Each sample was diluted by using the corresponding salt solutions with the concentration 0.1M, to produce concentrations of CMC in the range of 0.10-0.02g/L. The viscosity of the solution was determined by Ostwald glass capillary Viscometer (NO

11:75-1005, Nach Ostwald 486510, made by brand at W-Germany), thermostated with an accuracy of ± 0.015%, as well as to obtain linear and nonlinear regression line with corresponding equations and correction coefficients' (R^2) in order to assess the best model.

3. Results

The values of intrinsic viscosity of CMC solutions, which correspond to no sonication, 0.5 min, 5 min, 10 min, 30 min, or 60 min sonication treatments were calculated by appling Eqs. (4), (5) for estimation of intrinsic viscosities of CMC before and after sonication treatment. Which, (Fig. 2) represented the reducing viscosity Vs. CMC concentration: CMC solution (0.1 g/L) were premixed with 0.1 M NaCl, and then sonicated for the given time and (Fig. 3) represented the relative viscosity Vs. CMC concentration: CMC solutions (0.1 g/L) were premixed with 0.1 M NaCl, and then sonicated for the given time.

However, the results of our research showed an excellent fit to the model with correlation factor (R2=0.96) for the case of unsolicited solutions of CMC concentration ranging down to 0.02 g/L with 0.1M NaCl (Table 1). With sonication treatment, the intrinsic viscosities obtained by using the Huggins equation also show the reasonable correlation coefficient (R2 range from 0.72 to 0.97), which suggests that the Huggins equation is appropriate for determination of intrinsic viscosities of CMC solutions with polymer concentration higher than 0.02 g/L.

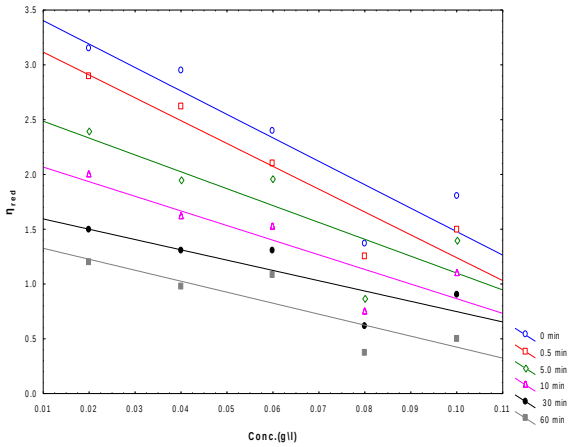

Fig. 2 CMC concentration Vs. reducing viscosity: CMC solutions (0.1 g/L) were premixed with 0.1 M NaCl, and then sonicated for the given time. After sonication, the sonication-treated solution was diluted with 0.1 M NaCl solution to produce polymer concentrations ranging from 0.10 to 0.02 g/L.

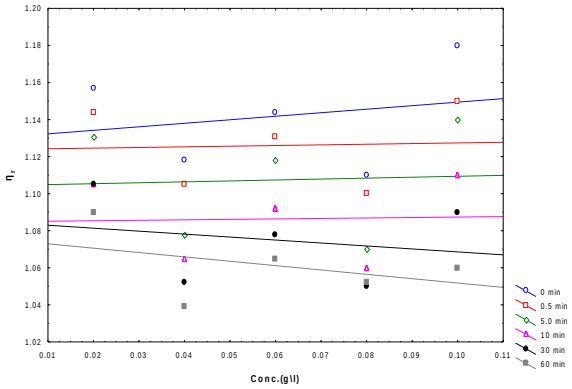

Fig. 3 CMC concentration Vs. relative viscosity: CMC solutions (0.1 g/L) were premixed with 0.1 M NaCl, and then sonicated for the given time. After sonication, the sonication-treated solution was diluted with 0.1 M NaCl solution to produce polymer concentrations ranging from 0.10 to 0.02 g/L.

As a result, to maintain the comparison properly, we use Eq. (4) as the best model for intrinsic viscosity determination because of its acceptable linear fit to data obtained from both sonicated and non-sonicated CMC solutions.

Table 1. Intrinsic viscosity and correlation coefficients obtained from the Huggins equation

Sonication time (min)	$[\eta]$ (L/g)	R^2
0	3.618	0.96
0.5	3.325	0.97
5	2.64	0.94
10	2.201	0.95
30	1.688	0.89
60	1.4265	0.72

Some different rate models have been proposed for the degradation of polymers, but in this study, a simple model was employed via viscometry. The data consists of Eq. (13) by considering that order reaction molar concentration is approximately -1, thus Eq. (14)

$$\Delta\eta^2 - \Delta\eta_0^2 = kt \qquad (14)$$

The plot of $(\Delta\eta^2 - \Delta\eta_0^2)$ versus sonication time for different CMC concentrations presented in figure 4. The apparent degradation rate constant defined in Eq. (14) can be estimated from the slops of the plots in figure 4 and shown in table 2. Based on that, rate constants were calculated. The calculated rate constants, k, are correlated in terms of revers solution concentration (Fig.5).

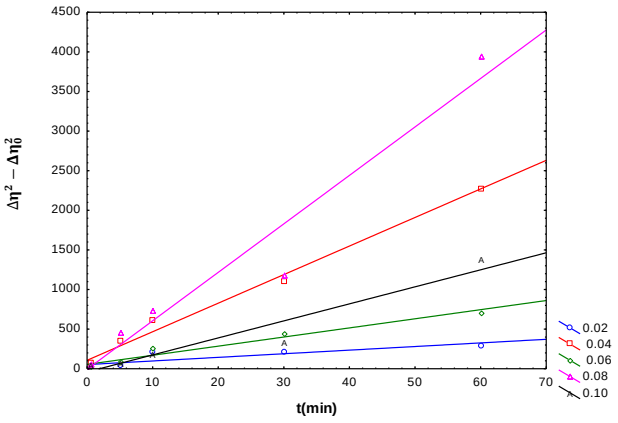

Fig. 4 The plot of $((\Delta\eta^2 - \Delta\eta_0^2$) versus sonication time for different concentrations of CMC in 0.1 M NaCl solution at 25^0C.

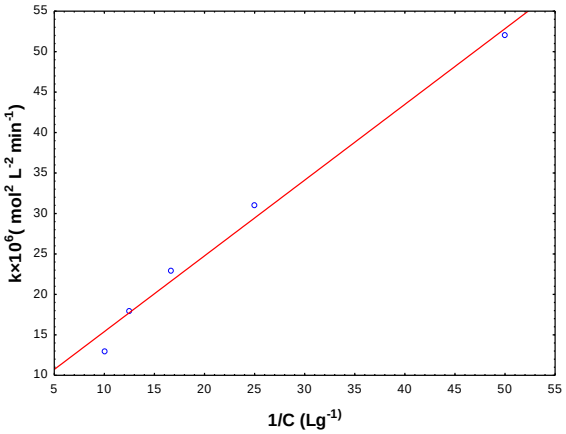

Fig. 5 The relationship between the calculated rate constants and reverse concentration of CMC in 0.1 M NaCl solution.

Table 2. Rate Constant and CMC Concentrations in 0.1 M NaCl Solution

K × 10^6 ($mol^2L^{-2}min^{-1}$)	52.0	31.0	23.30	18.10	13.20
Concentration (gL^{-1})	0.02	0.04	0.06	0.08	0.1

4. Discussion

When a plot a relative viscosity against concentration which is applied of the simplified Huggins equation (Eq. (5)) in which intermolecular interactions are not considered, the fitting linear plot could not be obtained by using this second model also this model has poor correlation coefficient values (0.15-0.440), with or without sonicated treatment. These results suggest that when molecular chains are long and tend to form entangled structures. The molecular interaction is essential and should not be neglected. On the contrary, since the molecular chains become shorter and stiffer, due to sonication treatment, the influence of molecular interaction on intrinsic viscosity becomes smaller and less critical.

The data in table 2 indicate that the rate constant of ultrasonic degradation decreases with increasing solution concentration.

The interpretation of these observations is that there is less overlap between polymer chains at low concentrations. Therefore, they are more susceptible to the hydrodynamic forces generated around cavitation bubbles.

5. Conclusions

In this work, the ultrasonic degradation of CMC in salt solutions was systematically studied. The rate and extent of degradation of polymer decrease with increasing solution concentration. With increasing solution concentration, their viscosities increase, and it reduces the shear gradients around the collapsing bubbles. Therefore, degradation rate decreases too. A simple kinetic model using viscosity data was used for studying the kinetics of degradation. This model optimally interpreted the experimental findings and thus, viscometry is a practical approach for monitoring the degradation of polymers in a solution.

Acknowledgements

The authors would like to thank Al-Jowfe Company for providing the necessary requirements for this reseach.

Conflict of interest: The authors declare that there are no conflicts of interest.

References

Ahlgren, J. A (1993). Characterization of xanthan gum degrading enzymes from a heat-stable , salt, tolerant bacterial consortium . Develop. Petro. Sci. 39: 55-63. doi:10.1016/S0376-7361(09)70049-4

Antti,G.; Pentti, P.; Hanna K (2008). Ultrasonic degradation of equeous carboxymethyl cellulose: effect of viscosity molecular mass, and concentration. Ultrason. Sonochem. 15: 644-648.doi:10.1016/j.ultsonch.2007.09.005

Bajpai, A. K; Giri, A (2003). Water sorption behavior of high swilling (carboxymethyl cellulose-g-Polyacrylamide) hydrogels and release of potassium nitrate as a grochemical. Carbohydr. Polym.53: 271-279. doi:10.1016 /S0144-8617(03)00071-7

Basedow, A. M.; Ebret, K. H.; (1977). Ultrasonic degradation of polumers in solution. Adv. Polym. Sci. 22: 83-148. doi:10.1007/3-540-07942-4_6

Capitani, D.; Porro, F.; serge, A. L (2000). High field NMR analysis of the degree of substitution in carboxymethyl cellulose sodium salt Carbohydr. Polym. 42: 283-286. doi:10. 1016/S0144-8617(99)00173-3

Christensen, B. E.; Smidsroed, O.; Elgseater, A.; Stokke, B. T(1993). Depolymerization of double-stranded xanthan by acid hydrolysis: Characterization of partially degraded double strands and single-stranded oligomers relased from the ordered structures. Macromolecules. 26: 6111-6120. doi:10.1021/ma00074a037

Clasen, C.; kulicke, W. M (2001). Determination of viscoelastic and rheo-optical material functions of water-soluble cellulose derivatives. Prog. Polym. Sci. 26:1839-1919. doi:10.1016/S0079-6700(01)00024-7

Elliot J H, Ganz A J (1974) Some rheological properties of sodium carboxymethyl cellulose solutions and gels. Rheol. Acta. 13: 670-674. doi:10.1007/ BF 01527058

Guo, J. H.; Skinner, G. W; Harcum, W. W.; Barnum, P. E (1998). Pharmaceutical applications of naturally occurring water-soluble polymers..Pharm. Sci. Technol. To. 1: 254-261. doi:10.1016/S1461-5347(98)00072-8

Kokol, V (2002). Interactions between Polysaccharide polymer thickener and bifunctional bireactive dye in the presence of nonionic surfactants Part1 , surface tension and rheological behavior of different polysaccharide solution. Carbohydr. Polym. 50: 227-236. doi:10.1016/S0144-8617(02) 00035-8

Lakshmi, D. S.; Trivedi, N.; Reddy, C. R. K (2017). Synthesis and characterization of seaweed cellulose derived carboxymethyl cellulose. Carbohydr. Polym. 157: 1604-1610. doi:10.1016/j.carbpol.2016.11.042

Lund, T.; Lecourtier, J.; Muller, G (1990). Properties of xanthan solutions after long-term heat treatment at 90^0C. Polym. Degrad. Stabil. 27: 211-225. doi:org/10.1016/0141-3910 (90)90110-S

Milas, M.; Rinando, M.; Tinland, B (1986). Comparative depolymerization of xanthan gum by ultrasonic and enzymic treatments. Rheological and structural properties. Carbohydr. Polym.6: 95-107. doi:10. 1016/ j.polymdegradstab.2011.01.026

Mohod, A. V.; Gogate, P. R (2011). Ultrasonic degradation of polumers: effect of operating parameters and intensification using additives for carboxymethyl cellulose (CMC) and polyvinyl alcohol (PVA). Ultrason. Sonochem .18: 727-734. doi:10. 1016/j.ultsonch.2010.11.002

Muchovà, M.; Ruźićka, J.; Julinorà, M.; Doleźalovà, M.; Houser, J.; Koutny, M.; Bunkovà, L (2009). Xanthan and gellan degradation by bacterial of activated sludge. Water Sci. Technol. 60: 965-973. doi:10.2166 /wst. 2009.443

Mulet, A.; Carel, J.; Benedito, J.; Rossello, C.; Simal, S (2002). Ultrasonic mass transfer enhancement in food processing. In J.Welti-Chanes & J.F. Velez-Ruiz (Eds.), Transport phenomena in food processing. Boca Raton: CRC press. pp, 265-277.

Pourjavadi, A.; Barzegar, Sh.; Mahdavinia, GR (2006). MBA-cross linked Na-Alg/CMC as smart Full-Polysaccharide Superabsorbent hydrogels. Carbohydr. Polym. 66: 386-395. doi:10. 1016 /j. carbpol.2006.03.013

Reynolds, M. A.; Aichelmann-Reidy, M. E.; Kasslois, J. D.; Parsad, H. S.; Dohrer, M. D(2007). Calcium Sulfate- carboxymethyl cellulose bone graft binder: Histologic and morphometeric evaluation in critical size defect. J. Biomed. Mater. Res. B. Appl. Biomater. Part B: Appl. Biomater. 83: 451-458. doi:10.1002/jbm.b.30815

Sakairi, N.; Suzuki, S.; Uneo, K.; Han, S.; Nishi, N.; Tokura, S (1998). .Biosynthesis of netero- Paysaccharides by acetobacterxylinum-synthesis and characterization of metal-ion adsorptive properties of partially carboxymethylated cellulose Carbohydr. Polym. 37: 409-414. doi:10.1016/S0144-8617 (97) 00226-9

Samant, S. K.; Singhal, R. S.; Kullkarni, P. R.; Regga, D. V (1993). Protein Polysaccharide interaction : A new approach in food formulation. Int. J. Food Sci. Technol. 28: 457-562. doi:10. 1016/S0144-8617(99) 00173-3

Santa-Comba, A.; Pereira, A.; Lemos, R.; Santos, D.; Amarante, J.; Pinto, M (2001). Evaluation of carboxymethyl cellulose, hydroxypropyl methly cellulose, and aluminum hydroxide as potential carriers for rhBMP-2. J. Biomed. Mater. Res. 55: 396-400. doi: 10.1002/1097-4636(20010605) 55:33 .0.CO; 2-Q

Soares, R. M. D.; Lima, A. M. F.; Olivera, R. V. B.; Pires, A. T. N.; Soldi, V (2005). Thermal degradation of biodegradable edible films based on xanthan and starches from different sources. Polym. Degrade. Stabil. 90: 449-454. doi:10.1016/j.polymdegradstab. 2005. 04.007

Srivastava, A.; Mishra, V.; Singh, P.; Srivastava, A.; Kumar, R (2012). Comparative study of thermal degradation behavior of graft copolymers of Polysaccharides and vinyl monomers. J. Therm. Anal. Cal. 107: 211-223. doi:10.1007/s10973-011-1921-y.

Taghizadeh, M. T.; Mehrdad, A (2003). Calculation of the rate constant for the ultrasonic degradation of equeous solutions of polyvinyl alcohol by viscometry. Ultrason. Sonochem.. 10: 309-313. doi:10.1016/ S 1350-4177(03)00110-X

Taghizadeh, M. T.; Abdullahi, R (2011). Sonolytic, Sonocatalytic and sonophotocatalytic degradation of chitosan in presence of TiO2. Ultrason. Sonochem. 18: 149-157. doi:10. 1016/j.ultsonch.2010.04.004

Zaleska, H.; Ring, S.; Tomasik, P (2001). Electosynthesis of potato starch-whey protein isolate complexes. Carbohydr. Polym. 45: 89-94. doi:10.1016/S0144-8617 (00)00239-3

Zaleska, H.; Ring, S.; Tomasik, P (2001). Electosynthesis of potato starch-casein complexes. Int. J. Food Sci. Technol. 36:509-515. doi:10.1046 /j.1365-2621.2001.00491.x

White, J. L.; Kim, K. J (2008). Thermoplastic and rubber compounds: Technology and physical chemistry. Munich: carl Hancer verlag.pp. 119-125.

Scientific Journal for the Faculty of Science-Sirte University Vol. 1, No. 1 October (2021) 39-46

Scientific Journal for the Faculty of Science-Sirte University
(SJFSSU)
Journal home page: http://journal.su.edu.ly/index.php/JSFSU/index

Comparison between Median Filter and Wiener Filter to Get High Accuracy for Blood Vessel Image Extraction

Akram Gihedan[1], Salma Albargathe[2], Mohamed Hasni[3], Waleed Khalafullah[4], Tarek Nagem[5]*

[1,2] *Computer Department, Art and Science Faculty , Omar Al-Mukhtar University-Branch of Algoba-Libya*
[3] *Computer Department, Art and Science Faculty, Omar Al-Mukhtar University-Branch of Derna-Libya*
[4] *Computer Department, Engineering Faculty, College of Computer Technology- Benghazi-Libya*
[5] *Computer Department, Engineering Faculty, The higher Institute of Engineering professional-Almajurie-Benghazi-Libya*

ARTICLE INFO

Article history:

Received 24 August -2021

Received in revised form 16 September 2021

Accepted 26 September 2021

Keywords:

Segmentation,

Computer Vision,

Image Processing,

Filtration.

ABSTRACT

With today's advancing technology, support of developing hardware and software systems, the developments in the field of medicine have increased considerably. In particular, medical image analysis and processing systems have taken a considerable lead. The development of an automatic system could provide great convenience for doctors and practitioners in the field. The image processing techniques proposed in this study can contribute to more effective analysis and more accurate diagnosis, regardless of the individual levels of experience of the users or particular situations and conditions such as fatigue or image quality. This paper presents a robust method for retinal blood vessel segmentation and some automatic algorithms for analyzing the vessel network and pixel classification into vessel and non-vessel .The aim of the work extraction or segmentation of retinal blood vessels used computer vision and image processing for getting high accuracy (comparison with manual) .Also We used the preprocessing techniques for enhancement of the image .And used two types of filter for comparing result to get best scenario. Also for simulation result we used the matlab and implement on DRIVE database.

1 Introduction

Fluorescein angiography (Wright, Young, Read, & Chang, 2018) is an early method for taking photographs of the fundus, or back of the eye, required the injection of fluorescein into blood stream to enhance the contrast of retinal blood vessels. However, with regarding advances in information and communication technology during last decade, digital fundus photography of retina has been developed. Fundus imaging is the process of obtaining the projection of the 3-D semitransparent retinal tissue onto the imaging plane as a 2-D representation using the reflected light and the image intensities to represent the amount of a reflected quantity of light. There are several reasons why digital fundus images have been widely used in many projects. Firstly, the publicity available databases have used fundus photographs of patients. Secondly this kind of photography is very useful for population-based and diagnose various type of systemic diseases such as diabetics, arteriosclerosis, and hypertension. Lastly and the most important advantage of corresponding images is possibility of precise measurement and monitoring of width and tortuosity of retinal blood vessels. The retina is a capillary semi-transparent and slightly pink-red color that covers the inside of the eyeball. The retina is a layer of the eye at the back of the eye that contains light-sensitive cells and nerve fibers that carry visual information to the brain and perform visual function.

Corresponding author:
E-mail: akram_kalil2010@yahoo.com
DOI: https://doi.org/10.37375/sjfssu.v1i1.74

The retina is basically made up of two main layers, the inner sensory layer (neurosensory) and the outer pigment layer. The inner sensory layer is composed of 10 separate cellular layers. The point where the picture falls is in the 9th floor. The diameter of this spot is about 1 mm. In addition, the retina, called the reticular layer, completely covers the inner posterior wall of the eyeball and is made up of millions of visual cells and neurons to which they are attached. The extensions of these nerve cells come together to form the visual nerve. The veins feeding these cells are also located in the retina layer as shown in (figure1).

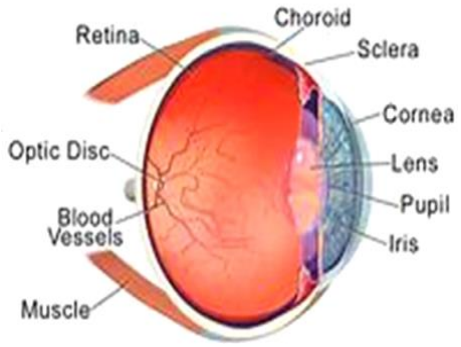

Figure 1. Anatomy of the Eye (Dolz-Marco et al., 2017)

Manual segmentation of the retinal blood vessels is arduous and time-consuming, and making a detailed segmentation can be challenging if the complexity of the vascular network is too high. Thus, segmentation extraction of blood vessel images is valuable, as it decreases the time and effort required, and in the best-case scenario, an automated algorithm can provide as good or better segmentation results as an expert by manual labeling. Automated blood vessel segmentation has faced challenges related to low contrast in images, wide range of vessel widths and variety of different structures in retinal images such as retinal image boundaries, optic disc and retinal lesions caused by diseases.

1.1 Related work

(Nguyen, Bhuiyan, Park, & Ramamohanarao, 2013) proposed a method of blood vessel segmentation using multi-scale line detection. The proposed method is based on changing the length of the line detector, and as a result of this process, multiple line detectors with different measurement values are collected. In order to maintain the efficiency of this method and eliminate the shortcomings of each individual line detector, the final segmentation of each retinal image is performed by linearly connected variable measurements. The performance of this method has been evaluated on 3 available declared databases, which are DRIVE, STARE and REVIEW. The proposed method achieves high accuracy on DRIVE and STARE databases compared to other existing methods. The precision for DRIVE is 0.9407 and for STARE it is 0.9324. These results are collected where there is a high density of vessels and difficult segmentation.

This method produces an accurate segmentation process on the central reflector vessel and it can be verified by visual inspection. On the other hand, the performance on the REVIEW database is also extremely accurate and close to the measurement provided by the experts. In addition, the proposed method has many advantages such as; rapid, primitive and stable segmentation stress to be overcome with high resolution retinal images. (Roychowdhury, Koozekanani, & Parhi, 2015) Proposes a method of segmentation of blood vessels based on the extraction of primary vessels and further classification. The proposed method presents a novel three-step vascular segmentation algorithm with the use of background images. In the first step, the green plane of the bottom image is accumulated and this image is processed before removing a directly concatenated image after high pass screening and what else is duplicated image for areas of vessels enhanced by morphological reconstruction. Key vascular regions are indicated as the intersection between the threshold version of preprocessed retinal images such as to phasic images and filtered images. Regions common to the high pass filter and the morphologically reconstructed image are ejected as primary veins.

The numbers of pixels specified are the main circuits which can increase or decrease when the pixel threshold value is changed. Furthermore all of the residual pixels from both binary images are classified with the aid of a Gaussian Mixture Model (GMM). After that A Gaussian Mixture Model classifier with 2-Gaussian is used for identifying the decent vessel pixels. This classifier uses a set of 8 features. These 8 features are extracted from neighbor pixel and first-second order gradient images. Subsequently the major parts of vessels will be combined with the classified vessel pixels. This proposed method requires short segmentation time while achieving well accuracy on retinal images. The accuracy of this proposed method is %95.2.

This method was tested on 3 avowedly available datasets, DRIVE, STARE and CHASE_DB1. This proposed method outperforms nearly most of the existing methods. Additionally required segmentation time of this method is approximately 8 seconds. The proposed method by (Marín, Aquino, Gegúndez-Arias, & Bravo, 2011) requires a time of 90 seconds to complete the process , while this proposed method by (Roychowdhury et al., 2015) needs one in ten time compared to Marin's method. (Lam, Gao, & Liew, 2010) proposes a vessel division procedure utilizing regularization and in view of multi concavity displaying. Recognizing vein in retinal pictures that has shiny and dim sores is a testing undertaking. To

overcome this problem this proposed method uses multi concavity modeling. This method uses both line-shaped concavity measure and differentiable concavity measure. The task of discriminable confocality is to treat bright lesions while line confocal deal with dark lesions that have a different intensity structure from the vessels in the retinal image which have a line pattern. Since the luminous lesions are of excessive intensity, the luminous lesions can be effectively separated from the circuit and not the circuit by measuring the level of the condenser. Vascular has a line-like intensity structure while dark lesions have an unstable shape.

The line curve is shown to cut the smoldering wound while preserving the position of the veins. To manage inappropriate agitation due to different circle strength in retinal images and to normalize the quality of noise release, a separately standardized gravimetric measurement is described. These 3 condensates measurements are relevant to a specific end goal of discriminating vessels in retinal imaging. Experimental sequelae of the proposed strategy give the best performance compared to existing strategies on distorted retinas, and the accuracy of this technique beats human witnessing ability, which those other existing strategies have not been able to implement. This proposed method can even show very remarkable effects on pathological retinas. The proposed method has an accuracy of 0.9556. MATLAB software was used for this method. The execution time for this method is 13 minutes. The result of this method is that most of the light and dark lesions are removed. (Al-Rawi, Qutaishat, & Arrar, 2007) proposed an improved matched filter for detecting blood vessels from retinal images.

In this proposed method matched filter's performance is improved by committing preferable filter coefficients. These improved filter coefficients were found by optimization methodology on retinal images that taken from DRIVE database. The original matched filter mainly had 3 parameters that control its response.

The outcome of this proposed matched filter is a sustained image. The new improved matched filter shows superior performance when compared to other matched filter containing methods. Output of this improved matched filter will be a sustained image, consequently a thresholding methodology should be evaluated in order to segment blood veins. Threshold value can be estimated experimentally. While the average value of threshold is working efficiently, a mechanized method for estimating the threshold valuation with utilizing the Euler number in the images and additionally it predicts the threshold valuation with utilizing the number of components that are in connection. Briefly the output of this sustained matched filter's image will be thresholded as long as initial regional minima occur. With using this proposed method, the accuracy of %95.1 is reached. (Xu & Luo, 2010) proposed a new method for detection of blood vessels in retinal images. This proposed method uses a method known as adaptive thresholding to generate a binary image and then large connected components such as large circuits will be extracted as well as the thinnest circuits. Most thin ships are classified using Vector Support Machines. With the use of a carrier vector machine, thin circuits with poor contrast can be identified.

The advantage of this proposed method is that it does not require heavy computation and additional manual intervention. This proposed method is tested on DRIVE database and reach mean sensitivity of %77 meantime reaching mean accuracy of %93.2. The comparison of their methods with other methods is shown in (Table1). Comparison of proposed methods' Average Accuracy (AAC).

Proposed method by	AAC
Marin et al (Marín et al., 2011)	0.9489
Shah et al (Shah, Tang, Faye, & Laude, 2017)	0.9479
Badsha et al (Badsha, Reza, Tan, & Dimyati, 2013)	0.9731
Miri et al (Miri & Mahloojifar, 2011)	0.9458
Ali et al(K. Ali, Jalil, Gull, & Fiaz, 2011)	0.9600
Nguyen et al (Nguyen et al., 2013)	0.9407
Akram et al (Akram & Khan, 2013)	0.9485
Roychowdhury et al(Roychowdhury et al., 2015)	0.9515
Lam et al(Lam et al., 2010)	0.9472
Fan et al (Fan, Lu, & Rong, 2016)	0.9580
Ali et al(A. Ali, Zaki, & Hussain, 2017)	0.9425
Eladawi etal (Eladawi et al., 2017)	0.9541
Ricci et al (Ricci & Perfetti, 2007)	0.9572
Zhang et al (Zhang, Zhang, Zhang, & Karray, 2010)	0.9484
Soares et al (Soares, Leandro, Cesar, Jelinek, & Cree, 2006)	0.9466
Bhuiyan etal (Bhuiyan, Nath, Chua, & Kotagiri, 2007)	0.9961
Al-Rawi etal (Al-Rawi et al., 2007)	0.9352
Xu et al (Xu & Luo, 2010)	0.9320

Table 1. The comparison of their methods with other methods

2. Materials and Methods

2.1 Sensitivity, Specificity and Accuracy

There are several terms that are commonly used along with the description of sensitivity, specificity and accuracy) Fawcett, 2006(. TP indicates positive pixels which have correctly been labeled positive, FP indicates incorrect negative pixels which have been labeled positive, FN indicates positive pixels which have incorrectly been labeled as negative pixels and TN indicates negative pixels which have correctly been labeled as negative. If a disease is proven present in a patient, the given diagnostic test also indicates the presence of disease, the result of the diagnostic test is considered true positive (TP). If a disease is proven absent in a patient, the diagnostic test suggests the disease is absent as well, the test result is true negative (TN). Both (TP) and (TN) suggest a consistent result between the diagnostic test and the proven condition (also called standard of truth). However, no medical test is perfect. If the diagnostic test indicates the presence of disease in a patient who actually has no such disease, the test result is false positive (FP). Crossing and branching in the veneer can complicate the image model. Most medical images pose significant problems in removing blood vessels, such as signal noise, image intensity shift, and image contrast mishandling.

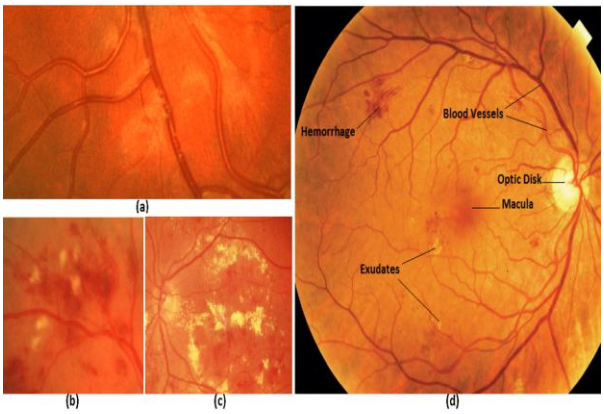

Figure 2. Morphology of retinal images: a) Central Vascular Reflex and Background Irregularity b) Cotton Wool Spots, c) Stiff Axes, d) Retinas an Atomic Structures.

However, no medical test is perfect. If the diagnostic test indicates the presence of disease in a patient who actually has no such disease, the test result is false positive (FP) (Rahebi & Hardalaç, 2014).

The sensitivity (TPR), specificity (TNR) and accuracy (ACC) are shown as equation (1), (2) and (3) respectively ()Fraz et al., 2012().

***Sensitivity** (TPR) = TP / (TP + FN) (1)

***Specificity** (TNR) = TN / (TN + FP) (2)

***Accuracy** (ACC) = (TP + TN)/(TP + FN + TN +FP) (3)

2.2 DRIVE Database

The DRIVE (Digital Retinal Images for Vessel Extraction) is a publicly available database. The photographs for the DRIVE database were obtained from a diabetic retinopathy screening program in The Netherlands. The screening population consisted of 400 diabetic subjects between 25-90 years of age (Staal, Abràmoff, Niemeijer, Viergever, & Van Ginneken, 2004).(Figure 3) shows retina images from the DRIVE database

(a)

(b)

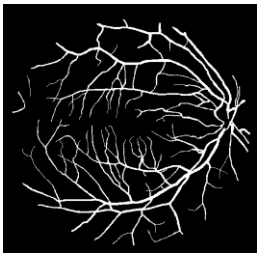

(c)

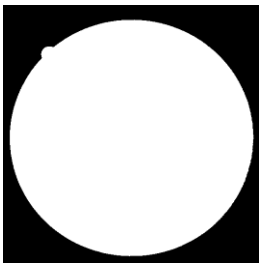

Figure 3. Retinal fundus image 02 from test set of the DRIVE database. a) Original RGB image b) Manual segmentation of blood vessels known as a ground

2.3 Proposed Method

The summary of method is shown in (figure 4).

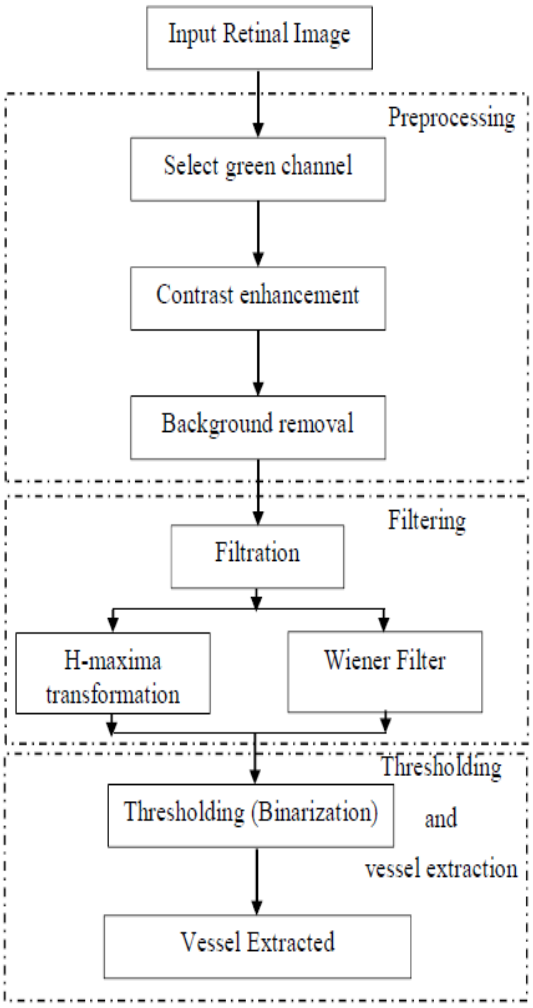

Figure 4. The summary of method

The steps of this flow chart are as following steps:

a. Input retina image from DRIVE database

b. Preprocessing:

- **Select green channel** an image from a standard digital camera will have a red, green and blue channel.
- **Contrast enhancement** for enhancement we used the Morphological structuring element.
- **Background removal** the light reflex of the retinal vessel is formed by the reflection from the interface between the blood column and vessel wall. For getting the foreground the median filter.

c. Filtration

Filters are commonly used to extract a desired signal from a background of random noise or deterministic interference. An image containing salt-and-pepper noise will have dark pixels in bright regions and bright pixels in dark regions so we used two types of filters for do comparing:

- **Median filtering with size 3*3**
  The median filter is a non-linear digital filtering technique, often used to remove noise from an image .The image obtained from top-hat transformation stage is further filtered using median filter to decrease the noise present.

- **Wiener filtering with size 3*3**
  The Wiener filter is a filter used to produce an estimate of a desired or target random process by linear time-invariant (LTI) filtering of an observed noisy process. Wiener filters are developed using time-domain concepts. They are designed to minimize the mean-square error between their output and a desired or required output.

d. Thresholding and vessel extraction

- Thresholding replace each pixel in an image.
- If Pixel values that are less than or equal to the threshold background.
- If Pixel values greater than the threshold foreground (vessels).
-

For getting high performance the vessel the binarization method is used.

The simplest way to use image binarization is to choose a threshold value, and classify all pixels with values above.

3. Results

This paper used 20 images from a ready-made DRIVE database to make the comparison process to get a better scenario when using two types of filters, where we found the best accuracy for the process of segmentation when using the median filter

The result for DRIVE database is shown in (table 2).

Image number	Accuracy Result Wiener filter	Accuracy Result Median filter
1	0.9520	0.963711
2	0.9510	0.961823
3	0.9302	0.951209
4	0.9505	0.960659
5	0.9364	0.958283
6	0.9443	0.95257
7	0.9319	0.957068
8	0.9172	0.95648
9	0.9489	0.961604
10	0.9277	0.962123
11	0.9415	0.958528
12	0.9392	0.957755
13	0.9442	0.954958
14	0.9429	0.96115
15	0.9051	0.96535
16	0.9587	0.962023
17	0.9520	0.960944
18	0.9498	0.963823
19	0.9587	0.970506
20	0.9391	0.963753

Table 2. Result for DRIVE database

The comparison between accuracy result wiener filter and median filter is shown in (figure 5).

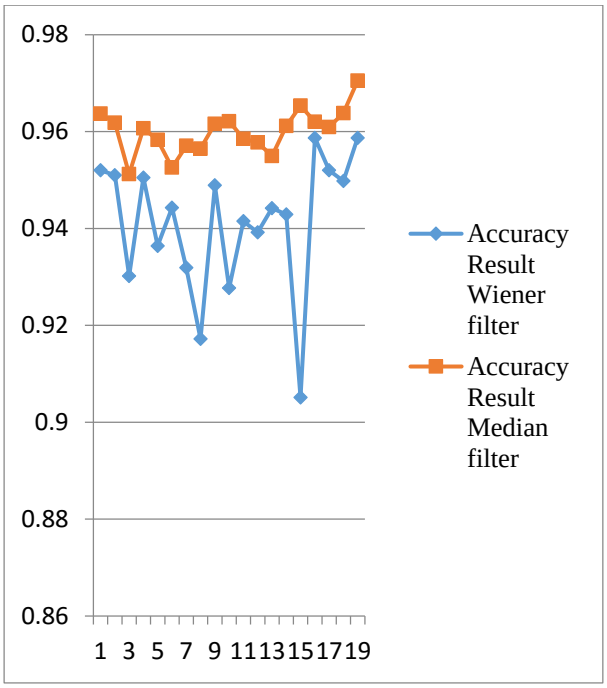

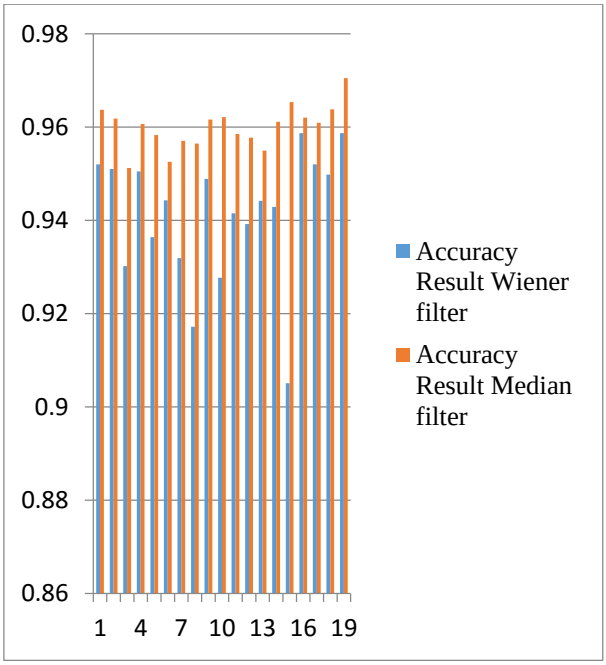

Figure 5. The comparison resulting between Wiener filter and Median filter

4. Discussion

This paper experimented on the database used and the differences were clear between the filters is shown in (figure 6):

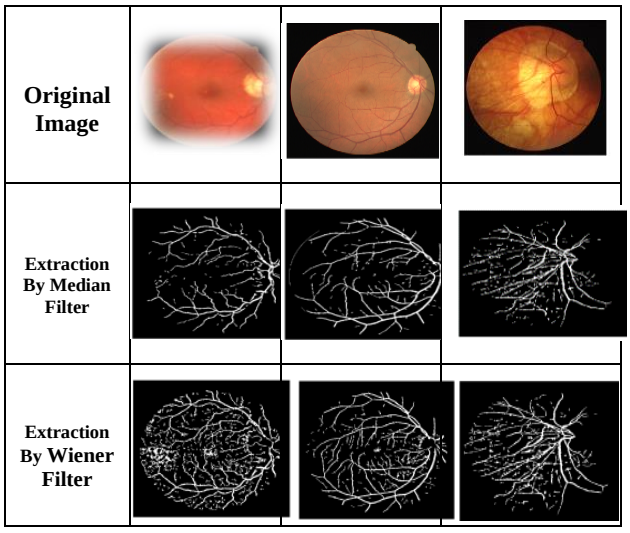

Figure 6. The result image of proposed method.

5. Conclusion

Extraction of blood vessels on retinal imaging will be of great benefit in the near future. These automated detection systems can reduce the workload for ophthalmologists. With the early detection system, patients can get real treatment at the right time. The preprocessing step must be processed to obtain a very precise value. During the preprocessing step, the contrast of the selected mesh image is enhanced to obtain a sharp image and remove an unwanted small object from the image. In addition, some of the grid images are noisy, indicating that this phase noise rejection problem is being solved. Pre-processing has been applied to the photos. We then corrected the changes in brightness in the grid image by applying the point processing described. As evidenced by simulation results, the results are better when using median filter to extract circuits.

Conflict of interest: The authors declare that there are no conflicts of interest.

References

Akram, M. U., & Khan, S. A. (2013). Multilayered thresholding-based blood vessel segmentation for screening of diabetic retinopathy. Engineering with computers, 29(2), 165-173.

Al-Rawi, M., Qutaishat, M., & Arrar, M. (2007). An improved matched filter for blood vessel detection of digital retinal images. Computers in biology and medicine, 37(2), 262-267.

Ali, A., Zaki, W. M. D. W., & Hussain, A. (2017). Blood vessel segmentation from color retinal images using K-means clustering and 2D gabor wavelet. Paper presented at the International Conference on Applied Physics, System Science and Computers.

Ali, K., Jalil, A., Gull, M. U., & Fiaz, M. (2011). Medical image segmentation using h-minima transform and region merging technique. Paper presented at the Frontiers of Information Technology (FIT), 2011.

Badsha, S., Reza, A. W., Tan, K. G., & Dimyati, K. (2013). A new blood vessel extraction technique using edge enhancement and object classification. Journal of digital imaging, 26(6), 1107-1115.

Bhuiyan, A., Nath, B., Chua, J., & Kotagiri, R. (2007). Blood vessel segmentation from color retinal images using unsupervised texture classification. Paper presented at the Image Processing, 2007. ICIP 2007. IEEE International Conference on.

Eladawi, N., Elmogy, M., Helmy, O., Aboelfetouh, A., Riad, A., Sandhu, H., . El-Baz, A. (2017). Automatic blood vessels segmentation based on different retinal maps from OCTA scans. Computers in biology and medicine, 89, 150-161.

Fan, Z., Lu, J., & Rong, Y. (2016). Automated blood vessel segmentation of fundus images using region features of vessels. Paper presented at the Computational Intelligence (SSCI), 2016 IEEE Symposium Series on.

Fawcett, T. (2006). An introduction to ROC analysis. Pattern recognition letters, 27(8), 861-874.

Fraz, M. M., Remagnino, P., Hoppe, A., Uyyanonvara, B., Rudnicka, A. R., Owen, C. G., & Barman, S. A. (2012). Blood vessel segmentation methodologies in retinal images–a survey. Computer methods and programs in biomedicine, 108(1), 407-433.

Lam, B. S., Gao, Y., & Liew, A. W.-C. (2010). General retinal vessel segmentation using regularization-based multiconcavity modeling. IEEE Transactions on medical imaging, 29(7), 1369-1381.

Marín, D., Aquino, A., Gegúndez-Arias, M. E., & Bravo, J. M. (2011). A new supervised method for blood vessel segmentation in retinal images by using gray-level and moment invariants-based features. IEEE Transactions on medical imaging, 30(1), 146-158.

Miri, M. S., & Mahloojifar, A. (2011). Retinal image analysis using curvelet transform and multistructure elements morphology by reconstruction. IEEE Transactions on Biomedical Engineering, 58(5), 1183-1192.

Nguyen, U. T., Bhuiyan, A., Park, L. A., & Ramamohanarao, K. (2013). An effective retinal blood vessel segmentation method using multi-scale line detection. Pattern recognition, 46(3), 703-715.

Rahebi, J., & Hardalaç, F. (2014). Retinal blood vessel segmentation with neural network by using gray-level co-occurrence matrix-based features. Journal of medical systems, 38(8), 85.

Ricci, E., & Perfetti, R. (2007). Retinal blood vessel segmentation using line operators and support vector classification. IEEE Transactions on medical imaging, 26(10), 1357-1365.

Roychowdhury, S., Koozekanani, D. D., & Parhi, K. K. (2015). Blood vessel segmentation of fundus images by major vessel extraction and subimage classification. IEEE journal of biomedical and health informatics, 19(3), 1118-1128.

Shah, S. A. A., Tang, T. B., Faye, I., & Laude, A. (2017). Blood vessel segmentation in color fundus images based on regional and Hessian features. Graefe's Archive for Clinical and Experimental Ophthalmology, 1-9.

Soares, J. V., Leandro, J. J., Cesar, R. M., Jelinek, H. F., & Cree, M. J. (2006). Retinal vessel segmentation using the 2-D Gabor wavelet and supervised classification. IEEE Transactions on medical imaging, 25(9), 1214-1222.

Staal, J., Abràmoff, M. D., Niemeijer, M., Viergever, M. A., & Van Ginneken, B. (2004). Ridge-based vessel segmentation in color images of the retina. IEEE transactions on medical imaging, 23(4), 501-509.

Wright, L., Young, R., Read, S., & Chang, E. (2018). Fluorescein Angiographic Evaluation of Peripheral Retinal Vasculature after Primary Intravitreal Ranibizumab for Retinopathy of Prematurity. Retina (Philadelphia, Pa.).

Xu, L., & Luo, S. (2010). A novel method for blood vessel detection from retinal images. Biomedical engineering online, 9(1), 14.

Zhang, B., Zhang, L., Zhang, L., & Karray, F. (2010). Retinal vessel extraction by matched filter with first-order derivative of Gaussian. Computers in biology and medicine, 40(4), 438-445.

Dolz-Marco, R., Gallego-Pinazo, R., Dansingani, K. K., & Yannuzzi, L. A. (2017). The history of the choroid. In J. Chhablani & J. Ruiz-Medrano (Eds.). Choroidal Disorders, 1(5), 1-5. Academic Press. https://doi.org/0.1016/b978-0-12-805313-3.00001-6

Scientific Journal for the Faculty of Science-Sirte University Vol. 1, No. 1 October (2021) 47-52

Scientific Journal for the Faculty of Science-Sirte University
(SJFSSU)
Journal home page: http://journal.su.edu.ly/index.php/JSFSU/index

Datura stramonium Leaf Extract Toxic Effects on Testis in Swiss Albino Mice *Mus Musculus*

*Soad Mohammed Alwirfli** [1], *Abdalla I. Mohamed,* [2] *Ateeqah Ghayth Alzwawy* [3], *Raja Abdullah Mohammed* [1]

[1]*Zoology Department, Arts and Science Faculty, Benghazi University Libya.*

[2] *Zoology Department, Science Faculty, Benghazi University, Libya.*

[3]*Zoology department, Science Faculty, Ajdabiya University, Libya.*

ARTICLE INFO

Article history:

Received 26 July 2021

Received in revised form 25 August 2021

Accepted 18 September 2021

Keywords:

Datura stramonium,

Male Mice,

Testis weigh,

Histopathology.

ABSTRACT

The notorious weed, jimson weed *(Datura stramonium L.*) is a hallucinogenic plant that is both toxic and medicinal. The presence of tropane alkaloids, which contain a methylation nitrogen atom (N-CH3) and inhibit neurotransmitters in the brain, is thought to be responsible for the plant's neurotoxicity. Toxic symptoms have been linked to the recreational use of *D. stramonium*, according to ethnomedicine.

This investigation has been designed to examine the toxicity and describe the possible changes in the structural function of vital organs, following the orally intubation of non-lethal doses of *D. stramonium* leaves crude aqueous extract. Through preliminary trials, crude aqueous extract. Of 200 mg leaves per kilogram body weight was established as a tolerable non-lethal dose. Three doses 0.36, 0.7, and 4 mg/kg were orally weekly, administered to the male mice in a 0.1 ml volume.

Acute toxicity studies were accomplished through oral intubation of three dosages in each case. Observation and mortality were reported for 24 .48, 72 hours.

Prolonged toxicity was performed through the administration of weekly, single doses oral for 40 days. The observation was made on the mice's testis weight and histological abnormality of a testis organ.

1 Introduction

All nightshades and agricultural plants, including potato, tomato, coffee, and pepper, belong to the genus Datura (Solanaceae). Genetic markers are frequently used in the classification of distinct species within the Datura genus, implying that this genus has a lot of variety owing to mutation.

Humans and other mammals are poisoned by all portions of Jimsonweed. Anticholinergic alkaloids are present in high concentrations in the plants. (block neurotransmitters) and have been used for its psychoactive effects. The concentration of toxins varies greatly from plant to plant making the risk of fatal overdose high (Mukhtar et al., 2019).

D. stramonium is used to treat ulcers, wounds, inflammation, rheumatism and gout, sciatica, bruising and swellings, fever, asthma and bronchitis, toothache, and other human illnesses in Ayurvedic medicine (Kirtikar et al., 1999). *D. stramonium* is used in a variety of folk medicine therapies. The medicinal uses of D. stramonium have been eclipsed by its acute toxic consequences in modern medicine (Gaire et al, 2013). The central nervous system is affected by significant doses of *D. stramonium*, resulting in symptoms such as confusion, odd behavior, hallucinations, and amnesia. Though death by *D. stramonium* poisoning is rare, recovery may take several days (Norton, 2008).

***Corresponding author:**
E-mail: soad.mohammed@uob.edu.ly
DOI: https://doi.org/10.37375/sjfssu.v1i1.54 **SJFSSU 2021**

Therefore, rigorous knowledge and understanding of the acute toxicity effects of this plant is undoubtedly need to be accounted for.

Tropane belladonna alkaloids, which have powerful anticholinergic effects, are the poisons in Jimson weed. Hyoscyamine (leaves, roots, seeds), hyoscine (roots), atropine (d,l-hyoscyamine), scopolamine (l-hyoscine), sitosterol, and proteins are all alkaloids.

1.1 Intoxication and Mode of Action

Consumption of *D. stramonium* interferes and obstructs the action of neurotransmitters in the nervous system. Datura toxins pass through the blood-brain barrier and block acetycholine production (The main neurotransmitter used by the parasympathetic nervous system). Atropine poisoning is very dangerous for children, and the prognosis is usually deadly. The State Chemical Laboratories in Agra, India, evaluated 2,778 deaths caused by consuming Datura from 1950 to 1965. Symptoms likely to be produced by tropane alkaloids such as scopolamine, hyoscyamine, and atropine include urinary retention, Dizziness, convulsions, fever, euphoria, hallucinations, short-term memory loss, and delirium are all symptoms of delirium.

Leaf alkaloids range from 0.25 to 0.45 percent, whereas seed alkaloids range from 0.47 to 0.65 percent. Hyoscine content in leaves is 0.1 percent, 0.05 percent in stems, and 0.1 percent in roots; and hyoscyamine content in leaves is 0.4 percent, 0.2 percent in stems, and 0.1 percent in roots (Kaur *et al*., 2020).

Sperm generation is controlled by the testis, which is the primary male reproductive organ. It is held in place by the scrotal sac's bilateral chambers. The production of spermatozoa from testis stem cells is a time-consuming process that takes approximately 64 days in humans and 48 to 53 days in rats.

Sertoli cells are important for spermatogenesis, but leydig cells are the main source of androgen synthesis. Both types of cells can be harmed by toxins and chemical medications.

A change in the functional integrity of these cells could induce a harmful disruption in hormonal balance, or disrupt the spermatozoa growth process, resulting in reduced male fertility (Adekomim, 2011).

The objective of this experiment is to evaluate the toxicity of *D. stramonium* to testis male Swiss albino mice and this has been achieved by conventional LD50 biochemical function tests in addition to the histo-physiology approach. Changes in behavior, physical activity, and body weight during the period of study have also been observed, Furthermore, the relative weight of testis.

2. Materials and Methods

2.1 Test Animals:

A total of 16 adult male and female Swiss albino mice Mus muscullus were brought, from the animal house of the faculty of Medicine, to the Zoology Department, University of Benghazi. The animals were reared in the laboratory.

2.2 The chemicals:

D. stramonium Hematoxylin, eosin and all other chemicals used in this study were of a technical grade with known structures and functions.

2.3. The experimentation

LD50 determination (Acute toxicity study):

The acute Toxicity of *D. stramonium* was evaluated through using five treatments 200, 100, 50, 25 and 12.5 mg of leaf extract per kg mice body weight. In addition to control treatment receiving only saline water.

Each treatment was replicated two times with four mice per replicate. Mice between the ages of 50 and 70 days were chosen at random for each treatment based on their body weight. The calculated doses (mg/kg) were orally delivered in a 0.1 ml solution through the mouth intubation. Observation were made on the behavior while other symptoms and mortalities were recorded on 24, 48, 72 and 96 hours post treatment.

2.4. Prolonged toxicity study:

A total of 36 male mice were used in this study. The animals were divided into three treatments each treatment contained three replicates and each replicate having three animals. The fourth treatment having 9 mice in three replicates formed the control .Treatment animals were intubated with 0.1 ml solution containing the specified treatment concentration 0.36, 0.7 and 4 mg/kg leaf extract per kg mice body weight, whereas, control mice were orally intubated with 0.1 ml of saline water .

2.5. Tissue Sample:

Testis of each animal were dissected out and weighted. After washing with normal physiology salin solution, the organs were transferred into glass containers containing formalin –acetic acid-alchol (FAA) fixative solution and kept for weighting and histological studies.

3. Results

In the acute toxicity symptoms were found to follow dose dependent acute toxicity to male mice receiving an orally single dose of various concentrations .

After 72hr of exposure no mortality was reported for the 200, 100, 50, 25, 12.5 mg/kg body weight .

Percent organ weight / body weight:

The effect of *D. stramonium* extract on the testis organ were measured through the relative organ weight per 100g body weight in each treatment and compare that with control treatment after 40 days of exposure.

Testis Weight

The relative weight mg testis weight/ 100 g body weight of control and D.stamonium treated male mice revealed a significant differences between control and treated mice (t-test p≤0.5). Control mice had significantly lower weight values compared to all treated mice . The mean±SD of testis weight were 0.71±0.28 for C1 ,0.60±0.21 for C2, 0.76±0.25 for C3 compared to only 0.36±0.11 for control.

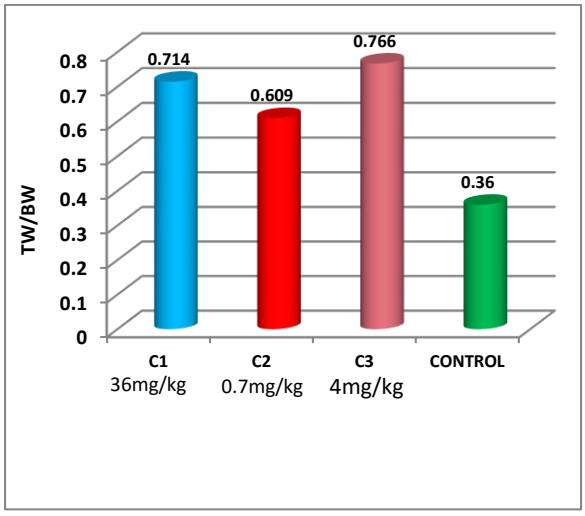

Figure 1: The relative weight mg Testis weight /100g body weight of control and *D. stramonium* treated male mice for 40 days of exposure.

Micromorphology of the organs :

A photomicrograph of the testis of the control group revealed some microstructural alterations due to multiple exposure of adult male mice to the given dose of *D. stramonium* leaves crude aqueous extract (Figure 1).

The seminiferous tubules with dense nuclei spermatogonia, (Figure 2). The portion of tubule in control group showed boundary tissue, spermatocytes, spermatids and spermatozoa, note the intact lining epithelium (Figure 3).

The histological changes in C2 and C3 treatments showed interruption of lining epithelial in somniferous tubule (Figure 4, 5 and 6) .

High magnification of the above section, showed portion of degeneration changes in lining epithelium (Figure 7) .

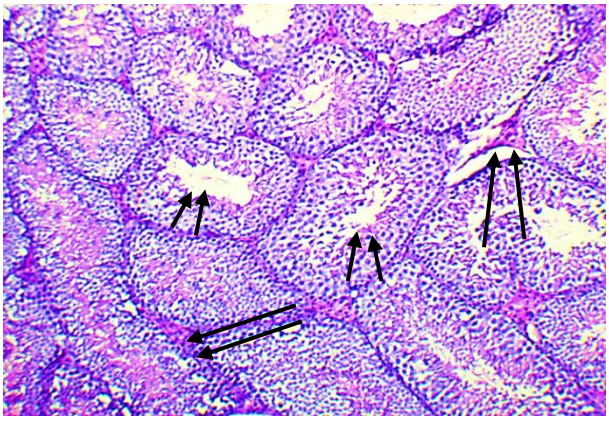

Figure 2: Lower photomicrograph of testis of control showing seminiferous tubules with dense nuclei spermatogonia (short arrow) slight amount of Interstitial connectiue tissue containg groups of leyding cells (arrows). (H&EX 100).

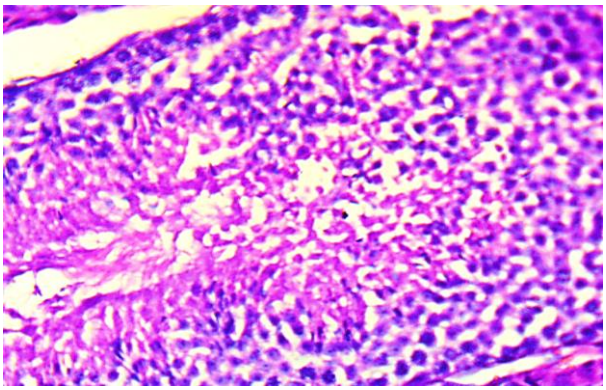

Figure 3: Photomicrograph of portion of one tubule in control group showing boundary tissue, spermatocytes, spermatids and spermatozoa in testis. Note intact lining epithelium. (H&E X400).

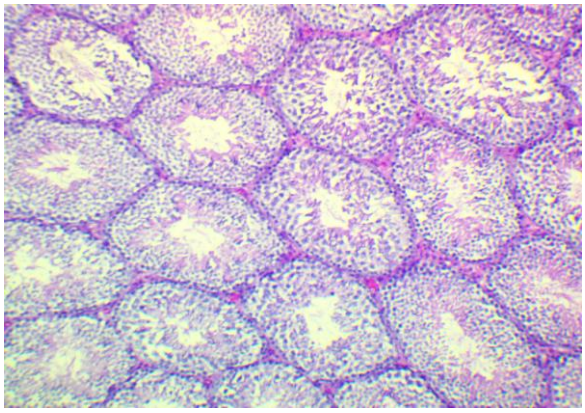

Figure 4: Photomicrograph of testis of treatment C2 showing interruption of lining epithelial in some seminiferous tubules.

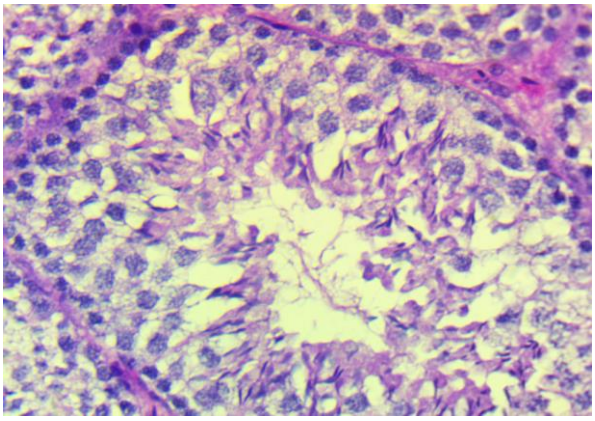

Figure 5: High magnification of the above section, showing portion of one tubule. Note marked degeneration changes in lining epithelium for testis. (H&E X 400).

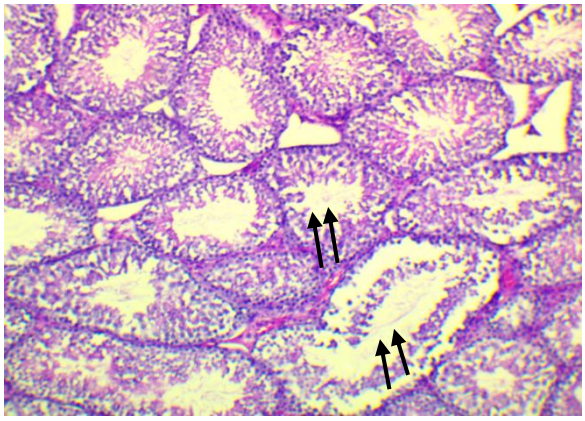

Figure 6: Photomicrograph of testis of treatment C3 showing interruption of lining epithelial in some seminiferous tubules (arrow). (H&E X 100).

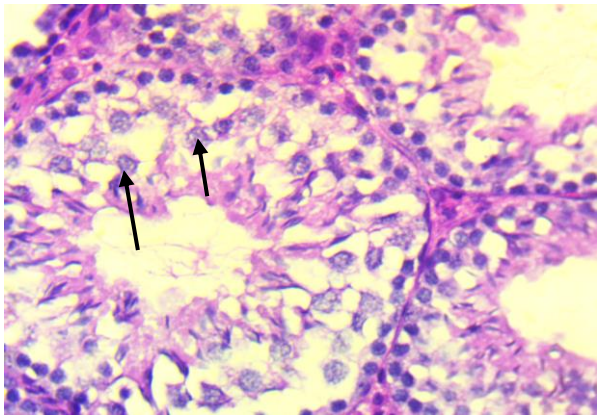

Figure 7: High magnification of the above section, showing portion of one tubule. Note marked degeneration changes in lining epithelium for testis (arrows). (H&E X 400).

4. Discussion

Close observation of the experimental animals have come in favor of optimal suitability of the laboratory conditions throughout period of the investigation. Handling of the males and females for breeding purposes have ensure the availability of the required number of males. This means that criteria such as hygienic measurements, ration, feeding and water , lighting and temperature were quite enough for well being of the males, pregnant females and growing offspring . Furthermore , males of the control treatment continued their normal activity and behavior until the end of the experiment. Males in the treatment group were given oral doses of *D. stramonium* leaves aqueous crude extract under the identical laboratory circumstances as the control group .Therefore contents of the crude aqueous extract collectively , should have stood behind the recorded changes in physical activity and behavior.

These contents should also be considered responsible for the observed deviation from normal that have been exhibited by other investigated selected parameters. Absence of mortalities in both control and extract treatment groups of animals confirmed the availability of sufficient survival requirements.

The toxicity of *D. stramonium* leaf extract was clearly observed in male mice that were exposed through oral doses . Symptoms of intoxication were easily detected . No mortality was detected in the higher used dose 200mg/kg . This result came in support of Antov *et al.*, (1991) who observed several signs of symptoms but no mortality .The toxic responses observed in the treated male mice was also supported by Bouzid *et al.*, (2002) who described similar symptoms of *D. stramonium* toxicity in humans.

The result of the toxicity obtained in this may indicate that *D. stramonium* is slightly toxic, however in reality that might not be the case when looking to previous authors who pointed the degree of this plant toxicity .

Therefore , the lake of mortality even in the higher used dose 200mg/kg leaf extract can be explained (1) most previous works were with the active ingredients of the plant , atropine and Scopolamine, whereas, our study was on the crud extract of the plant . (2) The extraction efficiency could have been low, resulting in a low percentage of the active component from the plant.(3) No organic solvent used in the extraction because the intention was on the whole plant constituents which is mostly used in the case of medication or poisoning and that synergism or antagonisms could happen in the two cases.

Furthermore, survival of the extract treatment male mice could be invested to point out to the employed tolerable non –lethal dose of the crude aqueous extract though it was repeated 4 times over 40 days weekly.

Several abnormal histological alterations seen in the testes of the animals in the treatment group, ranges from degeneration and disruption of the germ cells lining the somniferous tubules, and also the degeneration of the leydig cells. Reduction in the population of the germ cells was also seen in the histological profile of the testes obtained from the treatment group compared with the control group. This means that the number of viable sperm is decreasing, which could lead to infertility. Degenerative changes have been scientifically reported to result in cell death. There are two types of cell death, namely, apoptosis and necrosis (Cohen, 1993). Biochemically and morphologically, these two categories are distinct (Bose and Sinha, 1994). Apoptosis is a non-inflammatory response to tissue damage characterized by a series of morphological and biochemical alterations (Shen *et al*., 2002).

All parts of the plant are toxic because of their high tropane alkaloid level . Atropine and scopolamine have an approximate amount of 0.20 and 0.65 mg per flower, respectively. Because the average adult's suggested therapeutic dose of atropine plus scopolamine is 0.5 mg, it's easy to see how ingestion of just 10 blossoms can result in death. (Diker *et al*., 2007).

5. Conclusion

The weekly oral administration of non-lethal dose of D. stramonium leaves aqueous extract have been well tolerated by the male Swiss albino mice as judged by the mild transient neurotoxicity symptoms. Nevertheless, negative impacts have been observed on the body weight gain and on testis histology.

From the present study it is clear that the doses used in the acute toxicity study did not reveal in any degree of mortalities although stress symptoms were reported.

In the prolonged toxicity studies and at the designed 0.36, 0.7, 4 mg /kg concentration, significant changes in body weight between control and treatment were found.

Histological finding did reveal adverse effects on the testis .

Result of the present investigation has pointed out the necessity for systematic series of trials leading to the establishment of facts and solid information about the commonly used folk medication of this plant.

Acknowledgements

The authors thank Dr. Abdullah Ibrahim, Department of Zoology, Faculty of Science, University of Benghazi, for the guidance and inspiration. The authors also thank Dr. Mabrouka Al-Rafadi, Department of Zoology, College of Science, University of Benghazi; We also thank the lecturer, Umm Al-Ezz Gaddafi, the Higher Institute of Medical Professions, Benghazi.

Conflict of interest: The authors declare that there are no conflicts of interest.

References

Adekomi, DA. Musa, A. A. Tijani, A. A. Adeniyi TD. Usman, B. (2011). Exposure to smoke extract of Datura stramonium leaf:Some of its effects on the heart, liver, lungs, kidneys and testes of male Sprague Dawley rats. Journal of Pharmacognosy and Phytotherapy 3(5), pp. 67-75

Antov, G. Zaikov C, Bouzidi A, Mitova S, Michaelova A, Halkova J, Choumkov, N. (1991). Biochemical and histological changes after acute oral poisoning with the acetanilide herbicide acetochlor. J. Toxicol.Clin.11: 349-356.

Bose, S. Sinha, S. (1994). Modulation of Ochratoxin-Produced Genotoxicity in Mice by Vitamin C. *Food Chem. Toxicol.* 32: 533-537

Bouzid M., Allouche L, Houches B. (2002). Studies Epidemiological poisonous plants in the regions of Setif and Bordj Bou Arreridj. Algeria. *Bull. Inf. Toxicol.*, 18: 5- 10

Cohen J. (1993). Apoptosis. *Immunol. Today*, 14: 126-130.

Diker D, Markovitz, D, Rothman M,Sendovski U .(2007) Coma as a presenting sign of Datura stramonium seed tea poisoning . Eur J Int Med .18(4):336-338.

Gaire BP, Subedi L.(2013). A review on the pharmacological

and toxicological aspects of Datura stramonium L. *J Integr Med*. 11(2): 73-79.

Kaur, S. Pandey, N. Shallu (2020). Phytochemistry and Pharmacological Properties of Datura stramonium: An Analysis. *Ind. J.* Pure App. Biosc. 8(3), 92-105

Kirtikar KR, Basu BD. (1999). Indian medicinal plants. 2nd ed. Volume III. Dehradun: *International Book Distributors*. 1783-1787.

Mukhtar, Y. Tukur, S. Bashir, R. (2019). An Overview on Datura stramonium L.(Jimson weed):A Notable Psychoactive Drug Plant. American Journal of Natural Sciences Vol.2, Issue 1, pp 1- 9

Norton, S. (2008). Toxic effects of plants. In: Klaassen CD. Caserett and Doull's toxicology, the basic science of poisons. *7th ed. New York: McGraw Hil*l. 1110.

Shen, H. Dai, J. Chia, S. Lim, A. Ong, C. (2002). Detection of Apoptotic Alterations in Sperm in Subfertile Patients and their Correlations with Sperm Quality. J. Hum Reprod. 17: 1266-1273.

Scientific Journal for the Faculty of Science-Sirte University Vol. 1, No. 1 October (2021) 53-60

Scientific Journal for the Faculty of Science-Sirte University
(SJFSSU)
Journal home page: http://journal.su.edu.ly/index.php/JSFSU/index

Quality Assessment of Underground Water before and after Treatment: A Case Study of Tobruk City, Libya

*Mohamed Masoud**[1], Abdullah Abdullah[1], Anwar Abadelrahim[2] and Tahani Y. M. Aeyad[3]*

[1], [2] *Natural Resources Department, Tobruk, Libya University Libya*
[2] *Environmental Sciences Department, Tobruk, Libya University. Libya*
[3] *Chemistry Department, Benghazi University, Elmarj, Libya.*

ARTICLE INFO

Article history:

Received 15 August 2021
Received in revised form 27 September 2021
Accepted 12 October 2021

Keywords:

Tobruk,
Wells,
Underground water,
Treatment,
Pollutions.

ABSTRACT

The present study was carried out to assess the quality of various wells for drinking purposes and with regard to their current state of repair. Ten wells (W1, W2, W3, W4, W5, W6, W7, W8, W9 and S10) were selected in the study area. This study was designed to determine the physico-chemical and bacteriological quality of wells water before and after water treatment in east Libya, specifically in Tobruk. The bacterial load (E. Coli) of the water samples was determined using standard microbiological methods. Physicochemical properties including pH, total dissolved solids (TDS), electrical conductivity, and Na^+, K^+, Ca^{2+}, Cl^-, NaCl concentrations and total alkalinity were determined. The values obtained were compared with the World Health Organization (WHO) standards for drinking water. The results showed that E. Coli bacteria were present in some wells prior to treatment, but were *E. Coli*-free post-treatment. Furthermore, the physico-chemical parameters of the water samples were generally greater the limits recommended by the WHO with particularly high values seen in well W10, prior to treatment. However, only a few of the bacteriological and physicochemical parameters of the water samples remained above the tolerable limits recommended by the WHO (WHO, 2011) post-treatment. This suggests that regular monitoring and purification of boreholes to ensure good water quality is vital to maintaining the required health standards.

1 Introduction

The increase in the number of people who are today using underground water for different forms of human activity, such as freshwater, agriculture, industry, and other uses. In Libya, groundwater from wells represents the major sources of drinking water and water for domestic purposes (Salem & Alshergawi, 2013). Polluted water is main cause of diarrhoea worldwide (UNICEF, 2013) and this report showing that 2,000 children under 5 years old die every day all world due to diarrheal diseases, 90% of which are directly related to contaminated drinking water. Aquifers are a huge storehouse of Earth's water which is estimated to be about 94% of fresh water and people all over the world depend on groundwater in their daily lives (Heath, 1987). The cycle of groundwater begins with water falling on the land surface and slowly penetrating deep into the earth. Before reaching the ground, however, the rain comes into contact with bacteria and some of dissolved solids and suspended solids (Gibb, 1973). The source of diseases due to micro-organism and pollution related to drinking water from wells by non-suitable means used in treatment plants (Al-Azzawi, 2010). For this reason, the WHO has identified lack of access to clean drinking water as the most critical factor influencing the general health and wellbeing of populations in developing countries

Corresponding author:
E-mail Elwrfally@tu.edu.ly
DOI: https://doi.org/10.37375/sjfssu.v1i1.73

(Hoko, 2005). Overall, the provision of safe drinking water can help to reduce or eliminate preventable deaths (such as those emanating from waterborne diseases) and improve the quality of life for low-income households around the world (Lawson & Emmanuel, 2011). The main objective of this study is to evaluate the quality of borehole water in different communities in selected districts of Tobruk, Libya, and its nearby surrounding for drinking purposes. This study is considered to be the first of its kind to assess groundwater quality in this region. Therefore, this study will be an essential reference for decision makers with regard to regional groundwater management and protection.

1.1 The Geomorphology of the City:

The north-eastern coastal area of Libya is subdivided into two geomorphic units; the northern scarped terrain (Al Dafna plateau), which is marked by the presence of many prominent scarps running in an ESE-WNW direction and the southern part of Al Bardia area, which is flat and monotonous plain (El Deftar, 1977; Sweedan, 1977). Stratigraphically, the Al Dafna coastal plateau is formed of Late Eocene to Early-Middle Miocene succession and is subdivided into three formations: (i) the Al Khowaymat Formation (Late Eocene-Early Oligocene), which is considered to be the oldest rock unit in the region and that consists of limestone and dolomite. Glauconitic and Nummulite layers occur at the top of the section; (ii) the Al Faidiyah Formation: (Late Oligocene-Early Miocene), which consists of chalky limestone layers rich with fossils and carbonate mud. It constitutes 90% of the rocks that appear on the beach in the eastern region, starting from the city of Darnah, forming cliffs, terraces and sea heads; and (iii) the Al Jaghbub Formation (Early-Middle Miocene), which is a hard limestone with a yellowish-white colour but that can also be reddish in some parts and that covers most of Tobruk. Al Jaghbub Formation layers are the most widespread and distributed in the areas of the study with thicknesses reaching up to 34.5 metres (Adam, 2018).

1.2 The study area:

The study area lies in Tobruk, located in eastern Libya. It lies at latitude 32^0 04` 45" N and longitude $23^0$ 57` 20" E on the Mediterranean Sea coast of the eastern part of Libya. Comprising the east of the city at W1 Almnara Street, W2 Abdulmnam Ruad Area, W3 Aldaman Building, W4 Almokthar street, W5 Alnaser area, W6 Wadi Rasbuad, W7 Bab Elzuton area, W8 Alros area, W9 Akrom Alkhail (1), and W10 Akrom Alkhail (2), with the locations of underground water wells displayed in Fig. 1.

2 Materials and Methods: E-mail: E-mail:

2.1 Collection of Samples:

During two trips in the same month, Dec. 2020, twenty samples were collected from ten stations, with one sample from bottom of each well and the other from the surface after water treatment in all wells. The pHs were measured in situ using a portable pH because the parameters are likely to change during transport. **Fig. 2** shows the locations of the wells from which the water samples were collected at different locations in the Tobruk city area

2.2 Micro-analysis

The powder (Mac Conkey Agar) 49.5g was dissolved in 1L distilled water with swirling the water. The autoclave was running at 120°C for one minute, after cooling to room temperature, 1 ml of the sample was added and the sample was then left to grow for 84 hours in the lab at room temperature.

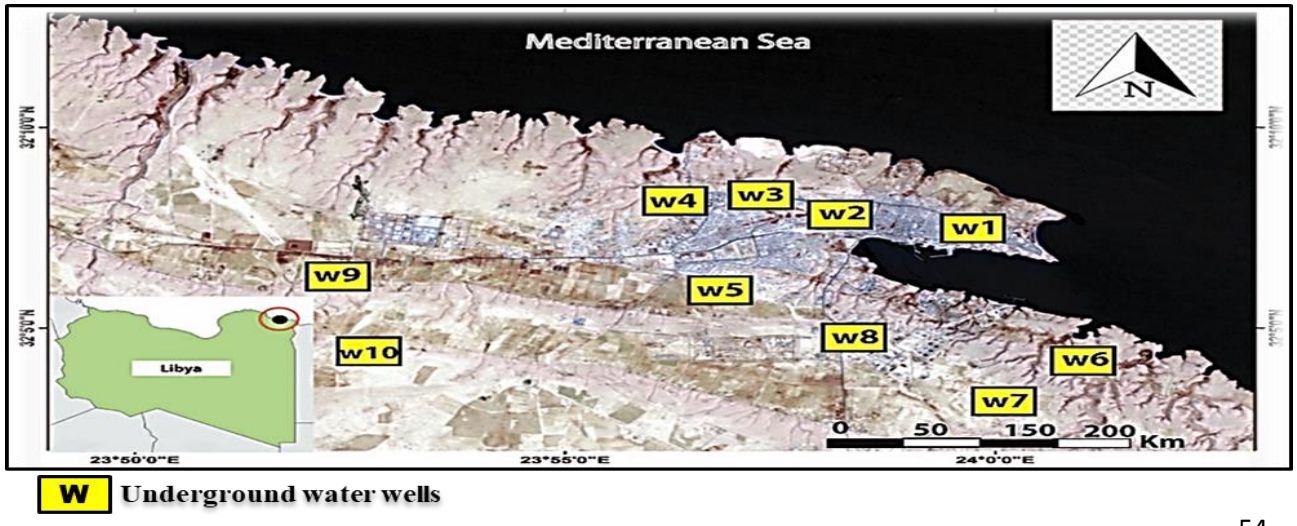

Fig. 1. Location of study area and groundwater samples.

Fig. 2. A and B are sample collections from Amanara Street prior to the treatment process. Pictures C and G show water samples being taken directly after treatment of the water, and pictures D and F illustrate water collections from Abd El mnam ruad station E, measuring Ph at the same time at Abd El mnam ruad station H.

2.3 physicochemical analysis

The various results obtained for the physicochemical analysis of the water samples from the various wells are presented in **Figs 3-9** and their data reported in **Table 2** in discussion section. pH was determined in this study using an "Inolab pH meter 720" which was equipped with a temperature compensating device. The instrument was calibrated using standard pH buffers (pH 4, 7, and 10) and the TDS of water samples. The TDS was determined using a "T.G.W" TDS meter. The instrument was calibrated using standard TDS buffers (1000 mg/L). Conductivity of water samples .The conductivity in µS/cm was determined by "Milwaukee". The instrument was calibrated using a standard conductivity buffer (4000 µS/cm), with sodium and potassium levels in water samples determined using a CARELYTE electrolyte analyser. A standard solution was prepared by dissolving 0.7915g KCl and 0.4715g NaCl in 1 L distilled water to produce a solution of 500 ppm K and 250 ppm Na. This solution was used as a stock solution and diluted to prepare the standard solutions used in the analysis. By plotting a graph of display readings against standards concentrations, and then taking a reading from the sample, the concentration of sodium

and potassium in the sample can be calculated from the calibration plot (Shibata Y, 1992). The chloride ion concentrations in the water samples were determined via titration of 10 mL water sample and 5 mL K_2CrO_4 (3.5 g potassium chromate in 1 L distilled water) against silver nitrate solution (3.7 g silver nitrate in 100 mL distilled water). The titration was performed until the colour of the solution changed to orange (Gaith G. A Jalgaif et al., 2018).

3 Results

3.1 Micro-analysis

Twenty water samples was taken on the same day and transferred directly to the Al-Aman Laboratory for chemical analysis within two hours for analysis at ambient temperature. **Table 1** shows that *E. coli* were present in most of the samples except for the water samples from wells W1, W7, and W10. The

corresponding results will be discussed in more detail in the dissection section.

Table 1. The *E. coli* detection in the samples.

Well Code	Sample No.	Microbiological Test	Result
W1	A*	Negative	-
	A**	Negative	-
W2	B*	Positive	*E. Coli* (+Ve)
	B**	Negative	-
W3	C*	Positive	*E. Coli* (+Ve)
	C**	Negative	-
W4	D*	Positive	*E. Coli* (++Ve)
	D**	Negative	-
W5	E*	Positive	*E. Coli* (+++Ve)
	E**	Negative	-
W4	D*	Positive	*E. Coli* (++Ve)
	D**	Negative	-
W5	E*	Positive	*E. Coli* (+++Ve)
	E**	Negative	-
W6	F*	Positive	*E. Coli* (+Ve)
	F**	Negative	-
W7	J*	Negative	-
	J**	Negative	-
W8	H*	Positive	*E. Coli* (+Ve)
	H**	Negative	-
W9	G*	Positive	*E. Coli* (+Ve)
	G**	Negative	-
W10	K*	Negative	-
	K**	Negative	-

Where: "*" and "**" are the number of samples before and after treatment, respectively.

3.2 Physicochemical analysis

3.2.1 5.2.1 pH

pH is an important parameter, which represents the degree of ionization of the medium studied; in this particular instance, it gives an indication on the level of the pollution of the water. The pHs of the samples before treatment range from 6.9 to 7.7, with an average of 7.30; after treatment, it ranged from 6.1 to 7.4 with an average of 6.5, as illustrated in Fig. 3 and Table 2.

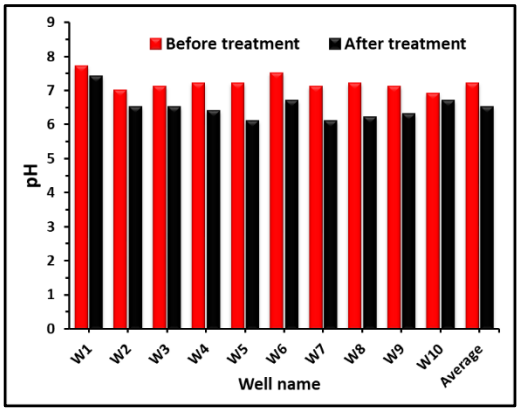

Fig. 3. Bar graph distribution for pH concentrations.

3.2.2 Total dissolved solids, TDS

TDSs are illustrated in Fig. 4. Their values before treatment fluctuated between 2850 and 14,640 mg/L, with an average of 6667 mg/L. The highest TDS value was recorded for W10. However, the TDS content after treatment was found to vary from 500 to 3300 mg/L, with an average of 1840 mg/L, and for which the highest TDS content was recorded for W8.

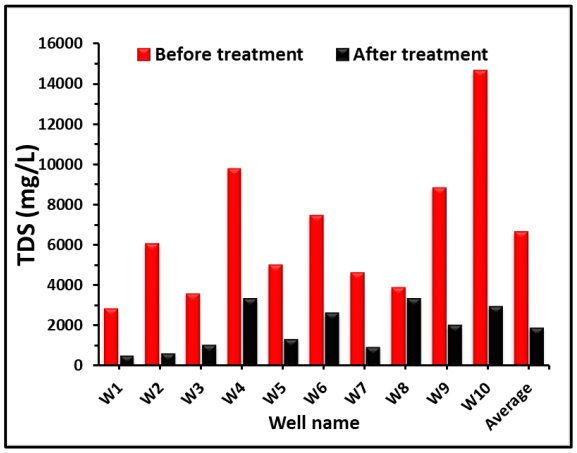

Fig. 4: Bar graph distribution for Total dissolved solids TDS concentrations.

3.2.3 Sodium ions, Na^+

The data obtained for sodium ion concentrations are given in Fig. 5. The results show that the Na concentrations prior to treatment varied from 1112 to 3556 mg/L, with an average 1937.2 mg/L, with the highest concentration recorded for W10, while after treatment it varied from 131.7 to 196.4 mg/L, with an average 161.39 mg/L and the highest concentration at W8.

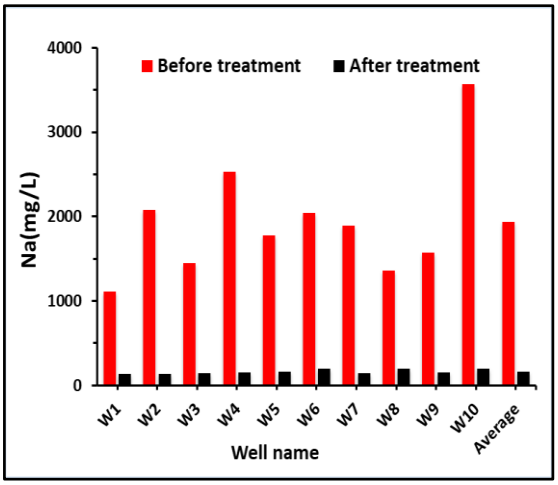

Fig. 5. Fig. 5. Bar graph distribution for sodium ion concentrations

3.2.4 Potassium ion, K^+

The distribution of potassium ion concentrations is shown in **Fig. 6**. This fluctuates between 108 to 22 mg/L prior to treatment, with an average of 54.9 mg/L. The highest K concentration of 108 ppm was recorded at Station 10. Akrom Alkhail (2). By contrast, K concentrations after treatment in the area of study ranged from 3.2 to 9.6 mg/L, with an average of 5.27 mg/L, with the highest concentration found at Station 4 (Almokthar Street).

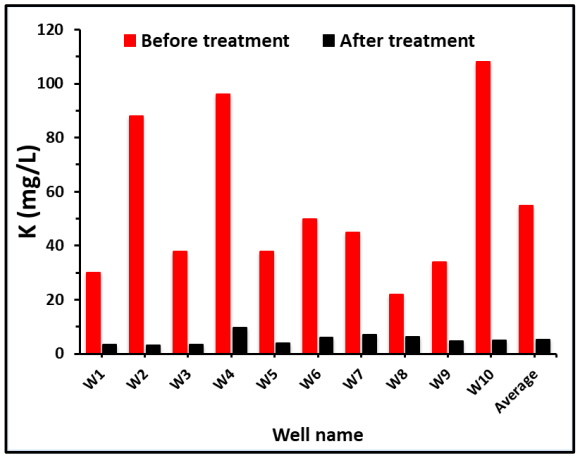

Fig. 6. Bar graph distribution for potassium concentrations.

3.2.5 Calcium ions, Ca^{2+}

Calcium ion concentrations are illustrated in Fig. 7. Prior to treatment, Ca^{2+} concentrations were found to vary from 400 to 1100 mg/L, with an average 809.4 mg/L. The highest concentration was seen at W10. After treatment, Ca^{2+} concentrations were found to range from 83.6 to 22 mg/L with an average of 56.95 mg/L, with stations W1, W2, W3, and W9 showing recorded values lower than the WHO permissible limits (WHO, 2011).

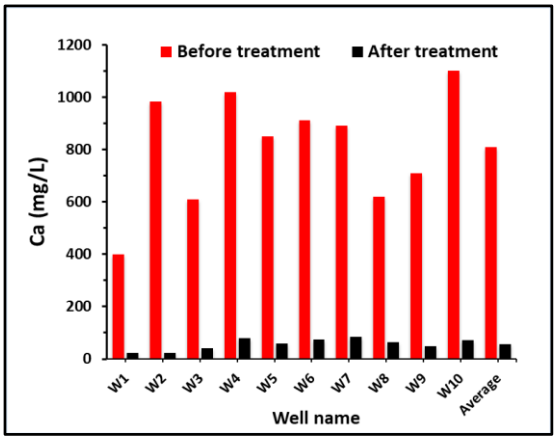

Fig. 7. Bar graph distribution for calcium ion concentrations.

3.2.6 Chloride ions, Cl^-

Chloride concentrations before treatment in the study area, as illustrated in **Fig. 8**, varied between 3130 and 6680 mg/L with an average of 4559.5 mg/L. On the other hand, after water treatment, Cl^- concentrations varied between 710 and 1065 mg/L, with an average of 710 mg/L.

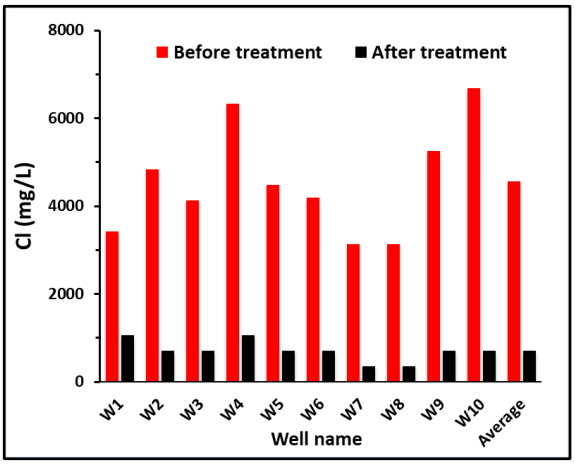

Fig. 8. Bar graph distribution for chloride ion concentrations**.**

3.2.7 Sodium chloride, NaCl

The data for sodium chloride concentrations are given in Fig. 9. The result before treatment showed that NaCl content ranged between 3940 and 9360

mg/L, with an average of 5964.5 mg/L, with the largest concentration recorded at Station 10. However, NaCl values after treatment were found to vary between 585 to 1755 mg/L, with an average of 1170 mg/L. Notably, the higher levels of NaCl concentrations were determined in five wells (W2, W3, W5, W9 and W10) than in compared to the other wells with the highest value of 1170 mg/L which are the same in five wells mentioned earlier.

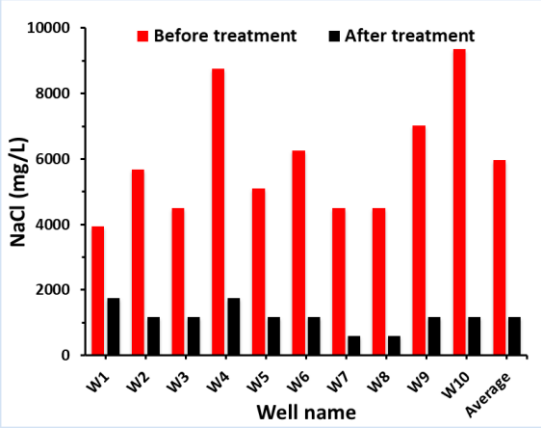

Fig. 9. Bar graph distribution for sodium chloride concentrations**.**

3.2.8. Electrical conductivity, E.C.

The conductivity of an electrolytic samples depends on its concentration were measured as shown Fig. 10 and their associated data are shown in Table 2. As expected prior to treatment of water the EC values ranged between 5.75 to 19.8 µS/Cm with an average of 12.148 µS/Cm which is considerably higher than permissible limit (1400 µmhos.cm^{-1}). It is possibly reflecting the water contains high levels of TDS because of naturally occurring elements and processes.

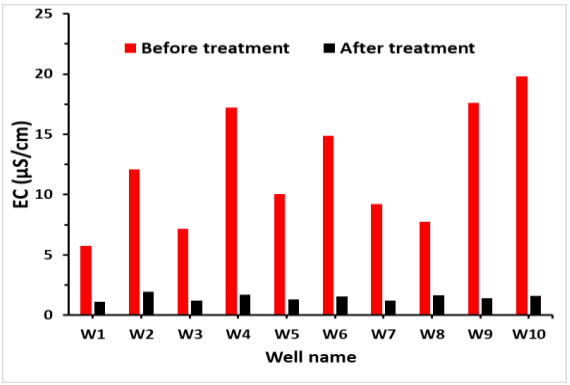

Fig. 10. Bar graph distribution for EC concentrations

4 Dissection

4.1 Micro-analysis

As can be observed from **Table 1**, prior to treatment all of the water samples tested positive for *E. coli* except for the water samples from W1, W7 and W10(2), whereas after treatment none of the wells tested positive. It is worth noting that the presence of *E. coli* in all the water sources indicate that they are not fit for human consumption without prior and adequate treatment. Several health risks have been associated with the consumption of water contaminated with faecal matter; indeed, this problem is exacerbated in children under the age of 5 and immuno-compromised adults (Diouf et al., 2014; Edokpayi, 2018; Joshua et al., 2018).

4.2 6.2 Chemical analysis

Acomparison of the physico-chemical characteristics of the studied water samples of drinking water wells has been made prior and after treatment and their data reported in Table 2, collected data revealed that there were considerable variations in physico - chemical properties of examined samples from the different localities and these properties will be discussed in detail below. As shown in Fig. 3 and Table 2, the pHs of the groundwater for all wells prior to treatment were within the range of 6.9 - 7.7 with a mean of 7.30, while after treatment were within the range of 6.1 to .7.4 with the mean of 6.75, indicating that the groundwater in the study area was initially slightly alkaline for most of the groundwater samples. Notably, all the samples tested in our study fell within limits of 6.5 to 8.5 required by the WHO's quality standards for groundwater (WHO, 2011).

The concentrations of TDS before and after treatment processes ranged from 2850 to 14,640 mg/L and 500 to 3,300 mg/L, with averages of 10,170 and 1900 mg/L, respectively Fig. 4 and Table 2,. This indicates that the quality of all groundwater in the study area could be classified as very hard water to TDS (Mohamed et al., 2018; Sawyer & McCarty, 1967; Todd, 1980). In this study, the concentrations of TDS are found above the WHO-allowable limit (WHO, 2011) for Libya 1000 ppm. Initially, the Na^+ concentration was determined to be between 1112 and 2532 mg/L with an average of 1937.2 mg/L, which was higher than WHO-permissible limits (Fig. 5 and Table 2). Although higher sodium levels do not pose a serious threat to human health, they create a risk to people on low sodium diets, as usually recommended for individuals

with hypertension and congestive heart failure. However, low levels of Na^+ were determined after treatment of water between of 131.7-196.1 mg/L with an average of 161.39 mg/L, which is well below the WHO-permissible limit (WHO, 2011) for Libya, of 200 ppm. The average concentrations of untreated water, the K^+, Ca^{2+}, Cl^- and NaCl were 5964.5, 4559.5, 809.4, and 54.9 mg/L, respectively, with an average of 5.27, 56.95, 710, and 1170 mg/L, respectively 108, 1100, 6680 and 9360 mg/L, respectively see Figures 6-9 and Table 2. After treatment, the concentrations of K^+, Ca^{2+}, Cl^-, and NaCl in the groundwater were 3.3–9.6, 22.0–83.6, 355-1065, 585–1755 mg/L, with averages of 5.27, 56.95, 710, and 1170 mg/L, respectively, and all their concentrations fall within WHO-permissible limits (WHO, 2011) for Libya at 40 ppm, 50 ppm, 250 ppm, and 250 ppm, respectively. The total alkalinity varied between 300–1100 mg/L and 200–600 mg/L for before and after treatment, respectively with a mean value of 650- 370 mg/L, respectively (Table 2).

The electrical conductivity is dependent on the concentrations, types of soluble ions, as well as the temperature of the water(Hem, 1985). In this study, the EC values before treatment ranged between 5.75 and19.8 µS/cm with a mean EC for all samples analysed of 12.14 µS/cm, which indicated a large variation in EC. High ECs were found in water samples from W10, W9 and W4 prior to treatment (Table 2). The desirable limit set for natural water as stated by the WHO (Mansour, 2013; Mudgal et al., 2009) should not exceed 1400 µmhos.cm^{-1}. However, it was observed that the conductivities of the water samples was influenced by TDS and, in general, water samples post-treatment had low electrical conductivities, and their ECs in the water samples ranged between 1.11-1.95 µS/Cm with an average of 1.46 µS/Cm, suggesting that they were all compliant with the WHO guidelines and were also safe for drinking purposes safe for drinking purposes.

Table 2. Results of the Physico-chemical properties for the Ten well samples investigated.

Well No.	Samples Test	pH	EC ms/cm	TDS	Na^+	K^+	Ca^{2+}	Cl^-	NaCl	Alkalinity
				gm/L						
W1	before	7.7	5.75	2850	1112	30	400	3420	3940	300
	after	7.4	1.11	500	131.7	3.3	22	1065	1755	200
W2	before	7.0	12.1	6040	2076	88	984	4840	5680	400
	after	6.5	1.95	600	134.5	3.2	23.5	710	1170	200
W3	before	7.1	7.16	3580	1444	38	610	4130	4510	500
	after	6.5	1.21	1000	147.3	3.5	41.2	710	1170	200
W4	before	7.2	17.22	9770	2532	96	1020	6325	8755	800
	after	6.4	1.67	3300	151.5	9.6	80.6	1065	1755	500
W5	before	7.2	10.02	5000	1776	38	850	4485	5095	700
	after	6.1	1.28	1300	165.6	4.0	58.2	710	1170	300
W6	before	7.5	14.87	7440	2044	50	910	4195	6265	1100
	after	6.7	1.53	2600	195.9	6.0	75.5	710	1170	500
W7	before	7.1	9.22	4630	1888	45	890	3130	4510	600
	after	6.1	1.19	900	144.8	7.0	83.6	355	585	400
W8	before	7.2	7.74	3900	1362	22	620	3130	4510	600
	after	6.2	1.66	3300	196.4	6.3	65.2	355	585	500
W9	before	7.1	17.6	8820	1572	34	710	5260	7020	800
	after	6.3	1.40	2000	150.1	4.8	48.3	710	1170	600
W10	before	6.9	19.80	14640	3566	108	1100	6680	9360	700
	after	6.7	1.58	2900	196.1	5.0	71.4	710	1170	300

5 Conclusion

The present study has provide information of underground wells in some locations in Tobruk city Libya. The data show from ten points that the microanalysis illustrate that there are three locations free from bacteria W1. W7. W10 this locations lead to good structure and a new area in the same time away from domestic sewage, while W7, W10 these locations located outside city center far away. From a water quality point of view, after treatment process most of the data for the physico-chemical parameters indicated tolerable quality

Therefore, the heavy reliance on borehole water in the study area calls for constant monitoring and design of regular purification strategies by government agencies concerned to ensure good water quality.

Acknowledgements

First of all, I would like to express my deep thanks to Allah, who guided me to bring forth this paper to light. I would like to sincerely thank to all people in my city who helping me to obtain water samples and for their support and continuous encouragements through the progress of this work.

Also, deep thanks to my friends Abdullah Abdullah, Anwar Abadelrahim and Tahani Y. M. Aeyad.

Conflict of interest: The authors declare that there are no conflicts of interest.

References

Adam, F. A. A. (2018). Petrographically and Mineralogical Studies on the Oligocene-Miocene formations of Al Bardia Coastal Area, East Tobruk City, Libya. Unpublished M.Sc. Thesis, Mansoura University, Egypt, 109 pp. .

Al- Azzawi, A. S. N., Ahala Vaiz Al guaharge, mead Adle Al-Taei,. (2010). Physical and chemical study of Iraqi and international mineral water available in local markets. The University of Babylon/Banking Journal of Science and Applied, 18(5).

Betz, J. B., & Noll, C. A. (1950). A total hardness determination by direct colorimetric titration. J. Amer. Water Works Assoc, 42, 49-56.

Diouf, K., Tabatabai, P., Rudolph, J., & Marx, M. (2014). Diarrhoea prevalence in children under five years of age in rural Burundi: an assessment of social and behavioural factors at the household level. Global Health Action, 7(1), 24895. doi:10.3402/gha.v7.24895

Edokpayi, J. N. R., Elizabeth T. Kahler, David M. Hill, Courtney L. Reynolds, Catherine. Nyathi, Emanuel. Smith, James A. Odiyo, John O. Samie, Amidou. Bessong, Pascal. Dillingham, Rebecca. (2018). Challenges to Sustainable Safe Drinking Water: A Case Study of Water Quality and Use across Seasons in Rural Communities in Limpopo Province, South Africa. Water, 10(2), 159.

El Deftar, T. I., B. (1977). Geological Map of Libya, scale 1: 250 000, sheet NH. 35-1. Al Bardia, Explanatory Booklet,. Industrial Research Center, SPLAJ, Tripoli, 93p.

Gaith G. A Jalgaif, Salah Ali M. Idris, Rabie Ali M. Maarouf, Ahmed M. Attia, & El-Naggar, M. M. (2018). International Journal of Environmental Chemistry. 2(1), 1-9.

Gibb, J. P. (1973). Water Quality and Treatment of Domestic Groundwater Supplies. URBANA: URBANA.

Heath, R. C. (1987). Basic Ground-Water Hydrology. U .S . GEOLOGICAL SURVEY. Dallas L . Peck, Director.

Hem, J. (1985). Study and interpretation of the chemical characteristics of natural water. (3rd edn. ed.). University of Virginia, Charlottesville, US University of Virginia, Charlottesville.

Hoko, Z. (2005). An assessment of the water quality of drinking water in rural districts in Zimbabwe. The case of Gokwe South, Nkayi, Lupane, and Mwenezi districts. Physics and Chemistry of the Earth, Parts A/B/C, 30, 859-866. doi:10.1016/j.pce.2005.08.031

Joshua, N. E., John O. Odiyo, Elizabeth, O. P., & Titus A.M. Msagati. (2018). Evaluation of Microbiological and Physicochemical Parameters of Alternative Source of Drinking Water: A Case Study of Nzhelele River, South Africa. Open Microbiol. J., 12, 18-27.

Lawson, O., & Emmanuel, L. (2011). Physico-Chemical Parameters and Heavy Metal Contents of Water from the Mangrove Swamps of Lagos Lagoon, Lagos, Nigeria. Advances in Biological Research, 5, 8-21.

Mansour, S. (2013). Physico-chemical Evaluation of Drinking Water Quality in Alshati District of Libya. IOSR Journal of Environmental Science, Toxicology and Food Technology, 4, 46-51; 10.9790/2402-0414651.

Mohamed, A. K., Liu, D., Mohamed, M. A. A., & Song, K. (2018). Groundwater quality assessment of the quaternary unconsolidated sedimentary basin near the Pi river using fuzzy evaluation technique. Applied Water Science, 8(2), 65. doi:10.1007/s13201-018-0711-0

Mudgal, K. D., Kumar, M., & Sharma, D. K. (2009). Hydrochemical analysis of drinking water quality of Alwar district. Rajastan. Nat. and Sci., 7(2), 30 – 39.

Salem, M., & Alshergawi, M. I. (2013). Physico-chemical Evaluation of Drinking Water Quality in Alshati District of Libya. IOSR Journal of Environmental Science, Toxicology and Food Technology, 4, 46-51.

Sawyer, C., & McCarty, P. (1967). Chemistry for sanitary engineers. McGraw-Hill, New York.

Shibata Y, M. T., Miyage H. (1992). Chemistry and Industrial Chemistry Journal of the Chemical Society of Japan.

Sweedan, A., and Issawi, B. (1977). Geological map of Libya, 1:250,000, Sheet NH 34-4. Bir Hacheim. Explanatory Booklet, Tripoli, LR.C.

Todd, D. (1980). Groundwater hydrology. . Wiley, New York.: Wiley, New York, US.

UNICEF. (2013). Children dying daily because of unsafe water supplies and poor sanitations and hygiene. United Nations Children Fund.

Scientific Journal for faculty of Science
Sirte University

sjsfsu@su.edu.ly
journal.su.edu.ly/index.php/JSFSU

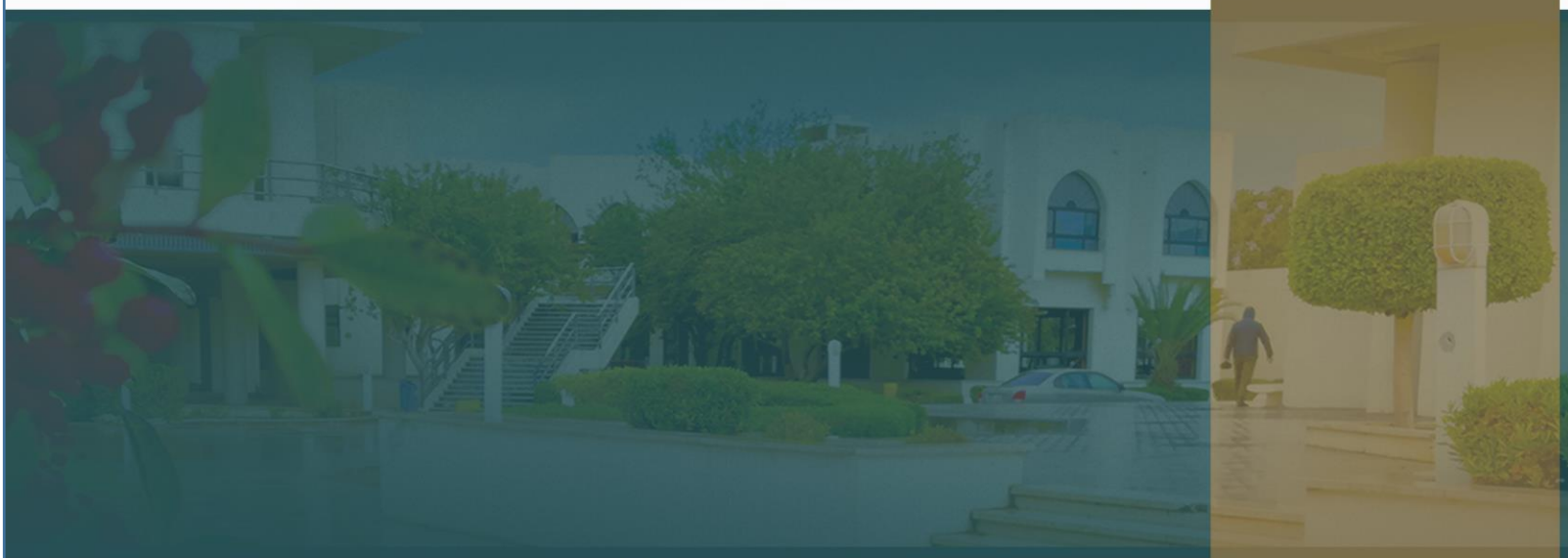

media92production@gmail.com
قسم الإنتاج الإعلامي جامعة سرت
تصميم : عبدالله نصرالدين